

Life Extension of Offshore Structures: A Conceptual Framework and Fatigue Damage Models

by

Ashish Aeran

Thesis submitted in fulfillment of
the requirements for the degree of
PHILOSOPHIAE DOCTOR
(PhD)



Faculty of Science and Technology
Department of Mechanical and Structural Engineering and Materials
Science
2019

University of Stavanger
N-4036 Stavanger
NORWAY
www.uis.no

©2019 Ashish Acran

ISBN: 978-82-7644-872-6
ISSN: 1890-1387
PhD: Thesis UiS No. 477

Preface

The thesis is submitted in partial fulfilment of the requirements for the degree of Doctor of Philosophy (PhD) at the University of Stavanger (UiS), Norway. The research work was carried out at the Department of Mechanical and Structural Engineering and Materials Science, Faculty of Science and Technology, UiS, during the period August 2015 to July 2019. During this period, the author also performed several departmental duties. The author was the main lecturer in Structural Mechanics II and Building Materials courses during the last 2 years. Also, several Bachelor/Master theses were supervised as both main supervisor and co-supervisor during the last 3 years. This work was fully funded by the Norwegian Ministry of Education and by the Department of Mechanical and Structural Engineering and Materials Science, UiS. The required PhD courses have also been completed at UiS.

This thesis is divided into two parts. Part I briefly presents the background, research gaps, objectives, main research outcomes, conclusions, recommendations and suggestions for future work. Part II comprises seven papers, of which four are journal papers and the remaining three are conference papers.

Ashish Aeran

Stavanger, Norway

Acknowledgments

First and foremost, I would like to thank my main supervisor, Associate Professor Sudath Siriwardane, for his immense support and guidance throughout this doctoral study. I am highly grateful to have had him as my supervisor, and his positive attitude has helped me in successfully completing this thesis. He has not only disseminated technical knowledge but also passed on valuable research ethics to me. It has been a great experience working with him. I would also like to thank my co-supervisors, Associate Professor Ove Mikkelsen and Professor Emeritus Ivar Langen, for their valuable comments and suggestions on my work.

I am also grateful to all my collaborators for their support and contributions. I would like to thank Professor Andrea Carpinteri, Professor Sabrina Vantadori and Dr. Daniela Scorza at the University of Parma, Italy. I would also like to express my gratitude to Professor Peter Starke and Ruth Acosta at the University of Applied Sciences, Kaiserslautern, Germany. Also, thanks to Professor Frank Walther at the TU Dortmund University, Germany. I have gained a great deal of knowledge and experience from all these collaborators.

I also extend my gratitude to friends and departmental colleagues for their support during the PhD period. Firstly, many thanks to Dr. Jithin Jose for his unconditional support during all these years at both personal and professional level. I would also like to thank Dr. Arvind Keprate, Dr. Endashaw Tesfaye, Dr. Adekunle Orimolade, Mr. Chavin Guruge and Mr. Nicolo Daniotti for the wonderful time and office chats. Also, many thanks to my colleague and friend (soon to be Dr.), Sindhu Kancherla, for all the encouragement and support throughout this journey that we started together four years back. This journey would have been so much tougher without these friends, and words are not enough to thank them all.

Acknowledgments

I am also thankful to administrative staff members at UiS for their support. Thanks to Mr. Norbert Puttkamer, Ms. Helga Hunnes Bøe, Ms. Elisabeth Stornes Paulsen, Ms. Kathrine Molde, Ms. Anne Karin Rafos, Ms. Cathrine Reilstad and Ms. Nina Stava for all the administrative support.

Finally, I would like to thank my parents and family for their unconditional love and support. Above all, thanks to God, the Almighty, for blessing me to complete this doctoral study successfully.

Abstract

Many offshore structures worldwide are approaching or have already exceeded their original design life. It is important to use the existing infrastructure efficiently and to estimate remaining service life accurately. Fatigue and corrosion are identified as main ageing mechanisms for these structures. Although, much research has been carried out on understanding these ageing processes, failure has occurred and is still occurring in offshore structures. Infact, for these structures, almost 25% of all structural damage requiring repair is classified as fatigue damage.

The assessment guidelines and recommendations are scattered across standard codes and research articles and these codes are not updated for recently proposed theories and models. There is a need to improve currently available guidelines to simulate structural degradation, to capture loading history more precisely, to consider the effect of localized corrosion on stress concentration factors, to select proper fatigue strength curves for corroded structural detail categories and to use more precise fatigue damage theories for a better estimation of remaining life. The Miner's rule, which is currently used in the codes, may lead to unreliable life predictions, as it does not capture loading sequence effects accurately. Moreover, commonly used approaches given in assessment standards do not capture the multiaxial fatigue accurately, and more accurate multiaxial damage theories are not updated in these standards. There is a need for more detailed assessment guidelines and more accurate uniaxial/multiaxial fatigue damage models for better estimation of remaining life.

To address the above-mentioned needs, a conceptual framework for structural integrity assessment of ageing offshore structures is proposed in this thesis. The proposed framework not only overcomes the deficiencies in the currently available guidelines but also includes recent

Abstract

research proposals available in the literature. The framework provides theories and guidelines necessary to predict the remaining fatigue life and check the structural adequacy in ULS, SLS and ALS during the whole extended service life. A new and accurate uniaxial fatigue damage model is also proposed for better estimation of remaining fatigue life. The model can be used for life predictions of ageing offshore structures, using nominal and hot-spot approaches. The proposed damage model does not require additional material parameters other than the code-given $S-N$ curves. Moreover, it does not require a full-range $S-N$ curve and can be easily applied by practising engineers using the partially known $S-N$ curves given in design standards. Finally, existing multiaxial fatigue damage theories based on the critical plane approach are also improved by proposing a new expression of the off-angle. The model can be used for better fatigue life predictions of ageing offshore structures. The proposed fatigue damage models are verified with experimental results for several materials, including S355 structural steel. The proposed framework and fatigue models are also applied to several case studies including welded joints and offshore jacket structures. Hence, the applicability and significance of proposed framework and damage models are confirmed.

Keywords: *Life extension, offshore jacket, structural degradation, corrosion, fatigue life, nonlinear damage models, multiaxial fatigue, critical plane approach*

Table of Contents

Preface	i
Acknowledgments	iii
Abstract	v
List of Papers	ix
Abbreviations	xi
Part I – Thesis Summary	xiii
Chapter 1 Introduction	1
1.1 Background	1
1.2 Problem statements	3
1.3 Research gaps	5
1.4 Objectives	12
1.5 Overview of the thesis	12
Chapter 2 Research Outcomes	13
2.1 Proposed framework for structural integrity assessment.....	14
2.2 Proposed uniaxial fatigue damage model	18
2.3 Proposed multiaxial fatigue damage model.....	24
Chapter 3 Summary and Conclusions	26
3.1 Summary	26
3.2 Concluding remarks	28
3.3 Suggestions for future work.....	31
References	32
Part II – Papers	43

List of Papers

- Paper I Aeran, A., Siriwardane, S. C., & Mikkelsen, O. (2016) Life extension of ageing offshore structures: Time dependent corrosion degradation and health monitoring. Proceedings of the 26th International Ocean and Polar Engineering Conference, ISOPE 2016, International Society of Offshore & Polar Engineers, Rhodes, Greece.
- Paper II Aeran, A., Siriwardane, S. C., Mikkelsen, O., & Langen, I. (2017) Life extension of ageing offshore structures: A framework for remaining life estimation. Proceedings of the 36th International Conference on Ocean, Offshore and Arctic Engineering, OMAE 2017, Volume 3A, Paper No. OMAE2017-62063, Trondheim, Norway.
- Paper III Aeran, A., Siriwardane, S. C., Mikkelsen, O., & Langen, I. (2017) A framework to assess structural integrity of ageing offshore jacket structures for life extension. *Marine Structures*, 56, 237–259.
- Paper IV Aeran, A., Siriwardane, S. C., Mikkelsen, O., & Langen, I. (2017) A new nonlinear fatigue damage model based only on S-N curve parameters. *International Journal of Fatigue*, 103, 327–341.
- Paper V Aeran, A., Siriwardane, S. C., Mikkelsen, O., & Langen, I. (2017) An accurate fatigue damage model for welded joints subjected to variable amplitude loading. Proceedings of the 1st Conference of

List of Papers

Computational Methods in Offshore Technology,
Volume 276, Stavanger, Norway.

Paper VI Aeran, A., Acosta, R., Siriwardane, S. C., Starke, P., Mikkelsen, O., Langen, I., & Walther, F. (2019) A nonlinear fatigue damage model: Comparison with experimental damage evolution of S355 (SAE 1020) structural steel and application to offshore jacket structures. *International Journal of Fatigue*, (under review).

Paper VII Aeran, A., Vantadori, S., Carpinteri, A., Siriwardane, S. C., & Scorza, D. (2019) Novel non-linear relationship to evaluate the critical plane orientation. *International Journal of Fatigue*, 124, 537–543.

Abbreviations

ALS	Accidental limit state
API	American Petroleum Institute
CPS	Cathodic protection system
DDCA	Double damage curve approach
DLDR	Double linear damage rule
DNV	Det Norske Veritas
EMU	Electrical mobile unit
HSE	Health and Safety Executive
ISO	International Standard Organization
KP	Key programmes
NCS	Norwegian Continental Shelf
OLF	Oil Industry Association
PSA	Petroleum Safety Authority
RBI	Risk-based inspection
SCF	Stress concentration factor
SHM	Structural health monitoring
SLS	Serviceability limit state
SWT	Smith-Watson-Topper
UKCS	United Kingdom Continental Shelf
ULS	Ultimate limit state
VAL	Variable amplitude load

Part I – Thesis Summary

Chapter 1 Introduction

1.1 Background

A number of offshore platforms worldwide are approaching or have already exceeded their design life [1-4]. More than 50% of offshore installations on the Norwegian Continental Shelf (NCS), the United Kingdom Continental Shelf (UKCS) and the Gulf of Mexico Shelf are currently operating beyond their original life [5-7]. This figure is roughly 70% for around 800 platforms in the Middle East region [8]. The replacement of all these structures at once presents an operational and technical challenge [9]. The use of infrastructure from an existing field is sometimes a precondition for the development of a newer oil/gas field [10]. The enhanced production and drilling techniques, falling profit margins due to low oil prices, uneconomical small field discoveries and plenty of remaining oil reserves in existing fields are factors which are also encouraging operators to undertake more life extension studies. It is important to use the existing infrastructure efficiently and to estimate its structural integrity and remaining service life.

Ageing was recently categorized as functional ageing, technological ageing, knowledge-based ageing and organizational ageing [4,11]. While functional ageing includes material degradation issues, such as fatigue, corrosion, dents, damages etc., technological ageing may refer to the old standards and regulations that are no longer considered sufficient for safe design. Knowledge-based ageing may occur in cases where original design documents have become outdated, due to the availability of new knowledge such as new analysis methods, new models, new standards, new knowledge about climate etc. Organizational ageing encompasses the ageing of personnel and insufficient competence. Though each of these key issues is important when addressing the problems of ageing, material degradation caused by fatigue and corrosion is a major cause of failures.

Introduction

Fatigue damage is caused by fluctuating stresses and may result in cracks after a certain number of stress cycles. Offshore structures are subjected to fatigue loading, mainly due to environmental wave loads during their service life. Fatigue is therefore a major hazard for these structures and in some cases fatigue cracking may reduce the overall structural integrity [12]. These structures are also subjected to corrosion, due to the harsh marine environment, which can cause severe material degradation, especially in the splash zone. Corrosion changes the mechanical properties (i.e. degrades the strength) of steel with time and can be broadly classified as uniform or localized [13]. Uniform corrosion is the most common form and can cause local structural collapse due to changes in structural stiffness [14]. Localized corrosion, such as pitting, and crevice corrosion, is restricted to small areas and can cause local stress concentrations [15]. Corrosion fatigue is the result of cyclic loading in a corrosive environment and may reduce the fatigue strength by more than 60% [16]. A corrosion protection system (CPS) is generally employed to counteract corrosion but has a typical life of only 5 to 15 years and is also ineffective in the splash zone due to the intermittent action of waves and tides [17]. The maintenance and repair of CPS for fixed offshore structures are generally very costly and sometimes impractical [18]. Other degradation mechanisms include erosion, creep, and accumulated plastic deformation, among others [11]. These ageing mechanisms can cause damage to the structure and can even lead to structural collapse.

Although much research is carried out on ageing processes, failure has occurred and is still occurring in offshore structures [19]. Infact, for offshore installations, almost 25% of all structural damage requiring repair is classified as fatigue damage [20-22]. Similarly, in the case of bridges, damage caused by fatigue accounts for 40% of the total damage [23]. Detailed investigations of failures, like those of Ranger I, Alexander Kielland, Ocean Ranger, West Vanguard and Ocean Odyssey, also highlighted fatigue as one of the major causes [24, 25].

Most of the currently available fatigue assessment approaches are based on the evaluation of stresses, followed by determination of fatigue damage using code-given $S-N$ curves and a damage theory [22]. The stresses are generally evaluated using nominal, hot-spot and notch approaches. Subsequently, detail category-based $S-N$ curves in design standards are used, together with Miner's rule, for fatigue life estimation of structural details, such as tubular joints. There are several uncertainties involved in these fatigue assessment approaches, which could be the reasons behind the above failures. These uncertainties can exist due to use of commonly available fatigue damage models, use of simplified relations in determining stress concentration factors at joints/discontinuities, dispersion in material characteristics of corroded members, lack of fatigue strength curves for corroded structural details, lack of loading history and etc. [26]. These uncertainties can increase the risk of failures. It is reported that the most severe accidents due to fatigue were caused by gross errors like faulty fatigue design checks and gross fabrication defects [26]. There is a need for improved design checks, using more detailed assessment guidelines and more accurate fatigue damage models. It is therefore important to understand the deficiencies in currently available guidelines and fatigue life assessment approaches and to propose more detailed guidelines/accurate fatigue damage models, to avoid such failures in future.

1.2 Problem statements

Based on the work of previous researchers in this field, the problem statements for this study are formulated as follows.

1. Currently available life assessment guidelines and recommendations are scattered across design and integrity assessment standards, and research articles. Moreover, these standards are not updated for recently proposed theories and models. There are still some deficiencies in the existing standards, which can be further improved.

Several initiatives have been taken for the development of life assessment guidelines. However, the information is not only scattered but is also not updated with recent research. In addition, there are still some deficiencies in existing guidelines. For instance, no detailed recommendations are provided on the simulation of time-dependent structural degradation (for both uniform and localized corrosion). There is also a need to improve currently available guidelines to capture loading history more precisely, to consider the effect of localized corrosion on stress concentration factors, to select proper fatigue strength curves for corroded structural detail categories and to use more precise fatigue damage theories for better estimation of remaining life [5].

2. Design and integrity assessment standards-recommended fatigue damage theory can lead to unreliable life predictions during fatigue life estimations based on nominal and hot-spot approaches. Commonly used damage theory has shortcomings, which may lead to inaccurate life predictions.

Offshore structures are subjected to variable amplitude loading (VAL) due to harsh environmental sea conditions [21, 22]. Under such VAL, the stress state is generally evaluated using nominal or hot-spot approaches. Subsequently, fatigue damage is determined using Miner's rule [27], which is still widely used in the fatigue design of steel structures, due to its simplicity and easy of application. Moreover, current design codes and standards, such as Eurocode, Det Norske Veritas (DNV), etc., also recommend the use of Miner's rule [28, 29]. However, Miner's rule-based life predictions are found to be unreliable, since it does not consider the loading sequence effects accurately [30, 31]. There is a need for an accurate uniaxial fatigue damage theory, for more accurate prediction of remaining life.

3. Design and integrity assessment standards do not capture the multiaxial stress state accurately, and recently proposed accurate multiaxial damage theories are not included in these standards.

Code-given approach, such as notch stress approach, is based on stress factors which does not represent the actual multiaxial stress state at the connections and discontinuities.

The structural detail category *S-N* curves in standard codes are based on uniaxial testing conditions. Under service loading conditions, the structural joints and connections are subjected to multiaxial stress state. Such a stress state is represented in terms of an equivalent uniaxial effective stress, using the stress concentration factors (SCFs) at these joints [21,22]. Such an equivalent effective stress together with Miner's rule is the most commonly used multiaxial fatigue criterion for the life assessment of structures. However, use of such factors does not represent the actual multiaxial stress state, and Miner's rule may lead to unreliable life predictions [32]. Also, the criteria cannot be used for multiplanar complex joints or stiffened joints [32]. Moreover, more accurate multiaxial damage theories, such as those based on grain scale meso-plasticity and critical plane approaches, are not updated in existing standard codes.

1.3 Research gaps

Several research works have been carried out to overcome the above stated problems. A literature survey of the conducted research in these areas is presented below, and the research gaps are identified for this work.

1. Research gaps in currently available life assessment guidelines

Over the past two decades, several initiatives have been taken for development of life assessment guidelines. Also, attention was paid on the development of risk-based inspection guidelines for the planning of inspection for fatigue cracks [33]. The Health and Safety Executive (HSE) launched several key programmes (KP) on the UKCS, including a detailed investigation of ageing installations [34-36]. On the NCS, the Norwegian Oil Industry Association (OLF), together with the Petroleum

Safety Authority (PSA), is establishing the necessary assessment guidelines [37-39]. The inclusion of the assessment procedures and frameworks for existing structures started in the mid-1990s with the insertion of a section in API RP 2A [40]. However, both the input and acceptance criteria given are tied to US waters. Subsequently, similar sections were added to ISO 2394 in 1996 [41]. This was followed by ISO 13822 in 2001 [42] and ISO 19900 in 2002 [43]. The last addition to the international standards was an assessment section in ISO 19902 in 2007 [44], but it contains only minimal detailed or quantitative information [3]. In the UK, a structural integrity management framework for jacket structures was issued by the HSE in 2009 but was again based on API and ISO standards [45]. Around the same time, OLF and PSA initiated a project to establish the necessary standards and guidelines for life extension projects in the NCS region [39]. The outcome was the establishment of a new NORSOK standard N-006 [46] and the issue of recommended OLF guidelines for the life extension of facilities [47]. In 2014, API released a new standard, API RP 2SIM [48]. In 2015, a new DNV guideline for fatigue cracks inspections was established using probabilistic methods [33]. It recommends the modelling of uncertainty variables (such as physical uncertainty, statistical uncertainty, measurement uncertainty) as stochastic variables, each having a defined probability distribution function, based on engineering judgement, past experience from similar problems or analytical results [49]. The British Standard BS 7910 is also an important document for probabilistic inspection planning methods such as risk-based inspections (RBI) [50,51]. In addition to above standards, some life assessment guidelines, which describe the overall assessment process, have been discussed by researchers in past [52-54].

The above standards and published literature provide a general overview of the life assessment issues in ageing structures. This available information is scattered across several standards and research articles. The ageing mechanisms are discussed in detail, including the various

types of material degradation. However, no detailed guidelines or recommendations are available for precise modelling and simulation of both uniform and localized corrosion. For instance, the rate of uniform corrosion is recommended to be taken based upon the relevant experience as per the NORSOK assessment standard. Also, members with localized corrosion are recommended to be treated as dented tubular members. Corrosion wastage models in the literature which have been verified against field measurements, are not included in the assessment guidelines. As a result, there are uncertainties among practising engineers while simulating material degradation, especially in the absence of field measurement data. Also, current assessment guidelines do not provide recommendations on several other issues, such as simulation of loading history, selection of fatigue strength curves for corroded structural detail categories and the use of more precise fatigue damage theories. In addition, there is currently no conceptual framework that provides recommendations on the above issues and covers both the assessment guidelines requirements along with recently proposed theories in literature. These deficiencies in current assessment guidelines and the available literature on life assessment are identified as research gaps for this study.

2. Research gaps in available uniaxial fatigue damage models

Several improvements have been proposed in the past to overcome the shortcomings of the commonly used Miner's rule. Among the first improvements was the Marco-Starkey model, proposed in 1954 [55]. This model has a stress-dependent parameter, C . However, determination of this parameter C is not possible unless it is matched with a physical variable that can be detected during the fatigue testing [56]. Several other models were proposed, subsequently, towards the end of the 1950s, but these required the determination of similar material parameters. Manson proposed a double linear damage rule (DLDR) in 1966, replacing the linear Miner's rule with a set of two lines converging at a knee point [57]. The DLDR was further improved, and the double

damage curve approach (DDCA) was proposed by Manson and Halford in 1981 [58]. However, both the DLDR and DDCA models failed to capture the loading sequence effects precisely. Many other damage models were proposed in the 1980s and 1990s, such as models by Lemaitre and Plumtree [59] and by Chaboche and Lesne [60]. These models were again based on material parameters, p , α , β , which can be determined only through the material testing. Although these models can be used for a few verified materials, their application to structural steel and structural detail categories is not found. As a result, even though some of above-mentioned models have shown good agreement with the experimental data for specific materials, they cannot be applied to structural detail categories using the standard codes [61]. A more detailed review of the damage models developed before 1998 can be found in an article by Fatemi and Yang [62]. These damage models are based on crack growth concepts, damage curve modifications, energy-based theories, and continuum damage mechanics. However, the application of these models is not found in the design standards, as they require testing for the determination of material parameters. There is a limited amount of such material testing data available for structural steel. Moreover, such material parameters cannot be used for fatigue assessment of structural details.

Material testing was performed by some researchers to establish fatigue damage behaviour in 1999. These tests were based on the exhaustion of material ductility and estimated the instantaneous damage in material for a given stress amplitude or range [63]. As a result, the damage evolution curves for a few materials were established, and these represent the variation in experimental observed damage with number of cycles to failure. Testing was also performed to develop damage models based on hardness increase during the fatigue of material [64]. Subsequently, damage models were proposed to fit such experimental data but were again dependent on material parameters, with application to specific materials. In 2005, Mesmacque et al. proposed a sequential law, which

does not require any material parameters other than the full-range $S-N$ curve [31]. The application of this model was demonstrated in steel bridges in 2008 [65]. Although the model can capture the loading sequence effects and predicts the fatigue life accurately, its requirement for a full-range $S-N$ curve restricts design application by practising engineers. Also, the design codes-given $S-N$ curves are based on detail categories, and the physical meaning of the intercept used for such details is not clear. Moreover, this law cannot be used with the design codes and standards having bilinear and trilinear $S-N$ curves. Some other proposed models do not require material testing and overcome the shortcomings of Miner's rule, using load interaction factors [66-68]. However, both the damage evolution curves, and the fatigue life predictions differ from experimental results, as will be shown later. A one-parameter fatigue damage model has also been proposed, based on the concept of iso-damage curves [69]. As mentioned in the discussion of this paper, the model is based on $S-N$ curves with a constant slope and is difficult to apply with bilinear or trilinear $S-N$ curves in the current codes and standards. Also, verification of model parameter b is required for structural steel.

Many other uniaxial fatigue damage models exist in the literature, based on the concepts of continuum damage mechanics, energy conservation and entropy change [70,71]. Again, these models depend on material parameters and cannot be applied for structural detail categories. Infact, most of the above-mentioned damage models cannot be used for fatigue assessment of structural detail categories, due to their dependence on material parameters. As a result, these models cannot be applied together with code-given $S-N$ curves for fatigue life assessment of offshore structures using nominal or hot-spot approaches.

3. Research gaps in available multiaxial fatigue damage models

Several criteria have been proposed in the past to capture the multiaxial stress state and can be broadly classified into four categories: (a) stress-

based criteria, (b) strain-based criteria, (c) energy-based criteria, and (d) fracture mechanics-based criteria [72]. While the stress-based criteria are suitable for high-cycle fatigue regime (where the major part of the lifetime is spent during the crack initiation stage) and strain-based criteria for low-cycle fatigue regime (where crack propagation takes a much larger amount of the overall fatigue lifetime), the energy-based criteria can be adopted for both these regimes [73-76]. Even though the strain energy is a scalar quantity, such a damage parameter can be used to evaluate the orientation of crack initiation and propagation, as is proved in Ref.[76]. However, energy criteria based on the SWT (Smith-Watson-Topper) parameter can lead to some uncertainty, since the cycles are extracted from the shear direction. This might result in scattering of results, as is reported in Ref.[76].

The critical plane-based approach is often recommended, providing high accuracy in the fatigue assessment of engineering components [77]. Strain energy-based criteria employing the critical plane concept have recently been proposed [78,79]. Towards the end of the 20th century, mesoscopic scale (grain scale) fatigue damage theories were developed, wherein some grains undergo local plasticity while the rest of the matrix behaves elastically [80-82]. Mesoscopic scale criteria were also used in conjunction with the critical plane-based approach and energy criteria [83,84]. Although these criteria yield good results, their application by practising engineers is still a challenge, since determination of the model parameters requires a complex error optimization process.

The stress-based criteria can be further categorized, based on the type of stress: empirical equivalent stress, stress invariants, average stress, and critical plane stress [85]. The earliest works included the classical yield theories of Lamé and Tresca, as well as the von Mises criterion, based on equivalent stress formulations [86]. Thereafter, several other formulations of equivalent stress were proposed, followed by criteria based on stress-invariants and averaged stress [87-91]. Although these

approaches give us unsatisfactory results, especially under non-proportional loading, the von Mises criterion is still widely used.

Towards the beginning of the 21st century, Carpinteri and co-workers proposed a multiaxial fatigue criterion, based on the critical plane approach, for the assessment of structural components under multiaxial constant amplitude cyclic loadings [92-95]. This criterion requires the determination of a critical plane orientation, followed by an equivalent stress evaluation performed on such a plane. It is noted that the critical plane may or may not be coincident with the fatigue fracture plane. In more detail, the evaluation of the critical plane orientation, according to the Carpinteri et al. criterion, is performed in two stages: first, averaged principle stress directions at the material verification point are computed; then, the normal to the critical plane, defined by means of an off-angle is estimated. Such an off-angle is a material characteristic, depending only on the fatigue strength ratio $\sigma_{af,-1}/\tau_{af,-1}$ of the material, being $\sigma_{af,-1}$ and $\tau_{af,-1}$, the fatigue strengths under fully-reversed normal stress and shear stress, respectively.

Several off-angle expressions have been proposed in the literature, the original one being a non-linear expression by Carpinteri et al. [91]. This expression can only be employed for materials with a fatigue strength ratio in the range from $1/\sqrt{3}$ to 1. Subsequently, some relationships have been presented by Walat et al. in 2014 [96]. Recently, in 2017, Carpinteri et al. proposed another off-angle expression [97]. Although such an expression provides more accurate fatigue lifetime results than those determined by using the original one, there are still slight deviations from the experimental results. Moreover, the expression does not exactly meet the boundary conditions for both elastic-brittle and elastic-plastic materials.

1.4 Objectives

Based on the problem statements and the identified research gaps, the main objectives of this thesis are to propose a conceptual framework and fatigue damage models for life assessment/life extension of offshore structures. These objectives are mentioned below in detail.

1. Propose a conceptual framework for structural integrity assessment and life extension of offshore structures.
2. Propose an accurate uniaxial fatigue damage model for a better estimation of fatigue life. The proposed model should not require material parameters other than the code-given $S-N$ curves and can be used together with nominal and hot-spot approaches.
3. Propose an expression of the off-angle, to obtain accurate multiaxial fatigue damage based on the critical plane approach. The proposed expression should be able to predict fatigue life of ageing offshore structures more accurately, using the notch stress approach.

1.5 Overview of the thesis

The thesis is organized in two parts. Part I is a summary of the thesis and briefly presents the introduction, research outcomes and conclusions. Chapter 2 briefly outlines the main research outcomes in the study. Chapter 3 presents the conclusions and suggestions for future research. Part II of the thesis is comprised of journal and conference articles published based on the outcomes of this study.

Chapter 2 Research Outcomes

The research was carried out to fulfil the identified research gaps, and the outcomes were published in international journals. The research results were also presented in international conferences and published in the conference proceedings. The present thesis is based on these published journals and conference proceedings, which also form the research outcomes from this study. These are listed below and are also included in the thesis. The research gaps and corresponding research outcomes are further summarized in Figure 1.

The research outcomes were published in the following papers :

Paper I (Conference paper) – Life extension of ageing offshore structures: Time dependent corrosion degradation and health monitoring.

Paper II (Conference paper) – Life extension of ageing offshore structures: A framework for remaining life estimation.

Paper III (Journal paper) – A framework to assess structural integrity of ageing offshore jacket structures for life extension.

Paper IV (Journal paper) – A new nonlinear fatigue damage model based only on S-N curve parameters.

Paper V (Conference paper) – An accurate fatigue damage model for welded joints subjected to variable amplitude loading.

Paper VI (Journal paper) – A nonlinear fatigue damage model: Comparison with experimental damage evolution of S355 (SAE 1020) structural steel and application to offshore jacket structures.

Paper VII (Journal paper) – Novel non-linear relationship to evaluate the critical plane orientation.

Research Gap 1	Research Gap 2	Research Gap 3
<p>Paper I Material degradation and SHM (ISOPE 2016)</p>	<p>Paper IV Proposed uniaxial fatigue damage model (International Journal of Fatigue 2017)</p>	<p>Paper VII Proposed multiaxial fatigue damage model (International Journal of Fatigue 2019)</p>
<p>Paper II Proposed conceptual framework (OMAE 2017)</p>	<p>Paper V Model application to welded joints (COTech 2017)</p>	
<p>Paper III Proposed conceptual framework and its applications (Marine Structures 2017)</p>	<p>Paper VI Model application to jacket structure (International Journal of Fatigue 2019)</p>	

Figure 1 Research gaps and corresponding outcomes from this thesis

2.1 Proposed framework for structural integrity assessment

A conceptual framework to assess structural integrity of ageing offshore jacket structures for life extension is proposed in Paper II [98] and Paper III [99]. A background for this work is also presented in Paper I [100].

2.1.1 Proposed conceptual framework

The proposed framework provides concepts, theories and guidelines for a more accurate estimation of remaining life. It provides recommendations on various issues, such as simulation of time-dependent structural degradation, precision of loading history, effect of localized corrosion on stress concentration factors, selection of proper fatigue strength curves, determination of stress cycles and planning for mitigation and strengthening. Recently suggested, more precise fatigue damage theory is also included in the proposed framework. Recommendations are also made on strengthening mitigations and inspection/maintenance plans during the extended life. The proposed framework can be used for both deterministic and probabilistic analysis approaches. While the deterministic approach requires the use of design values (mean plus two standard deviation) of the parameters in the proposed framework, the probabilistic approach involves the use of a distribution function for each of these parameters. These distribution functions can be imported in simulation tools employing the probabilistic finite element method, and hence the failure probability of the structure can be determined. The use of such probabilistic tools can be computationally demanding for complex structures.

The framework is divided into five blocks, Blocks A to E. A brief outline of various fatigue assessment approaches is presented with recommendations for selecting a suitable approach in Block A. Recommendations are made on the simulation of structural degradation and past loadings in the available finite element models in Blocks B and C. Guidelines on the selection of the proper fatigue strength curve for the selected detail are also included, followed by damage calculations using Miner's rule and the recently developed damage theories in Block D. Remaining life is estimated at the end, and recommendations are made on possible strengthening mitigations in Block E. These blocks are shown in Figures 2 to 4. More details can be found in the published article [99].

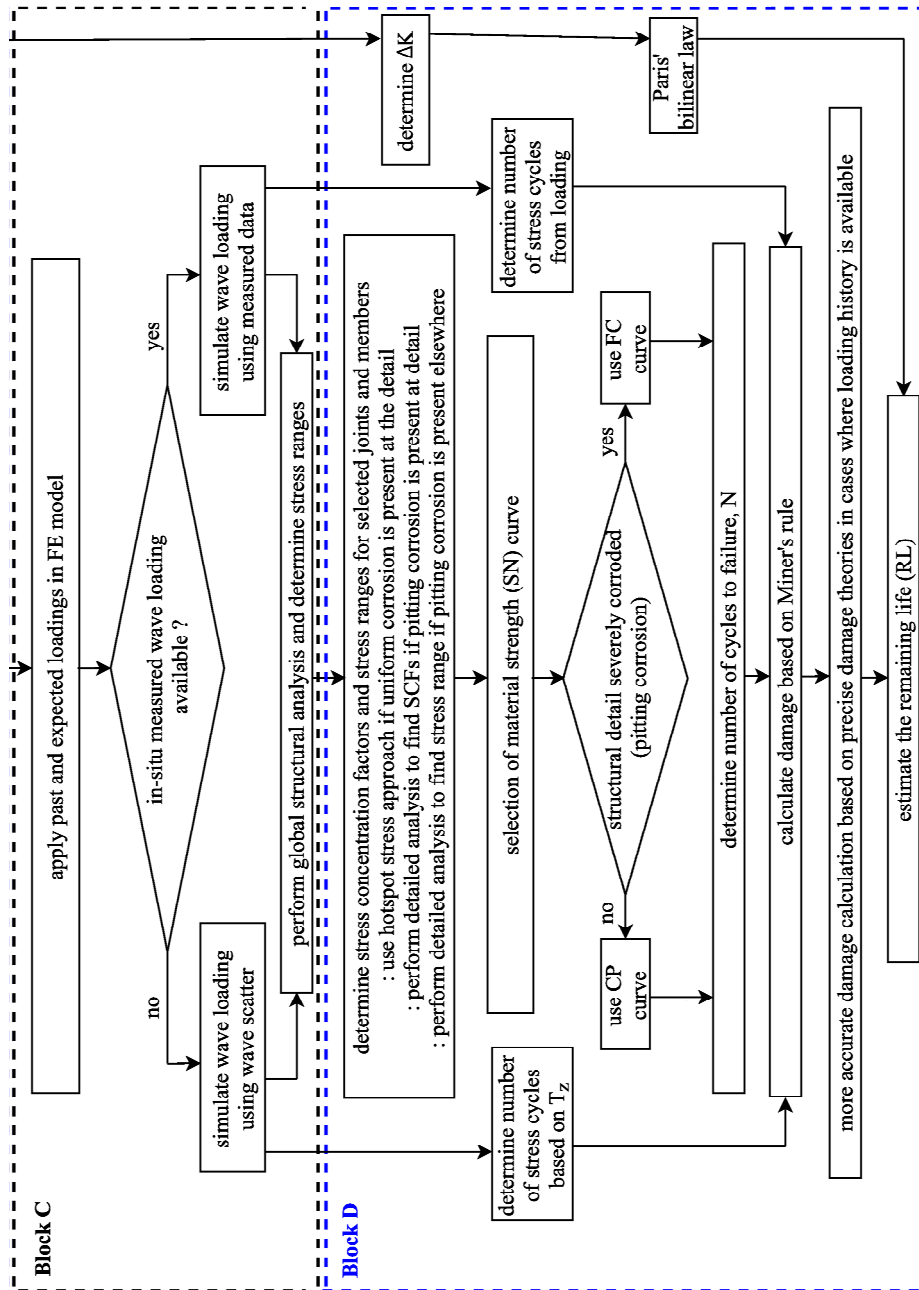


Figure 3 Block C and Block D of the proposed framework [99]

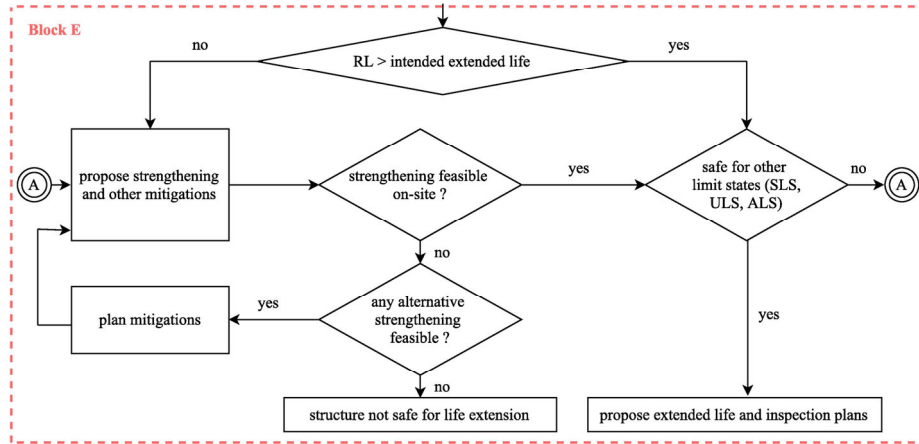


Figure 4 Block E of the proposed framework [99]

2.1.2 Application of proposed framework

The proposed framework is applied to a case study performed on an old existing jacket type of platform. The jacket is assessed for its structural integrity, and its remaining life is estimated using the proposed framework. The obtained assessment results are compared with conventional assessment approaches for several joints. The remaining life of one of the joints in the splash zone is found to be one year using the conventional approach, compared to ten years using the proposed framework. Recommendations are also made to increase the fatigue life of these joints in the splash zone, by means of fatigue improvement techniques. Hence, the significance of the proposed framework is confirmed. More details can be found in the published article [99].

2.2 Proposed uniaxial fatigue damage model

A new and easy-to-apply fatigue damage model is proposed and published in Paper IV [101]. The applications of the proposed model to welded joints and jacket structure are shown in Paper V [102] and Paper VI [103], respectively. The proposed model does not require any material parameters and depends only on commonly available $S-N$ curves. The

model can be applied to several engineering applications by practising engineers using the $S-N$ curves in design codes and standards.

2.2.1 Proposed damage index

A new damage index is proposed, as shown in Eq. (1). The fatigue damage, D , can be represented by the absolute value of proposed D_i , as shown in Eq. (2).

$$D_i = 1 - \left[1 - \frac{n_i}{N_i}\right]^{\delta_i} \quad (1)$$

$$D = Abs(D_i) \quad (2)$$

where n_i is the number of cycles for stress amplitude (or range) σ_i , N_i is the corresponding number of cycles to failure, which can be obtained from the $S-N$ curve, and Abs represents the absolute value. The model parameter δ_i can be determined using $S-N$ curve and is given in Eq. (3).

$$\delta_i = \frac{-1.25}{\ln N_i} \quad (3)$$

2.2.2 Proposed damage transfer concept

A new damage transfer concept is proposed for a more reliable estimation of the fatigue life. This concept is based on the use of fatigue damage evolution curves and a proposed load interaction factor. The proposed interaction factor is given by Eq. (4).

$$\mu_{i+1} = \left(\frac{\sigma_i}{\sigma_{i+1}}\right)^2 \quad (4)$$

where σ_i and σ_{i+1} are the two adjoining stress levels, and μ_{i+1} represents the load interaction between these stress levels. Suppose a material is subjected to a certain stress amplitude (or range) σ_i , for n_i number of cycles at load level i . The number of cycles to failure for this stress state

is N_i and can be determined from the $S-N$ curve of the material. The fatigue damage from this stress range can be determined using the proposed damage model and can be written as shown in Eq. (1).

In the proposed damage transfer concept, it is required to transfer the same damage to the next stress amplitude (or range) σ_{i+1} , using the proposed load interaction factor, μ_i . By doing so, the effective number of cycles $n_{(i+1), eff}$ can be determined, corresponding to the stress range σ_{i+1} , using Eq. (5) and Eq. (6).

$$D_i = 1 - \left[1 - \frac{n_{(i+1), eff}}{N_{i+1}} \right]^{\frac{\delta_{i+1}}{\mu_{i+1}}} \quad (5)$$

$$n_{(i+1), eff} = \left[1 - (1 - D_i)^{\frac{\mu_{i+1}}{\delta_{i+1}}} \right] \cdot N_{i+1} \quad (6)$$

Considering n_{i+1} as the number of cycles for stress state σ_{i+1} , the total number of cycles for loading step $i+1$ can be written using Eq. (7):

$$n_{(i+1), total} = n_{(i+1), eff} + n_{(i+1)} \quad (7)$$

Subsequently, the cumulative damage at loading step $i+1$ is written as:

$$D_{i+1} = 1 - \left[1 - \frac{n_{(i+1), total}}{N_{i+1}} \right]^{\delta_{i+1}} \quad (8)$$

The corresponding fatigue damage can be determined using Eq. (9):

$$D = Abs (D_{i+1}) \quad (9)$$

This damage transfer technique is continued until the fatigue damage D becomes one, denoting fatigue failure. The damage transfer concept is explained using a simple flowchart in Figure 5 and more details can be found in the published article [101].

Research Outcomes

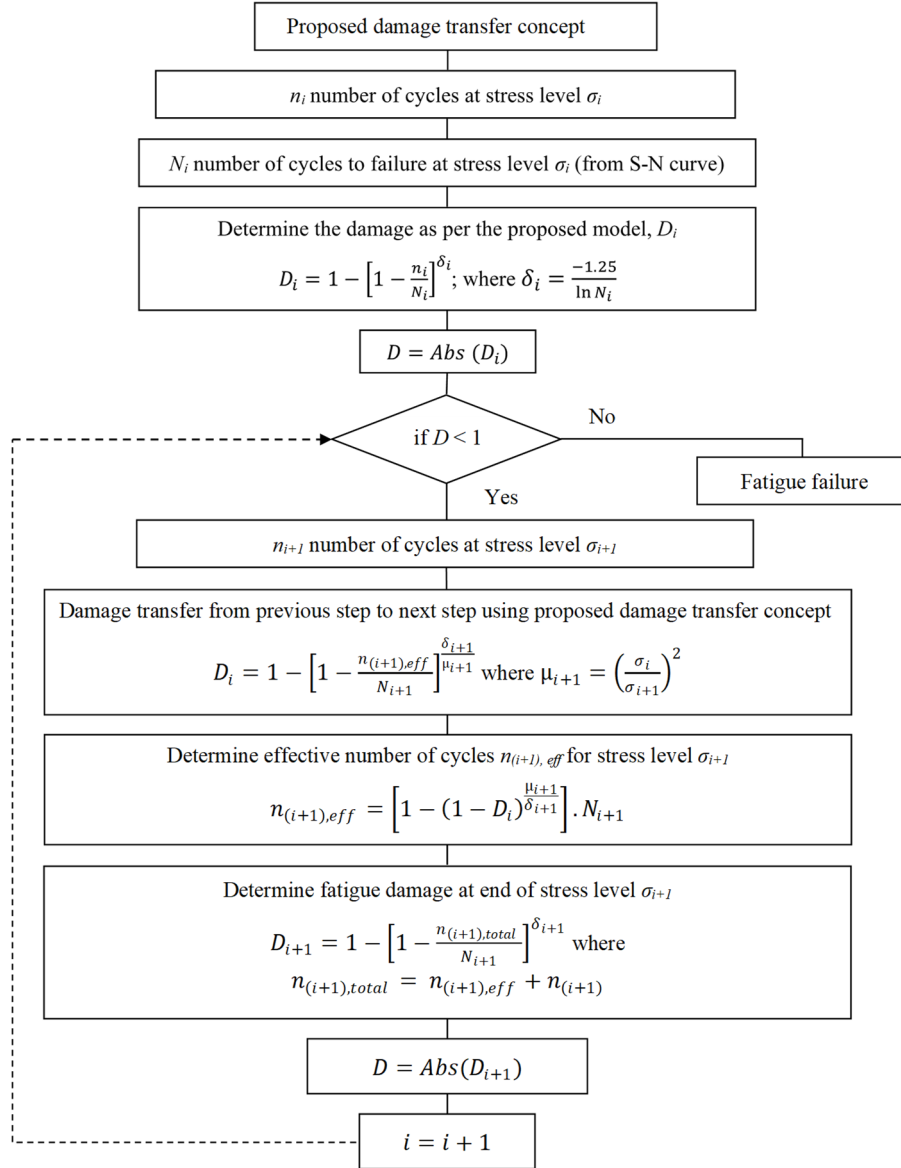


Figure 5 Flow chart of the proposed damage transfer concept [101]

2.2.3 Verification of proposed model with experimental data

The proposed model is verified with experimental data for both the damage curves and fatigue life estimations of several materials. The model is firstly verified by comparing the experimental results for damage evolution curves. The verification is shown for C 45 and 16 Mn steels, and the results can be found in Paper IV [101]. Verification is also shown for S355 structural steel, and the results can be found in Paper VI [103].

The model is also verified with the experimental fatigue lives of several materials, using a new damage transfer concept to estimate fatigue life. The proposed damage model and the associated damage transfer concept are applied to predict the fatigue life of several materials subjected to multilevel block loadings. The results are compared with experimentally obtained fatigue lives to demonstrate the accuracy of the proposed model. The fatigue lives predicted by the proposed model are also compared with those predicted by other models. The verification is performed for six materials that are selected based on their practical applicability to the structural engineering field. More details and results can be found in Paper IV [101].

2.2.4 Application of proposed model to welded joints

The proposed model is applied to butt, and fillet welded joints and the results are shown in Paper V [102]. These joints are subjected to block loading and variable amplitude loadings. These welded joints are used in several engineering applications, such as vehicles, electrical mobile units (EMUs), etc., and an accurate prediction of life is necessary for the safety of both passengers and vehicles [104, 105]. The proposed model is firstly applied to these joints under the given block loading conditions, and predicted lives are compared with experimental results. The applicability and the accuracy of the proposed model under block conditions are henceforth confirmed. The application of the proposed model is also shown on these welded joints subjected to random variable amplitude

loadings (VAL). The fatigue life of these joints is predicted using the proposed model. The lives are also predicted using Miner's rule, recommended by standard codes and standards such as Eurocode. The detail category $S-N$ curves for the joints are taken from the Eurocode. The cycle counting is performed using the rainflow counting method. Finally, the damage accumulation curves are obtained, and fatigue lives from the proposed model are compared with those obtained using Miner's rule. More details and results can be found in Paper V [102].

2.2.5 Application of proposed model to jacket structure

The proposed model is applied to a bottom-fixed offshore jacket structure, and fatigue damage is estimated for one of the joints. The damage is also computed using the conventional approach, and results are compared. All results are presented in Paper VI [103]. The considered platform is supported on an 8-legged jacket structure installed in a water depth of 123 metres. The topsides and jacket weights are 23,600 tons and 17,400 tons, respectively. The structure is modelled in Sesam GeniE software [106]. The hydrodynamic parameters for jacket members are considered as per the design basis of the structure and the NORSOK standard [107]. A time-domain fatigue analysis is performed for one of the joints of the jacket structure for the selected waves, as per design basis. The fatigue damage is evaluated for one of the joints, using the hot-spot stress approach.

There are significant deviations between the fatigue damage predicted using the proposed model and using a conventional approach. The predicted damage is almost seven times less than that predicted using Miner's rule after 25 years' lifetime. However, the damage using the proposed model is more than three times less than that using Miner's rule at the end of 40 years. These observations in the damage deviations confirm the nonlinear behaviour of fatigue damage evolution in the material and structure. More details and results can be found in the

published article [103]. Hence, the applicability and significance of the proposed model has been established.

2.3 Proposed multiaxial fatigue damage model

The multiaxial fatigue criteria based on the critical plane approach is further improved. The critical plane approach proposed by Carpinteri et al. requires determination of critical plane orientation, using an off-angle. A novel relationship to estimate the critical plane orientation is proposed and published in Paper VII [108].

2.3.1 Proposed relationship

A novel relationship to compute the off-angle is proposed, to improve fatigue life estimation deduced through the Carpinteri et al. criterion. The proposed relationship is given in Eq. (10). It can be used for a more accurate estimation of the off-angle and thereby of the critical plane orientation. Subsequently, better fatigue life estimations are obtained under multiaxial loading conditions. Such a relationship is implemented in the stress-based critical plane criterion by Carpinteri et al., which is applicable to any material under multiaxial constant amplitude fatigue loading. The proposed expression has three parameters, governing the peak value, slope and inflection point of the curve, respectively. A parametric study is also performed to analyse the influence of each of these parameters on the shape of the proposed curve. More details can be found in the published article [108].

$$\beta \left(\frac{\sigma_{af,-1}}{\tau_{af,-1}} \right) = \frac{a}{1 + e^{-b[(\sigma_{af,-1}/\tau_{af,-1}) - c]}} \quad (10)$$

where ratio $\sigma_{af,-1}/\tau_{af,-1}$ is the fatigue strength ratio, and a b c are the parameters.

2.3.2 Verification with experimental data

The proposed expression of the off-angle is verified with the experimental fatigue lives of several materials subjected to biaxial loading conditions. The considered materials are six type of steels (D30, 982FA, SM45C, SUS304, 10HNAP and 30CrNiMo8), three types of cast iron (GGG40, GTS45 and IC2), brass (CuZn40Pb2) and aluminium alloy (PA4 or 6082-T6). All the specimens are smooth, and the loading data is taken from other researchers. The fatigue strengths under both normal and torsion loading are also known, together with the corresponding loading cycle numbers N_0 and N_0^* , respectively. The fatigue life for each test carried out on these materials has been computed by employing both the novel relationship and the original off-angle expression; such results have then been compared with the experimental fatigue life. These results can be found in the published article [108].

Chapter 3 Summary and Conclusions

3.1 Summary

In the present thesis, a detailed study of the life extension of offshore structures is carried out, and a conceptual framework and, fatigue damage models are proposed for remaining life estimation of ageing offshore structures. The main motivation for this study was the ageing problems in offshore structures, with more than 50% of these structures worldwide operating beyond their design lives. The replacement of these structures at once is technically challenging, as well as expensive. Moreover, falling profit margins due to low oil prices, uneconomical small field discoveries and plenty of remaining oil reserves in existing fields are encouraging factors for more life extension studies.

Ageing is mainly characterized by fatigue and corrosion among others. Although much research has been carried out on understanding these ageing processes, especially over the last two decades, failure has occurred and is still occurring in offshore structures. A literature review was initially carried out, and research problems/research gaps were formulated for the study. It was found that there is a need for more detailed assessment guidelines, giving concepts and recommendations on the simulation of structural degradation, simulation of loading history, selection of fatigue strength curves for corroded structural detail categories and on the use of more accurate uniaxial and multiaxial fatigue damage theories.

A conceptual framework to assess the structural integrity of ageing offshore jacket structures for life extension is proposed. The proposed framework not only overcomes the shortcomings in the currently available guidelines but also includes recent research proposals available in the literature. The framework provides concepts, theories and guidelines for a more accurate estimation of remaining life. It provides

Summary and Conclusions

recommendations on various issues, such as simulation of time-dependent structural degradation, precision of loading history, effect of localized corrosion on stress concentration factors, selection of proper fatigue strength curves, determination of stress cycles and planning for mitigation and strengthening. Recently suggested, more precise fatigue damage theory is also included in the proposed framework. Recommendations are also made on strengthening mitigations and inspection/maintenance plans during the extended life. The application of the proposed framework to an existing jacket type platform is shown. The jacket is assessed for its structural integrity, and its remaining life is estimated. Hence, the significance of the proposed framework is confirmed.

A new uniaxial fatigue damage model is also proposed. It can be used for accurate remaining life prediction of ageing offshore structures, using nominal and hot-spot approaches and code-given $S-N$ curves. The proposed model does not require additional material parameters and depends only on commonly available $S-N$ curves. It can be applied to several engineering applications by practising engineers, using the $S-N$ curves given in design codes and standards. The proposed model is verified with experimental data for both the damage curves and fatigue life estimations of several materials. Application of the proposed model to welded joints and to an existing aged platform structure is also shown.

A novel expression of the off-angle is also proposed, to improve critical plane approach based multiaxial fatigue damage theories. This damage model can be used for better fatigue life predictions, using the notch stress approach. The new expression depends only on the fatigue strength ratio of the material and can be used for more accurate determination of the critical plane. This leads to better fatigue life estimations under multiaxial loading conditions, using Carpinteri et al. criterion, together with the proposed expression. The proposed expression is applied to several material tests under biaxial loading conditions, and the results are

compared with those obtained using an earlier expression of the off-angle.

3.2 Concluding remarks

The following concluding remarks are made, based on the outcomes of this study.

1. A conceptual framework is proposed, to assess the structural integrity of existing aged offshore structures for possible life extension. The significance of the proposed framework is highlighted through a case study on an existing jacket structure. The framework is an attempt to provide more detailed case-dependent guidelines, by adding relevant theories and models, which can capture the time-dependent structural degradation more precisely than currently available assessment guidelines and standards. It caters to the needs of practising engineers, by providing recommendations on various issues such as simulation of structural degradation in the absence of any corrosion measurements, precision of loading history, as well as the effect of localized corrosion on stress concentration factors. Suggestions are also made on the determination of stress cycles and the selection of a suitable fatigue strength curve, particularly for severely corroded details. Recently developed fatigue damage theories are also included for more accurate estimation of remaining life.

The simulation of structural degradation using the proposed framework is compared with the conventional approach, through the case study. Conventionally, either structural degradation is not modelled for cases of mild corrosion or model parameters are taken on the conservative side to represent patch corrosion. The model parameters recommended in the proposed framework constitute an attempt to reduce such variability in the selection of

Summary and Conclusions

model parameters. The remaining fatigue life of critical joints is found more accurately, using the proposed framework approach, as compared to the conventional approach. The structure can also be assessed for other limit states, using the framework. Strengthening/inspection plans for extended life are also recommended. It can be concluded that the proposed framework provides an accurate prediction of remaining life, and the framework is a currently required tool to assess the structural integrity of an ageing jacket structure for possible life extension.

2. A new uniaxial fatigue damage model is proposed. The proposed damage model can be used for accurate remaining life prediction of ageing offshore structures, using nominal and hot-spot approaches and code-given $S-N$ curves. The proposed model does not require any material parameters, other than the commonly available $S-N$ curve parameters, which are generally used with Miner's rule. The major advantage of the proposed model is that it does not require extensive material testing or modifications to the $S-N$ curve. Also, unlike earlier models, the proposed model can be applied to design detail categories, using the corresponding partially known $S-N$ curve in the design standards. Therefore, the proposed model can be easily implemented by practising engineers for fatigue analysis of several engineering problems. The model is verified with both the damage evolution curves and fatigue life estimations. It is concluded that the damage curves plotted using the proposed model are in good agreement with the available experimental data for the considered materials, including S355 structural steel. The model is further verified with fatigue life predictions under two-level and multilevel block loading for six materials. It is concluded that, using the proposed model, the life predictions are better than those from the widely used Miner's rule, as well as those from some of the recently developed models.

Summary and Conclusions

The applicability, validity and significance of the proposed model is also highlighted, by comparing its predicted fatigue lives with the experimentally observed fatigue lives of welded joints used in several engineering applications. The predicted fatigue lives of these joints are found to be in good agreement with the experimental results under block loadings. Results are also obtained for these joints subjected to variable amplitude loadings. Significant differences between the fatigue lives calculated by both the proposed model and Miner's rule underline the significance of having accurate fatigue damage models for structural detail categories. Finally, application is also shown to an offshore jacket structure. The fatigue damage in one of the joints is evaluated using the proposed approach and results are also compared with the conventional approach. It is concluded that the proposed model leads to a more accurate prediction of damage and also confirms the nonlinear behaviour of fatigue damage evolution in the material and structure. It is concluded that the proposed model can therefore be used for better fatigue life predictions and can be applied by practising engineers using only the code-given $S-N$ curves.

3. A novel off-angle relationship to evaluate the critical plane orientation is proposed, to improve multiaxial fatigue damage theories. This damage model can be used for better fatigue life predictions, using the notch stress approach. The proposed relationship is used in conjunction with Carpinteri et al. criterion, to improve the accuracy in fatigue life estimation of any material under multiaxial constant amplitude fatigue loading. Several tests on materials under biaxial loading are available in the literature. The fatigue life for each test examined has been computed by employing both the novel relationship and the original off-angle expression, and then such results have been compared with the experimental fatigue life. A good agreement has been observed

between experimental data and theoretical life estimations when the novel relationship is used, since the mean square error is equal to about 2, while such an error is equal to about 3 when the original expression is adopted.

It is concluded that the novel relationship, used together with the Carpinteri et al. criterion, is a useful tool to obtain life estimations for any material under multiaxial loading. Such a relationship should be further assessed in the case of both different materials and different loadings.

3.3 Suggestions for future work

The limitations of the current study and identified suggestions for future work are mentioned below.

1. The proposed framework considers only the functional ageing characterized by fatigue and corrosion. Other aspects such as erosion, creep, and accumulated plastic deformation have not been considered. Moreover, technological ageing, knowledge-based ageing and organizational should also be considered wherever applicable. The significance of the proposed framework should be further highlighted using a few more case studies. Thereafter, the proposed framework and given model parameters may be adopted in the assessment standards in future.
2. The proposed uniaxial and multiaxial models have been verified for several materials, including S355 structural steel. The applicability, significance and validity of these damage models can be further verified through more case studies in the future. Thereafter, the proposed models may be adopted in the design standards in future for a more accurate estimation of fatigue life.

References

- [1] Ersdal, G. (2005) Assessment of existing offshore structures for life extension. Doctoral thesis, University of Stavanger, Norway.
- [2] Stacey, A., Birkinshaw, M., & Sharp, J. V. (2008) Life extension issues for ageing offshore installations. Proceedings of the 27th International Conference on Offshore Mechanics and Arctic Engineering, Estoril, Portugal.
- [3] Zettlemyer, N. (2010) Life extension of fixed platforms. Tubular Structures XIII, 3–13.
- [4] Ersdal, G., Sharp, J. V., & Galbraith, D. (2014) Ageing accidents – suggestions for a definition and examples from damaged platforms. Proceedings of the 33rd International Conference on Offshore Mechanics and Arctic Engineering, San Francisco, California.
- [5] Ersdal, G., Sharp, J. V., & Stacey, A. (2019) Ageing and life extension of offshore structures. Wiley, UK.
- [6] Stacey, A., & Sharp, J. V. (2011) Ageing and life extension considerations in the integrity management of fixed and mobile offshore installations. Proceedings of the 30th International Conference on Ocean, Offshore and Arctic Engineering, Rotterdam, The Netherlands.
- [7] Rusell, J., & Keith, I. (2014) The challenges of extending the life of UK offshore installations. International Petroleum Technology Conference, Doha, Qatar.
- [8] Nezamian, A., & Iqbal, K. (2015) Requalification and extension of service life and integrity requirements for offshore structures in Middle East. International Petroleum Technology Conference, Doha, Qatar.
- [9] Osmundsen, P., & Tveteras, R. (2003) Decommissioning of petroleum installations—major policy issues. *Energy Policy*, 31(15), 1579–1588.
- [10]. Alveberg, L. J., & Melberg, V. E. (2013) Facts 2013 Norwegian petroleum sector. Report by the Ministry of Petroleum and the

References

Norwegian Petroleum Directorate, Publication number: Y-0103/14 E, ISSN 1502–5446.

[11] Hornlund, E., Ersdal, G., Hinderaker, H. R., Johnsen, R., & Sharp, J. V. (2011) Material issues in ageing and life extension. Proceedings of the 30th International Conference on Ocean, Offshore and Arctic Engineering, Rotterdam, The Netherlands.

[12] Stacey, A., & Sharp, J. V. (2007) Safety factor requirements for the offshore industry. *Engineering Failure Analysis*, 14(3), 442–258.

[13] Garbatov, Y., Soares, C. G., Parunov, J., & Kodvanj, J. (2014) Tensile strength assessment of corroded small-scale specimens. *Corrosion Science*, 85, 296–303.

[14] Popoola, L. T., Grema, A. S., Latinwo, G. K., Gutti, B., & Balogun, A. S. (2013) Corrosion problems during oil and gas production and its mitigation. *International Journal of Industrial Chemistry*, 4(1), 4–35.

[15] Adasooriya, N. D., & Siriwardane, S. (2014) Remaining fatigue life estimation of corroded bridge members. *Fatigue and Fracture of Engineering Material and Structures*, 37(6), 603–622.

[16] Zhang, W., & Yuan, H. (2014) Corrosion fatigue effects on life estimation of deteriorated bridges under vehicle impacts. *Engineering Structures*, 71, 128–136.

[17] Dong, W., Moan, T., & Gao, Z. (2012) Fatigue reliability analysis of the jacket support structure for offshore wind turbine considering the effect of corrosion and inspection. *Reliability Engineering & System Safety*, 106, 11–27.

[18] Det Norske Veritas (2010) Cathodic protection design. DNV-RP-B401, October 2010.

[19] Moan, T. (2007) Accidents and near-misses in the offshore oil and gas industry – how and why. Norsk Offshore Day, Oslo.

[20] Haagenen, P. J. (1997) Fatigue of tubular joints and fatigue improvement methods. *Progress in Structural Engineering and Materials*, 1, 96–106.

[21] Almar-Naess, A. (1985) *Fatigue handbook*. Tapir Publishers, Trondheim, Norway.

References

- [22] Lotsberg, I. (2016) Fatigue design of marine structures. Cambridge University Press, Cambridge.
- [23] Kuhn, B., & Lukic, M. (2007) Assessment of existing steel structures: Recommendations for estimation of remaining fatigue life. JRC technical report.
- [24] Almar-Naess, A. A., Haagenen, P. J., Lian, B. B., Moan, T. T., & Simonsen, T. T. (1984) Investigation of the Alexander L. Kielland failure—metallurgical and fracture analysis. ASME. Journal of Energy Resources Technology, 106(1), 24–31.
- [25] Moan, T. (2007) Accidents and near-misses in the offshore oil and gas industry -how and why. Norsk Offshore Day, Oslo.
- [26] Moan, T. (2005) Reliability-based management of inspection, maintenance and repair of offshore structures. Structure and Infrastructure Engineering, 1(1), 33–62.
- [27] Miner, M. A. (1945) Cumulative damage in fatigue. Journal of Applied Mechanics, A-159–64.
- [28] Eurocode 3 (2010) Design of steel structures – Part 1-9: Fatigue, NS-EN 1993-1-9:2005 +NA:2010, 2010.
- [29] Det Norske Veritas (2016) Fatigue design of offshore steel structures; 2016. DNVGL-RP-C203, 2016.
- [30] Suresh, S. (1998) Fatigue of materials. Cambridge University Press, Cambridge, UK.
- [31] Mesmacque, G., Garcia, S., Amrouche, A., & Rubio-Gonzalez, C. (2005) Sequential law in multiaxial fatigue, a new damage indicator. International Journal of Fatigue, 27(4), 461–7.
- [32] Saini, D. S., Karmakar, D., & Ray-Chaudhuri, S. (2016) A review of stress concentration factors in tubular and non-tubular joints for design of offshore installations. Journal of Ocean Engineering and Science, 1, 186–202.
- [33] Det Norske Veritas (2015) Probabilistic methods for planning of inspection for fatigue cracks in offshore structures. DNVGL-RP-0001, May 2015.

References

- [34] Stacey, A., & Birkinshaw, W. (2008) Initiatives on structural integrity management of ageing North Sea installations. Proceedings of the 27th International Conference on Offshore Mechanics and Arctic Engineering, Estoril, Portugal.
- [35] Stacey, A. (2011) KP4: Ageing and life extension inspection programme for offshore installations. Proceedings of the 30th International Conference on Ocean, Offshore and Arctic Engineering, Rotterdam, The Netherlands.
- [36] H.S.E. (2012) Key Programme 4 (KP4) Ageing and life extension. An interim report by the offshore division of HSE's Hazardous Installations Directorate, UK.
- [37] Ersdal, G., & Selnes, P. O. (2010) Life extension of ageing petroleum facilities offshore. Society of Petroleum Engineers International Conference, Rio de Janeiro, Brazil.
- [38] Ersdal, G., & Hornlund, E. (2008) Assessment of offshore structures for life extension. Proceedings of the 27th International Conference on Offshore Mechanics and Arctic Engineering, Estoril, Portugal.
- [39] Selnes, P. O., & Ersdal, G. (2011) Industry developed guidelines and standards for ageing and life extension. Proceedings of the 30th International Conference on Ocean, Offshore and Arctic Engineering, Rotterdam, The Netherlands.
- [40] American Petroleum Institute (2000) Recommended practice for planning, design and constructing fixed offshore platforms—working stress design. API RP 2A-WSD, December 2000.
- [41] International Standards Organization (1996) General principles on reliability for structures. ISO 2394, December 1996.
- [42] International Standards Organization (2001) Bases for design of structures – Assessment of existing structures. ISO 13822, December 2001.
- [43] International Standards Organization (2002) Petroleum and natural gas industries – General requirements for offshore installations. ISO 19900, December 2002.

References

- [44] International Standards Organization (2007) Petroleum and natural gas industries – Offshore structures, fixed offshore structures. ISO 19902, December 2007.
- [45] H.S.E. (2009) Structural integrity management framework for fixed jacket structures. A report by Atkins Limited for the HSE, UK.
- [46] NORSOK Standard (2009) Assessment of structural integrity for existing offshore load-bearing structures. N-006, March 2009.
- [47] Norwegian Oil and Gas Association (2008) Recommended guidelines for the assessment and documentation of service life extension of facilities. OLF Guideline No. 122, June 2008.
- [48] American Petroleum Institute (2014) Recommended practice for the structural integrity management of fixed offshore structures. API RP2 SIM, November 2014.
- [49] Det Norske Veritas (2015) Probabilistic methods for planning of inspection for fatigue cracks in offshore structures. DNVGL-RP-C210, November 2015.
- [50] British Standard Institution (2013) Guide to methods for assessing the acceptability of flaws in metallic structures. BS 7910, December 2013.
- [51] JCSS (2001) Probabilistic Model Code. Published on the website <http://www.jcss.ethz.ch/JCSSPublications/PMC/PMC.html>.
- [52] Nezamian, A., & Altmann, J. (2013) An oil field structural integrity assessment for re-qualification and life extension. Proceedings of the 32nd International Conference on Ocean, Offshore and Arctic Engineering, Nantes, France.
- [53] Sharp, J. V., Terry, E. G., & Wintle, J. (2011) A framework for the management of ageing of safety critical elements offshore. Proceedings of the 30th International Conference on Ocean, Offshore and Arctic Engineering, Rotterdam, The Netherlands.
- [54] Liu, H., Shi, X., Chen, X., & Liu, Y. (2015) Management of life extension for topsides process system of offshore platforms in Chinese Bohai Bay. *Journal of Loss Prevention in the Process Industries*, 35, 357–365.

References

- [55] Marco, S. M., & Starkey, W. L. (1954) A concept of fatigue damage. *Transactions ASME* 7, 6, 626–62.
- [56] Hwang, W., & Han, K. S. (1986) Cumulative damage models and multi-stress fatigue life prediction. *Journal of Composite Materials*, 20(2), 125–53.
- [57] Manson, S. S., Freche, J. C., & Ensign, C. R. (1967) Application of a double linear damage rule to cumulative fatigue. *Fatigue Crack Propagation*, ASTM STP 415, 384–412.
- [58] Manson, S. S., & Halford, G. R. (1981) Practical implementation of the double linear damage rule and damage curve approach for treating cumulative fatigue damage. *International Journal of Fracture*, 7, 169–92.
- [59] Lemaitre, J., & Plumtree, A. (1979) Application of damage concepts to predict creep-fatigue failures. *Journal of Engineering Materials and Technology*, 101(3), 284–92.
- [60] Chaboche, J. L., & Lesne, P. M. (1988) A non-linear continuous fatigue damage model. *Fatigue & Fracture of Engineering Materials & Structures*, 11(1), 1–17.
- [61] Goodin, E., Kallmeyer, A., & Kurath, P. (2004) Evaluation of nonlinear cumulative damage models for assessing HCF/LCF interactions in multiaxial loadings. *Proceedings of the 9th National Turbine Engine High Cycle Fatigue (HCF) Conference*; 2004 March 16–19; Pinehurst, North Carolina, US.
- [62] Fatemi, A., & Yang, L. (1998) Cumulative fatigue damage and life prediction theories: a survey of the state of the art for homogeneous materials. *International Journal of Fatigue*, 20(1), 9–34.
- [63] Shang, D. G., & Yao, W. X. (1999) A nonlinear damage cumulative model for uniaxial fatigue. *International Journal of Fatigue*, 21(2), 187–94.
- [64] Pavlou, D. G. (2002) A phenomenological fatigue damage accumulation rule based on hardness increasing, for the 2024-T42 aluminum. *Engineering Structures*, 24(11), 1363–8.
- [65] Siriwardane, S., Ohga, M., Dissanayake, R., & Taniwaki, K. (2008) Application of new damage indicator-based sequential law for remaining

References

- fatigue life estimation of railway bridges. *Journal of Constructional Steel Research*, 64, 228–37.
- [66] Kwofie, S., & Rahbar, N. (2013) A fatigue driving stress approach to damage and life prediction under variable amplitude loading. *International Journal of Damage Mechanics*, 22(3), 393–404.
- [67] Liakat, M., & Khonsari, M. M. (2014) An experimental approach to estimate damage and remaining life of metals under uniaxial fatigue loading. *Materials & Design*, 57, 289–97.
- [68] Lv, Z., Huang, H. Z., Zhu, S. P., Gao, H., & Zuo, F. (2015) A modified nonlinear fatigue damage accumulation model. *International Journal of Damage Mechanics*, 24(2), 168–81.
- [69] Rege, K., & Pavlou, D. G. (2017) A one-parameter nonlinear fatigue damage accumulation model. *International Journal of Fatigue*, 98, 234–46.
- [70] Santecchia, E., Hamouda, A. M. S., Musharavati, F., Zalnezhad, E., Cabibbo, M., El Mehtedi, M., & Spigarelli, S. (2016) A review on fatigue life prediction methods for metals. *Advances in Materials Science and Engineering*, 9573524, 1–26.
- [71] Silitonga, S., Maljaars, J., Soetens, F., & Snijder, H. H. (2013) Survey on damage mechanics models for fatigue life prediction. *Heron*, 58(1), 25–60.
- [72] Wei, H., & Liu, Y. (2017) A critical plane-energy model for multiaxial fatigue life prediction. *Fatigue & Fracture of Engineering Materials & Structures*, 40, 1973–1983.
- [73] Zhu, S. P., Liu, Y., Liu, Q., & Yu, Z. Y. (2018) Strain energy gradient-based LCF life prediction of turbine discs using critical distance concept. *International Journal of Fatigue*, 113, 33–42.
- [74] Zhu, S. P., Yu, Z. Y., Liu, Q., & Ince, A. (2018) Strain energy-based multiaxial fatigue life prediction under normal/shear stress interaction. *International Journal of Damage Mechanics*, 28(5), 708–739.
- [75] Feng, E. S., Wang, X. G., & Jiang, C. (2019) A new multiaxial fatigue model for life prediction based on energy dissipation evaluation. *International Journal of Fatigue*, 122, 1–8.

References

- [76] Portugal, I., Olave, M., Urresti, I., Zurutuza, A., López, A., Muñiz-Calvente, M., & Fernández-Canteli, A. (2019) A comparative analysis of multiaxial fatigue models under random loading. *Engineering Structures*, 182, 112–122.
- [77] Zhu, S. P., Yu, Z. Y., Correia, J., De Jesus, A., & Berto, F. (2018) Evaluation and comparison of critical plane criteria for multiaxial fatigue analysis of ductile and brittle materials. *International Journal of Fatigue*, 112, 279–288.
- [78] Carpinteri, A., Berto, F., Campagnolo, A., Fortese, G., Ronchei, C., Scorza, D., & Vantadori, S. (2016) Fatigue assessment of notched specimens by means of a critical plane-based criterion and energy concepts. *Theoretical and Applied Fracture Mechanics*, 84, 57–63.
- [79] Lu, C., Melendez, J., & Martínez-Esnaola, J. M. (2018) Modelling multiaxial fatigue with a new combination of critical plane definition and energy-based criterion. *International Journal of Fatigue*, 108, 109–115.
- [80] Papadopoulos, I. V., Davoli, P., Gorla, C., Filippini, M., & Bernasconi, A. (1997) A comparative study of multiaxial high-cycle fatigue criteria for metals. *International Journal of Fatigue*, 19, 219–235.
- [81] Morel, F. (1998) A fatigue life prediction method based on a mesoscopic approach in constant amplitude multiaxial loading. *Fatigue & Fracture of Engineering Materials & Structures*, 21, 241–256.
- [82] Dang, Van K., Bignonnet, A., Fayard, J. L., & Janosch, J. J. (2001) Assessment of welded structures by a local multiaxial fatigue approach. *Fatigue & Fracture of Engineering Materials & Structures*, 24, 369–376.
- [83] Morel, F., Palin-Luc, T., & Froustey, C. (2001) Comparative study and link between mesoscopic and energetic approaches in high cycle multiaxial fatigue. *International Journal of Fatigue*, 23, 317–327.
- [84] Huyen, N., Flaceliere, L., & Morel, F. (2008) A critical plane fatigue model with coupled meso-plasticity and damage. *Fatigue & Fracture of Engineering Materials & Structures*, 31, 12–28.
- [85] Liu, Y., & Mahadevan, S. (2005) Multiaxial high-cycle fatigue criterion and life prediction for metals. *International Journal of Fatigue*, 27, 790–800.

References

- [86] von Mises, R. (1913) Mechanik der festen Körper im plastisch-deformablen Zustand. Nachrichten von der Gesellschaft der Wissenschaften zu Göttingen. Mathematisch-Physikalische Klasse, 582–592.
- [87] Gough, H. J., & Pollard, H. V. (1935) The strength of metals under combined alternating stresses. Proceedings of the Institution of Mechanical Engineers, 131, 3–18.
- [88] Crossland, B. (1956) Effect of large hydrostatic pressures on the torsional fatigue strength of an alloy steel. Proceedings of the International Conference on Fatigue of Metals, Institution of Mechanical Engineers, London, 184–194.
- [89] Papadopoulos, I. V. (2001) Long life fatigue under multiaxial loading. International Journal of Fatigue, 23, 839–849.
- [90] Li, B., & De Freitas, M. (2002) A procedure for fast evaluation of high-cycle fatigue under multiaxial random loading. Journal of Mechanical Design, 124, 558–563.
- [91] You, B. R., & Lee, S. B. (1996) A critical review on multiaxial fatigue assessments of metals. International Journal of Fatigue, 18, 235–244.
- [92] Carpinteri, A., & Spagnoli, A. (2001) Multiaxial high-cycle fatigue criterion for hard metals. International Journal of Fatigue, 23, 135–145.
- [93] Carpinteri, A., Spagnoli, A., & Vantadori, S. (2009) Multiaxial fatigue life estimation in welded joints using the critical plane approach. International Journal of Fatigue, 31, 188–196.
- [94] Carpinteri, A., Spagnoli, A., & Vantadori, S. (2011) Multiaxial fatigue assessment using a simplified critical plane-based criterion. International Journal of Fatigue, 33, 969–976.
- [95] Carpinteri, A., Spagnoli, A., Vantadori, S., & Bagni, C. (2013) Structural integrity assessment of metallic components under multiaxial fatigue: The C–S criterion and its evolution. Fatigue and Fracture of Engineering Materials and Structures, 36, 870–883.

References

- [96] Walat, K., & Łagoda, T. (2014) Lifetime of semi-ductile materials through the critical plane approach. *International Journal of Fatigue*, 67, 73–77.
- [97] Carpinteri, A., Kurek, M., Łagoda, T., & Vantadori, S. (2017) Estimation of fatigue life under multiaxial loading by varying the critical plane orientation. *International Journal of Fatigue*, 100, 512–520.
- [98] Aeran, A., Siriwardane, S. C., Mikkelsen, O., & Langen, I. (2017) Life extension of ageing offshore structures: A framework for remaining life estimation. *Proceedings of the 36th International Conference on Ocean, Offshore and Arctic Engineering, OMAE 2017, Volume 3A, Paper No. OMAE2017-62063, Trondheim, Norway.*
- [99] Aeran, A., Siriwardane, S. C., Mikkelsen, O., & Langen, I. (2017) A framework to assess structural integrity of ageing offshore jacket structures for life extension. *Marine Structures*, 56, 237–259.
- [100] Aeran, A., Siriwardane, S. C., & Mikkelsen, O. (2016) Life extension of ageing offshore structures: Time dependent corrosion degradation and health monitoring. *Proceedings of the 26th International Ocean and Polar Engineering Conference, ISOPE 2016, International Society of Offshore & Polar Engineers, Rhodes, Greece.*
- [101] Aeran, A., Siriwardane, S. C., Mikkelsen, O., & Langen, I. (2017) A new nonlinear fatigue damage model based only on S-N curve parameters. *International Journal of Fatigue*, 103, 327–341.
- [102] Aeran, A., Siriwardane, S. C., Mikkelsen, O., & Langen, I. (2017) An accurate fatigue damage model for welded joints subjected to variable amplitude loading. *Proceedings of the 1st Conference of Computational Methods in Offshore Technology, Volume 276, Stavanger, Norway.*
- [103] Aeran, A., Acosta, R., Siriwardane, S. C., Starke, P., Mikkelsen, O., Langen, I., & Walther, F. (2019) A nonlinear fatigue damage model: Comparison with experimental damage evolution of S355 (SAE 1020) structural steel and application to offshore jacket structures. *International Journal of Fatigue*, (under review).

References

- [104] Wang, W., Li, Q., Liu, Z., & Wang, B. (2009) Experimental study on fatigue performance and damage model of aluminum alloy welding joints for high-speed train car body. Fourth International Conference on Experimental Mechanics; International Society for Optics and Photonics, 75225I-75225I.
- [105] Zou, H., Li, W., Li, Q., & Wang, P. (2010) Probabilistic fatigue property of aluminum alloy welded joint for high-speed train. *Advanced Materials Research*, 118, 527–31.
- [106] Det Norske Veritas (2014) Concept design and analysis of offshore structures. Sesam user manual Genie Vol. 1, March 2014.
- [107] Standard NORSOK (2017) Actions and action effects. 2017. N-003, January 2017.
- [108] Aeran, A., Vantadori, S., Carpinteri, A., Siriwardane, S. C., & Scorza, D. (2019) Novel non-linear relationship to evaluate the critical plane orientation. *International Journal of Fatigue*, 124, 537–543.

Part II – Papers

Paper I

**Life Extension of Ageing Offshore Structures: Time
Dependent Corrosion Degradation and Health Monitoring**

Conference Paper

*International Ocean and Polar Engineering Conference,
ISOPE 2016*

Rhodes, Greece.

Not yet available in Brage due to copyright.

Paper II

**Life Extension of Ageing Offshore Structures: A
Framework for Remaining Life Estimation**

Conference Paper

*International Conference on Ocean, Offshore and Arctic Engineering,
OMAE 2017*

Trondheim, Norway.

Not yet available in Brage due to copyright

Paper III

**A Framework to Assess Structural Integrity of Ageing
Offshore Jacket Structures for Life Extension**

Journal Paper

Marine Structures

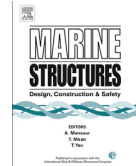
November 2017, Volume 56, Pages 237-259.



Contents lists available at ScienceDirect

Marine Structures

journal homepage: www.elsevier.com/locate/marstruc



A framework to assess structural integrity of ageing offshore jacket structures for life extension



Ashish Aeran*, Sudath C. Siriwardane, Ove Mikkelsen, Ivar Langen

Department of Mechanical and Structural Engineering and Materials Science, University of Stavanger, P.O. Box 8600 Forus, N-4036, Stavanger, Norway

ARTICLE INFO

Article history:

Received 16 December 2016

Received in revised form 23 June 2017

Accepted 15 August 2017

Available online 30 August 2017

Keywords:

Structural degradation

Life extension

Offshore jacket

Fatigue

Corrosion

ABSTRACT

The structural integrity assessment of ageing structures for possible life extension has been identified as a growing challenge in the oil and gas industry worldwide. Although the available guidelines provide a general assessment process, it is necessary to have more detailed guidelines. This can be achieved by adding relevant theories and models which can capture time-dependent structural degradation more precisely. To address this, a new framework for possible life extension is proposed in this paper. The proposed framework provides more precise corrosion models, new damage theories and assessment guidelines to predict the remaining fatigue life and check the structural adequacy in all the limit states during the whole extended service life. Initially, the paper presents the proposed framework in detail. The framework approach is then applied to an ageing jacket as a case study and results are compared with conventional approach. The proposed approach results in a remaining life of ten years as compared to one year using the conventional approach. Thus, the jacket structure can be safely operated for an additional nine years using the proposed approach. Recommendations are also made on increasing the remaining fatigue life using life improvement techniques. Finally, the applicability, significance and validity of the proposed framework are discussed.

© 2017 Elsevier Ltd. All rights reserved.

1. Introduction

A number of offshore platforms worldwide are approaching or have already exceeded their design life [1–8]. More than 50% of offshore installations on the Norwegian Continental Shelf (NCS), the United Kingdom Continental Shelf (UKCS) and the Gulf of Mexico Shelf are currently operating beyond their original life [3,9–12]. This figure is around 70% for around 800 platforms in the Middle East region [13]. The replacement of all these structures at once presents an operational and technical challenge [14,15]. The use of infrastructure from an existing field is sometimes a precondition for the development of a newer oil/gas field [16]. The enhanced production and drilling techniques, falling profit margins due to low oil prices, uneconomical small field discoveries and plenty of remaining oil reserves in existing fields are factors which are also encouraging operators to undertake more life extension studies. It is important to use the existing infrastructure efficiently and estimate its structural integrity and remaining service life more accurately.

* Corresponding author.

E-mail addresses: ashish.aeran@uis.no (A. Aeran), sasc.siriwardane@uis.no (S.C. Siriwardane), ove.mikkelsen@uis.no (O. Mikkelsen), ivar.langen@uis.no (I. Langen).

Ageing was recently categorized as functional ageing, technological ageing, knowledge based ageing and organizational ageing [8,17–20]. While the functional ageing includes material degradation issues such as fatigue, corrosion, dents, damages etc., technological ageing may refer to the old standards and regulations that are no longer considered sufficient for safe design. Knowledge based ageing may occur in cases where original design documents have become outdated due to availability of new knowledge such as new analysis methods, new models, new standards etc. Organizational ageing is the ageing of personnel and insufficient competence. While each of these key issues are important while addressing the problems of ageing, material degradation caused by fatigue and corrosion is a major cause of failures. Fatigue is a major hazard for offshore structures and in some cases fatigue cracking may reduce the overall structural integrity [21]. Corrosion changes the mechanical properties (i.e. degrades the strength) of steel with time [22]. Uniform corrosion is the most common form and can cause local structural collapse due to changes in structural stiffness [3,23,24]. Localized corrosion such as pitting and crevice corrosion is restricted to small areas and can cause local stress concentrations [25]. Corrosion fatigue is the result of cyclic loading in a corrosive environment and may reduce the fatigue strength by more than 60% for various corrosion levels [26]. A corrosion protection system (CPS) is generally employed to counteract corrosion but has a typical life of only 5–15 years [27]. It is ineffective in the splash zone due to the intermittent action of waves and tides [28]. Also, localized corrosion can start even before CPS loses its effectiveness [29]. The maintenance and repair of CPS for fixed offshore structures are generally very costly and sometimes impractical [30]. Other degradation mechanisms include erosion, creep, hydrogen related cracking, damage, blockages and accumulated plastic deformation [19,20]. It is reported that more than 60% of leaks on hydrocarbon systems are caused by ageing processes [18]. These ageing mechanisms can cause serious damage and even lead to major structural collapse. Although much research is carried out on ageing processes, failure has occurred and is still occurring in offshore structures [31]. Also, there are several uncertainties involved in fatigue assessment of ageing structures. These uncertainties can exist due to stochastic nature of the wave motion, dispersion in material characteristics of corroded members, scatter in the considered *S-N* curve for corroded detail, use of empirical relations in determining of stress factors and others. Such uncertainties together with poor inspection planning increases the risks of failures [32]. It is reported that the most severe accidents induced by fatigue were caused by gross errors like the absence of fatigue design check, bad design detailing and gross fabrication defects [32]. There is a need for detailed design checks using more precise assessment guidelines and a better understanding of complex ageing mechanisms.

Over the past two decades, a significant amount of research has been carried out to understand ageing and associated mechanisms. A number of initiatives have been taken in respect of the development of assessment guidelines and a framework for the life extension of aged structures. Also, attention was paid on the development of risk based inspection guidelines for the planning of inspection for fatigue cracks [33]. The Health and Safety Executive (HSE) has launched several key programmes (KP) on the UKCS, including a detailed investigation of ageing installations [34–36]. On the NCS, the Norwegian Oil Industry Association (OLF), together with the Petroleum Safety Authority (PSA), is establishing the necessary assessment guidelines [4,10,37]. The inclusion of the assessment procedures and frameworks for existing structures started in the mid-1990s with the insertion of a section in API RP 2A [38]. However, both the input and acceptance criteria given are tied to US waters. Subsequently similar sections were added to ISO 2394 in 1996 [39]. This was followed by ISO 13822 in 2001 [40] and ISO 19900 in 2002 [41]. The last addition to the international standards was an assessment section in ISO 19902 in 2007 [42], but it contains only minimal detailed or quantitative information [5]. In the UK, a structural integrity management framework for jacket structures was issued by the HSE in 2009 but was again based on API and ISO standards [43]. Around the same time, OLF and PSA initiated a project to establish the necessary standards and guidelines for life extension projects in the NCS region [37]. The outcome was the establishment of a new NORSOK standard N-006 [44] and the issue of recommended OLF guidelines [45] for the life extension of facilities. In 2014, API released a new standard, API RP 2S1M [46]. In 2015, a new DNV guideline was established on the use of probabilistic methods for planning of inspections for fatigue cracks in offshore structures [33]. It recommends the modelling of uncertainty variables (such as physical uncertainty, statistical uncertainty, measurement uncertainty) as stochastic variables, each having a defined probability distribution function based on engineering judgement, past experiences from similar problems or analytical results [47]. The British Standard BS 7910 is also an important document for probabilistic inspection planning methods such as RBI [48]. In addition to the above standards, life assessment guidelines and frameworks, which describe the overall assessment process, were discussed by researchers in the past [19,49–51]. These standards and the published literature provide a general assessment process for offshore structures and some procedures for the fatigue integrity assessment of details which cannot be inspected for fatigue cracks. However, it is advisable to have more detailed guidelines for offshore jackets; this can be achieved by adding relevant theories and models, which can capture the time-dependent structural degradation more precisely. Recommendations, which can estimate structural degradation in the absence of any corrosion measurement data or in cases where no significant corrosion is observed, are also necessary. The available guidelines are not sufficient to choose precise fatigue strength curves, which represent the time-dependent localized structural changes such as localized corrosion, dent, cracks, etc. Furthermore, recently proposed fatigue damage theories have not been included for a more accurate estimation of remaining fatigue life.

To overcome the above problems, this paper proposes a new framework for structural integrity assessment for the life extension of ageing jacket structures. The proposed framework provides the theories and guidelines necessary to predict the remaining fatigue life and check the structural adequacy in ULS, SLS and ALS during the whole extended service life. The proposed framework also provides recommendations on various issues such as simulation of time-dependent structural degradation, precision of loading history, effect of localized corrosion on stress concentration factors, selection of proper

fatigue strength curves, determination of stress cycles and planning for mitigation and strengthening. Recently suggested, more precise fatigue damage theory is also included in the proposed framework. Initially, the paper presents the proposed framework in detail. Then, the significance of ageing is highlighted quantitatively through a case study performed on an ageing offshore jacket structure. The structure is assessed using the proposed framework, as well as conventional approaches, and the remaining lives are compared. Finally, conclusions are drawn and recommendations are made on the use of the proposed framework for a more precise structural integrity assessment.

2. Proposed framework for structural integrity assessment and life extension

This section proposes a framework for structural integrity assessment and a more precise estimation of the remaining life of an ageing jacket structure. The assessment should be carried out for all limit states, i.e. ULS, SLS, ALS and FLS. The FLS is considered the most critical limit state as fatigue is the primary source of failure in welded structures and the remaining life is mainly governed by fatigue criteria [52,53]. The FLS being the most critical limit state may not always be true, particularly in benign waters. However, almost 25% of all structural damage requiring repair on offshore installations is classified under fatigue damage [54]. Fatigue in interaction with corrosion results in corrosion fatigue and can reduce the remaining life quite significantly. The uncertainty in the input parameters, such as loading history and stress concentration factors, also affects the remaining life predictions. It is important to determine these parameters more precisely for a more accurate prediction of the remaining life. The proposed framework provides precise corrosion models, new damage theories and assessment guidelines to predict the remaining fatigue life more accurately. The structural adequacy is checked for all other limit states as well. Finally, recommendations are made on strengthening mitigations and inspection/maintenance plans during the extended life. It is noted that, for a single structure, the assessment procedure might involve going through all paths of the framework, depending on the different degradation states of the fatigue critical details. Also, the proposed framework can be used for both deterministic and probabilistic analysis approaches. While the deterministic approach requires the use of design values (mean plus two standard deviation) of the parameters in the proposed framework, the probabilistic approach involves the use of a distribution function for each of these parameters. These distribution functions can be imported in probabilistic finite element method employed simulation tools and hence the failure probability of the structure can be determined. The use of such probabilistic tools can be computationally demanding for complex structures.

The framework is divided into five blocks, block A to block E, as shown in Fig. 1. These blocks include several stages of an assessment process from data collection to strengthening mitigations. A brief outline of various fatigue assessment approaches is presented with recommendations for selecting a suitable approach in Block A. Recommendations are made on the simulation of structural degradation and past loadings in the available finite element models in Block B and Block C. Guidelines on the selection of the proper fatigue strength curve for the selected detail are also included, followed by damage calculations using Miner's rule and the recently developed damage theories in Block D. Remaining life is estimated at the end, and recommendations are made on possible strengthening mitigations in Block E. The proposed framework is shown in Fig. 1, and a detailed explanation about each block is given in the following sub-sections.

2.1. Data collection, screening and selection of fatigue assessment approach (Block A)

Data and information collection is the first and one of the most important stages in an assessment study. The details of the data collection, screening and selection of fatigue assessment approaches are shown in Block A of the framework presented in Fig. 1. Documentation from the design phase and operational phase, as well as from the expected extended phase, should be collected as explained below.

2.1.1. Documentation during design, fabrication and installation phase

These include design documents, structural drawings, loading details, structural calculations, available finite element models, as well as fabrication and installation reports. Any reports of accidents during the lifting, transportation and installation phase should be collected. In addition, it is important to collect all the initial codes and standards used during the design phase.

2.1.2. Documents during the operational phase

These include documentation of any accidents and incidents during the service life, damage and modifications to the structure, risk assessment reports, as well as any modified finite element models of the structure. It is important to collect all inspection and maintenance reports, as well as any material-testing reports, to document the status of the structural degradation and any potential fatigue cracks. It is also important to list all the findings and repairs that are carried out during the operational phase.

2.1.3. Documents during the extended life phase

These include expected operational as well as environmental loads. Information regarding any modifications required to cater for future needs, in terms of both technology and equipment, should be collected. The current set of codes and standards addressing the life assessment and life extension also need to be documented.

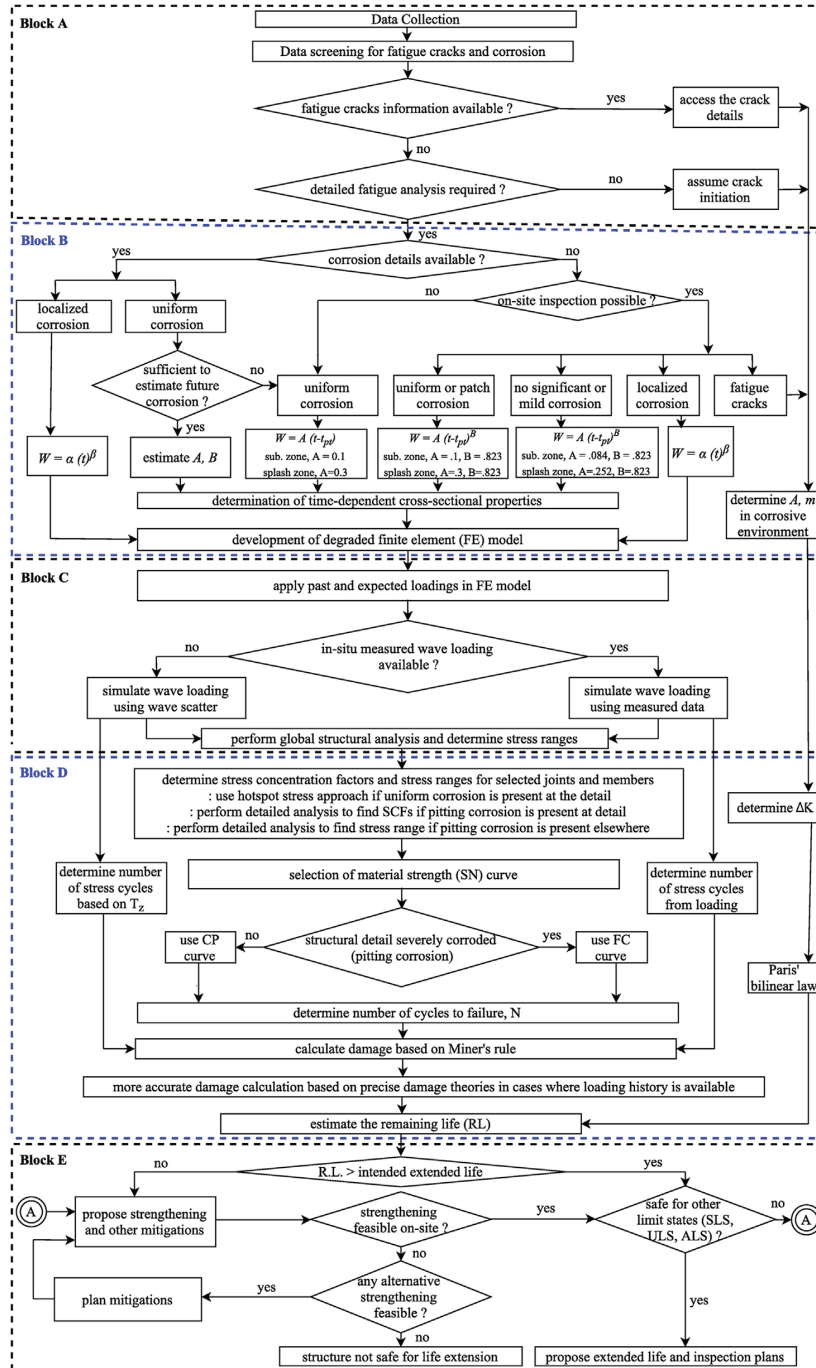


Fig. 1. Proposed framework for structural integrity assessment and life extension of ageing offshore structures.

2.1.4. Selection of fatigue assessment approach

The collected data should be screened for all structural degradation information, including extent of structural degradation, member thickness measurements and fatigue cracks. The selection of a suitable fatigue assessment approach is an essential part of any assessment process. For offshore structures, two well-known fatigue life assessment approaches are: (a) the damage tolerance approach and (b) the safe life approach [55,56]. The damage tolerance approach assumes the existence of a fatigue crack and then estimates the future life, using crack propagation theories, while the safe life approach estimates the crack initiation and propagation life, using detailed category-based fatigue strength curves. It is known that the crack initiation life of a structural element is much higher than the crack propagation life [56]. The industry practice for the fatigue design of offshore jacket structures is based on the use of the safe life approach and is also recommended in design standards [57,58]. Moreover, it is recommended that the damage tolerance approach be used where fatigue crack information is available, such as in cases of existing ageing structures. In such cases, the safe life approach is no longer applicable after a crack has initiated. The linear elastic fracture mechanics can describe the probable crack behaviour and its propagation towards the final failure.

2.1.4.1. Safe life approach – S-N method. The safe life approach is based on S-N curves of detail category. In this assessment method, a more accurate prediction of remaining life can be made using recently proposed precise damage theories [59–61]. For a detailed fatigue assessment of tubular joints in jacket structures, hot spot stress based T curve should be carefully chosen based on the extent of corrosion at the joint [58]. In cases where detailed fatigue assessment is not required, remaining life can be predicted by assuming a crack initiation and using the damage tolerance approach based on linear elastic fracture mechanics.

2.1.4.2. Damage tolerance approach - linear elastic fracture mechanics method. This method is based on the crack growth law, which can be represented by several models [48,62–64]. The most frequently used conventional model is Paris' law as given in Eq. (1) [65].

$$\frac{da}{dN} = A(\Delta K)^m \quad (1)$$

where da/dN is the crack growth rate, ΔK is the stress intensity factor range, A and m are the constants that depend on material and the applied conditions, including environment and cyclic frequency. A re-assessment of the available test data for fatigue crack growth rates was made in 1998 to capture the environmental effect on these constants and recommendations are also available on the use of more precise two-stage relationships [48,66–68]. The stress intensity range ΔK can be expressed as shown in Eq. (2).

$$\Delta K = K_{max} - K_{min} \quad (2)$$

where K_{max} and K_{min} are the maximum and minimum stress intensity factor corresponding to maximum and minimum stress ranges. The stress intensity factors for tubular joints can be determined numerically using a finite element or boundary element analysis of the joint. Alternatively, analytical solutions are provided by standards, which are deduced from semi-elliptical cracks in plates [48]. The other parameters of the crack propagation curve (A , m) can also be found in standards [48].

2.2. Simulation of degradation and development of degraded FE models (Block B)

The structural degradation should be simulated, and degraded FE models should be developed as per Block B of the framework presented in Fig. 1. The collected data is further screened for all available structural degradation information. This includes all the past inspection reports and thickness measurement records, as well as the current status of degradation in the structure. It is recommended that the finite element (FE) model of the structure should first be developed using this available information. Any geometrical modifications to the structure during the installation and operational phase should be modelled. The jacket and the topside should be modelled in finite element software using the beam/frame elements. In addition, precise modelling of the foundation should be carried out, using the available soil stiffness information. The finite element model should be verified against any available structural dynamic response measurement data; modifications should then be performed to account for the effect of time-dependent structural degradation of the structure. This model is named the “degraded FE model”, and the simulation of degradation is explained in detail below.

2.2.1. Simulation of uniform corrosion

Uniform corrosion is the most common form of corrosion and is uniformly distributed on the surface. This results in the reduction of member thickness and thereby the reduction of the effective cross-sectional properties of the members, such as effective area, second moment of area, torsional constants and warping constants. This may cause change in the overall stiffness of the structure and the structural response (i.e. stress, displacement and dynamic characteristics). It is essential to accurately include the time-dependent effect of uniform corrosion in the finite element model, using suitable corrosion wastage models. Several studies have shown that uniform corrosion can be simulated with a good approximation by a

nonlinear function [69–75]. The nonlinear corrosion wastage model assumes no degradation in the first phase when the protection system is effective. This is followed by a nonlinear process of growth over time, as shown in Eq. (3).

$$W(t) = A(t - t_{pt})^B \quad (3)$$

where $W(t)$ is the thickness wastage in millimetres, t is the lifetime and t_{pt} is the corrosion protection time in years. The model has two parameters, A and B , whose values should be precisely determined. The standard deviation of the thickness wastage is given by Eq. (4) [76,77].

$$\sigma_{W(t)} = 0.67 W(t) \quad (4)$$

2.2.2. Simulation of localized corrosion

Pitting is a localized form of corrosion and is regarded as one of the most hazardous types of corrosion for offshore structures [78,79]. Such localized corrosion is very likely to occur in the splash zone area, where corrosion protection systems (CPS) are ineffective [80]. Also, pitting corrosion may even start before the CPS loses its complete effectiveness [29]. Although pitting corrosion has no significant effect on the global stiffness of the structure, it can cause local stress concentrations at the structural detail and thus reduce the fatigue life [25,81,82]. It is therefore essential to take pitting corrosion into account, while determining stress concentration factors at the corroded structural detail. It is recommended that, in addition to the global structural analysis, a local stress analysis be performed near the pits to determine secondary stresses and estimate the fatigue life more precisely. The pit depth has been acknowledged as a critical factor for pitting corrosion and is the key parameter to describe the pitting rate [78]. The propagation of pit depth is conventionally described by a power-law model [83], analogous to that for uniform corrosion, and is shown in Eq. (5). Moreover, no coating period (t_{pt}) is considered, as pitting corrosion can start even in the presence of CPS.

$$W(t) = \alpha(t - t_i)^\beta \quad (5)$$

where $W(t)$ is the propagation of pit depth, t_i is the pit nucleation time and t is the pit propagation time. In practice, the time for the pit nucleation (t_i) is negligible compared to the pit propagation time [84]. Hence the pit growth is usually described by Eq. (6).

$$W(t) = \alpha(t)^\beta \quad (6)$$

The α and β are model parameters and should be determined precisely. Wang et al. [85] also proposed a simple engineering model by adopting a two-parameter (m, α) Weibull function to describe the growth of macro-pits in the function of exposure time, as given in Eq. (7). The corresponding pit growth rate is given by Eq. (8).

$$W(t) = d_m \{1 - \exp[-[\alpha(t - t_i)]^m]\} \quad (7)$$

$$W_I(t) = d_m m \alpha (t - t_i)^{m-1} \exp[-[\alpha(t - t_i)]^m] \quad (8)$$

where m and α are the shape and scale parameters respectively, and d_m is the long-term pit depth. For the shape parameter greater than 1, the pit growth rate shows an increasing phase, followed by a maximum and a decreasing phase. The pitting corrosion rates drop monotonically for $m \leq 1$. This new model is only applicable to the growth phase of macro-pits. More guidelines on the selection of these parameters can be found in Wang et al. [85].

2.2.3. Time-dependent sectional properties of corroded cross sections

The cross-sectional properties of the members or locations where uniform or patch corrosion is observed should be modified as per the time-dependent thickness reduction, Eq. (3). These modified cross-sectional properties are used to develop a degraded FE model. Such a change is not required for members where pitting corrosion is observed, as there is no significant loss of material and hence no significant reduction in the stiffness.

The effective cross-sectional area of a corroded section is given by

$$A_{eff}(t) = A_0 - \sum_{i=1}^n W_i(t) l_i \quad (9)$$

where A_{eff} is the effective area, A_0 is the initial cross-sectional area, l_i is the length of uniform corrosion spread over the cross section at the i^{th} corroded surface, as shown in Fig. 2(a). The $W_i(t)$ is the average corrosion penetration in mm at the i^{th} corroded surface of the cross section, and t is the age in years.

The reduction in the member cross section shifts the neutral axis by a distance, $e(t)$. This shift can be obtained using Eq. (10).

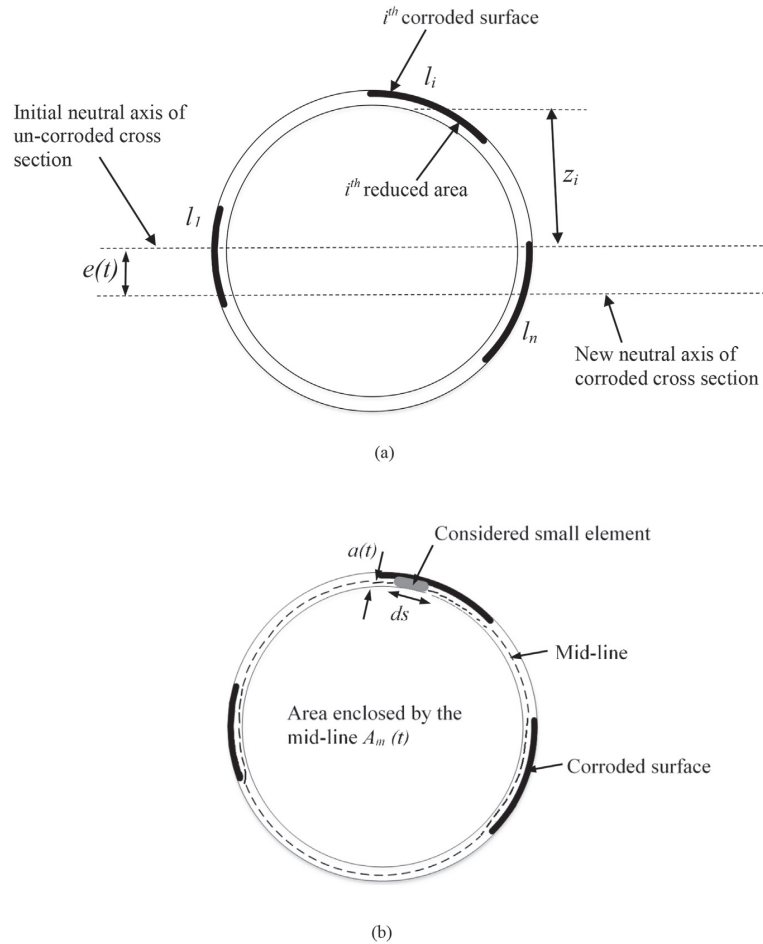


Fig. 2. Schematic representations of (a) effective cross-sectional parameters of corroded tubular cross section (b) torsional parameters of corroded tubular cross section.

$$e(t) = \frac{\sum_{i=1}^n W_i(t) l_i z_i}{A_{\text{eff}}(t)} \quad (10)$$

where z_i is the height from the initial neutral axis to the centroid of the i^{th} reduced area (i.e. lost area at the i^{th} surface).

The effective second moment of area of the corroded cross section is calculated about the new neutral axis and can be obtained using Eq. (11).

$$I_{\text{eff}}(t) = I_0 + A_0 e(t)^2 - \sum_{i=1}^n \left\{ \Delta I_i + W_i(t) l_i [z_i + e(t)]^2 \right\} \quad (11)$$

where I_0 is the second moment of area of the uncorroded cross section, ΔI_i is the second moment of i^{th} reduced area about its own neutral axis.

The effective torsional constant for the closed cross section of a corroded member can be obtained using Eq. (12).

$$I_{T,eff}(t) = \frac{4A_m(t)^2}{\oint ds/a(t)} \quad (12)$$

where $A_m(t)$ is the area enclosed by the midline of the cross section as shown Fig. 2(b). The enclosed area $A_m(t)$ keeps shifting with time due to a continuous shift in the midline as a result of corrosion. The ds is the developed midline length and $a(t)$ is the thickness of the considered small element of the cross section.

The thickness $a(t)$ of the considered small element of the cross section can be written at a time t using Eq. (13).

$$a(t) = a_0 - W(t) ; \text{ when } t > t_{pt} ; a(t) = a_0 ; \text{ when } t \leq t_{pt} \quad (13)$$

where a_0 is the thickness of an uncorroded small element, $W(t)$ is the average corrosion penetration in mm at the considered location and t_{pt} is the corrosion protection time in years.

2.2.4. Parameters of uniform corrosion model

The average corrosion penetration is the corrosion wastage due to uniform corrosion and can be determined using Eq. (3). The values of parameters A and B can be determined by fitting previous corrosion measurements with a proposed nonlinear variation in Eq. (3). However, if the corrosion details are insufficient for the estimation of the above parameters, it is recommended that the values be selected conservatively from Table 1. The values of these parameters can be found in the work of several researchers [27,28,32,76,77]. It is suggested to ignore any remaining potential of sacrificial anodes. This is to have some conservatism in the estimation of remaining life.

2.2.5. Parameters of localized corrosion model

In addition to accounting for uniform corrosion in global analysis, it is recommended that a local stress analysis be performed near the pits to determine secondary stresses, if precise fatigue assessment is required. The pits can be simulated as per the corrosion model explained in Eq. (6). The parameters α and β can be taken based on the material type, as per Table 2 [86,87].

2.2.6. Parameters of crack growth law in marine environment

The material parameters, A and m , in Paris' law, are influenced by the surrounding environment and need to be correctly determined for offshore structures in the marine environment. For welded joints, use of mean plus two standard deviation values with stress ratio, $R \geq 0.5$ is recommended for conservatism and to allow for the influence of residual stresses [48]. The values of the parameters, A and m , for the crack growth law in Eq. (1), are given in Table 3 [48].

Table 1
Mean values of model parameters for uniform corrosion [27,28,32,76,77].

Inspection findings	Splash zone area		Other areas	
	$A(mm)$	B	$A(mm)$	B
Not performed – unmanned facility or high costs involved	0.3	1	0.1	1
Severe corrosion found – uniform corrosion with many patches and pitting corrosion	0.3	0.823	0.1	0.823
No significant corrosion – slight uniform corrosion with few patches	0.252	0.823	0.084	0.823

Table 2
Model parameters for pitting corrosion [86,87].

Material type	Parameters	
	$\alpha (mm)$	β
Carbon steel in sea water	0.092	0.511
Mild steel in sea water	0.0028	0.3877

Table 3
Parameters of crack growth law in marine environment (recommended values for stress ratio $R \geq 0.5$) [48].

Marine environment	Stage A		Stage B		Intersection between Stage A and B $\Delta K_0 (N/mm^{3/2})$
	A^a	m	A^a	m	
Free corroding environment	1.72×10^{-13}	3.42	7.48×10^{-7}	1.11	748
Cathodic protection at -850 mV	2.10×10^{-17}	5.10	2.02×10^{-11}	2.67	290
Cathodic protection at -1100 mV	2.10×10^{-17}	5.10	1.02×10^{-7}	1.40	415

^a For da/dN in $mm/cycle$ and ΔK in $N/mm^{3/2}$.

2.2.7. Feasibility of on-site inspections

In cases where degradation/corrosion information is not available, it is recommended to explore the possibilities of on-site inspections. These inspections can be limited and should contain at least some thickness reduction measurements, along with photographs. Several non-destructive monitoring techniques are used in industry for evaluating the corrosion resistance of materials and detecting fatigue cracks without causing damage. A brief description of non-destructive testing (NDT) methods is presented by past researchers [88–90]. Simpler detection methods like general visual inspection (GVI) and close visual inspection (CVI) cannot be used to detect small fatigue cracks. In such cases, other methods like flooded member detection (FMD), eddy current (EC), magnetic particle inspection (MPI) and alternating current field measurement (ACFM) should be used together with the probability of detection (PoD) curves. Among these, EC method may be preferred for ease of measurement and for its provision of a direct measurement of thickness loss, i.e., corrosion rate [91]. The PoD curves represent the probability of detecting a crack depending on the method used and working conditions such as location of crack with respect to water level or the visibility conditions at hot spot areas [47,92]. The distribution functions for the PoD curves are dependent on qualification and execution of work but can also be taken from recommended guidelines [47]. While doing the on-site inspections, special attention should be paid to the hot spot areas in the splash zone.

The degraded FE model should be developed based on the on-site inspection findings. The uniform or patch type of corrosion can be simulated using the model parameters given in Table 1. It is advisable to take parameters on the conservative side if inspections are not performed or if the details are subjected to severe corrosion. Any findings of localized pitting corrosion should be accounted for precisely to determine the model parameters of Eq. (6) or to check the accuracy of the available/determined model parameters of the pitting corrosion wastage model given in Table 2. The stress concentration factors should be calculated in cases where pitting corrosion is observed at the fatigue critical details. Localized corrosion found on the members should be accounted for by modelling them in detail and performing a more detailed local stress analysis. As discussed above, the modification of cross-sectional properties should not be required for the members/locations where pitting corrosion has been recognized, if there is no significant change in the stiffness or stability of the member. It is recommended that the damage tolerance approach be used in cases where fatigue cracks are found during the on-site inspections. The parameters of the bilinear law should be determined based on the extent of corrosion at the crack location and as per Table 3.

2.2.8. Corrosion fatigue

The mechanical degradation of material, when the structure is subjected to repetitive cyclic stress in the presence of a corrosive environment, is corrosion fatigue. This is a failure mechanism which is not yet fully understood [93]. However, it can have a significant impact on the fatigue life, reducing it by more than 60% for various corrosion levels [26]. Although the precise modelling of this mechanism is a complex task, it is essential to take it into reasonable consideration for life extension.

2.3. Simulation of loading and structural analysis (Block C)

The past and future loading should be applied, and structural analysis should be performed as per Block C of the framework presented in Fig. 1. The collected data should be screened for all past loadings over the design life of the structure. These include operational loads as well as environmental loads. The operational loads should be updated for any changes during the lifetime of the structure, based on inspection and maintenance records. In cases where sufficient information is not available or data records are missing, it is recommended that operational load values be taken from the design standards [38,42,58,94]. Any additional requirements for higher operational loadings during the extended life should be simulated in the degraded FE model. The environmental loads include mainly the wave and the current loading. It is advisable to use a 100-year return period wave for ultimate limit state assessment and a 10000-year return wave for accidental limit state assessment. The wave and current parameters for the above-mentioned return periods can be taken from the original design documents. In cases where the information is missing, the recommendation is to take these values from the design standards [38,42,58,94]. For the fatigue limit state assessment, the data collected during the operational phase should be screened for any records of real wave measurements. Such available data should be employed for estimating the past and future wave loading on the structure at the specified location. In cases where no wave measurement data is available, the wave environment can be approximately simulated using the long-term wave scatter diagram for the specified location. The wave scatter diagrams can be either found in the design documents or taken from design standards.

The structure should be analysed for past as well as future loadings. The load cases and load combinations can be made as per the standards for the various limit states. It is recommended to first perform a quasi-static analysis to ascertain the overall integrity of the structure. A linear elastic analysis should be performed for a preliminary estimation of the overstressed members in ultimate limit state. Such a preliminary analysis is required to screen critical locations for a detailed fatigue assessment. In cases where preliminary analysis results are found to be severe with plenty of overstressed locations, performing a nonlinear analysis is recommended for more precise analysis. The nonlinear analysis should capture both the geometrical and the material nonlinearities. Based on the ultimate limit state preliminary analysis, critical locations should be identified for a detailed fatigue assessment. For a detailed fatigue assessment, a suitable fatigue assessment method should be selected depending upon the sensitivity of the structure to dynamic effects.

2.3.1. Fatigue assessment methods for jacket structures

Two different methods are used for the fatigue analysis of jacket structures. These are deterministic discrete wave fatigue analysis (deterministic fatigue analysis) and frequency response fatigue analysis (frequency domain fatigue analysis, spectral fatigue analysis or stochastic fatigue analysis). The deterministic approach requires calculation of fatigue damage for each sea state in the wave scatter diagram to determine the total fatigue damage. This approach is traditionally preferred for jacket structures in low to moderate water depths as these are not sensitive to dynamic effects [47,53,58,94]. A stochastic fatigue analysis is generally performed for structures with significant dynamic response such as deep-water structures and requires the determination of hydrodynamic transfer functions [47,53,58,94]. It is recommended to perform a deterministic fatigue analysis for jacket types structures in low to moderate water depths [47,53,58,94]. For deep-water jackets with a fundamental natural period exceeding 2.5 s, a deterministic fatigue analysis may still be recommended by determining a dynamic amplification factor using recommended guidelines [47,53].

The fatigue assessment should be performed for the critical locations using the available loading history or wave scatter diagram. It is advisable to apply wave loading from 0 to 180° at 30-degree spacing. A suitable wave theory should be used, depending upon the water depth at the location as well as the wave parameters [95,96]. The wave loads should be applied, together with permanent and variable loads, to capture the mean stress effects. The load combinations should be as per standard codes and guidelines. A nonlinear structural analysis is recommended for the determination of stresses in the members for each sea state of the wave scatter diagram.

2.4. Stress evaluation and estimation of remaining fatigue life (Block D)

Analysis should be performed to determine stress ranges and to estimate the remaining fatigue life as per Block D of the framework presented in Fig. 1.

2.4.1. Evaluation of stress ranges at the critical locations

The analysis should be performed for each sea state of the wave scatter, and the maximum stress range should be determined for all the members at the critical joints/locations identified in Section 2.3. The hot spot stress (HSS) approach is widely used for the fatigue assessment of jacket structures. The presence of uniform corrosion reduces the member thickness uniformly and hence it is still reasonable to use the HSS approach for such cases. The stress concentration factors (SCFs) can be determined as per standard codes and guidelines, and the superposition method can be applied to determine the maximum hot spot stress range [58]. The HSS approach can also be applied at the joint detail if localized corrosion is present at a distance of more than four times the member thickness [58]. In cases where localized corrosion is present at the detail, a comprehensive detailed local analysis is recommended. This can be done by making a separate finite element model of the detail, including the pits and a more refined mesh. The local secondary stress state should be determined, and use of the notch stress approach is advised for fatigue life assessment. In the presence of localized corrosion away from the joint detail (at a distance of more than four times the member thickness), a comprehensive detailed local analysis should be performed separately. The member with pits should be modelled considering required mesh sensitivity, and local stresses should be evaluated to identify the most critical locations. The maximum stress ranges at this location can then be utilized to determine the fatigue life, using a suitable *S-N* curve. Alternatively, the pits can also be assumed to be dents, and the stress concentration factors can be determined using the formulae for dents provided in the standards or textbooks [97]. The stress ranges are employed for fatigue life estimation, using either the safe life or the damage tolerance approach. Life estimation using the safe life approach is firstly discussed; this is followed by the damage tolerance based linear elastic fracture mechanics method.

2.4.2. Selection of fatigue strength (*S-N*) curve

The selection of a suitable *S-N* curve depends on the type of detail category and the method used for stress evaluation. The current state of degradation at the detail category also influences the selection of *S-N* curve, as surface roughness and hydrogen embrittlement are the governing factors of fatigue strength. It is recommended to use a free corrosion (FC) curve in the cases where severe uniform and pitting corrosion are found at the detail. The cathodic protection (CP) *S-N* curve can be used for corrosion-free details. For tubular joints in jacket structures, hot spot stress based T curve can be selected from design standards and recommended practices [58]. The number of actual stress cycles (*n*) can be determined using the zero up-crossing time period for the corresponding sea state of the wave scatter diagram [58,98]. The stress cycles can be counted from the measured wave loading history, if available.

2.4.3. Calculation of fatigue damage

The yearly fatigue damage for each sea state can be calculated using Miner's rule [56,99]. The yearly fatigue damage covering all sea states can be calculated using Eq. (14) as per standard codes [100].

$$D_L = \sum_{i=1}^{n_s} D_i P_i \quad (14)$$

where D_L is the yearly fatigue damage covering all sea states, n_s is the number of discrete sea states in the wave scatter diagram, D_i is yearly fatigue damage for individual sea states and P_i is the sea state probability. A design fatigue factor (DFF)

should be considered in the damage calculations depending upon the consequence of fatigue failure and the probability of inspection and repair. The DFF can be obtained from the design standards and recommended practices [47,58,94,101]. A high value of DFF represents a reduced probability of fatigue cracking and a value of 10 is recommended for areas not accessible for inspection and repair. This value can also be used if it is desired to omit future scheduled inspections during the extended life of the structure.

The fatigue damage can be determined using the Miner's rule where loading history is unknown. However, under variable amplitude loading conditions, Miner's rule can lead to unreliable predictions of remaining life, since it did not properly take into account the loading sequence effect [56,59,102]. In cases of existing ageing structures where loading history might be known, it is recommended to use the recently proposed "sequential law" [59,60] to capture the load sequence effect more precisely. This paper presents only a summary of the sequential law. It can be explained briefly by assuming a component subjected to a certain stress range, σ_i , for n_i number of cycles at load level i . This results in a residual life of the component: $(N_i - n_i)$ cycles at load level, i . The stress, $\sigma_{(i)eq}$, which corresponds to the failure life $(N_i - n_i)$ is obtained from the S-N curve and is named as i^{th} level damage stress amplitude or stress range. The new damage indicator, D_i , can then be written as

$$D_i = \frac{\sigma_{(i)eq} - \sigma_i}{\sigma_u - \sigma_i} \quad (15)$$

where σ_u is the intercept of the S-N curve with the ordinate at one quarter of the first fatigue cycle. Assuming that the same damage is transformed to the next load level $i+1$, the damage equivalent stress at level $i+1$ can then be calculated. Subsequently, the corresponding equivalent number of cycles to failure and the residual life at the load level $i+1$ can be obtained using the S-N curve. The cumulative damage at load level $i+1$ can then be defined. The above procedure is followed until the cumulative damage becomes unity and a more precise estimation of remaining fatigue life is obtained. A detailed description of the sequential law, including the damage stress model and the new damage indicator D_i , can be found in work by previous researchers [59,60].

2.4.4. Selection of crack propagation curve

In cases where the linear elastic fracture mechanics method is adopted to estimate remaining life, it is recommended that a suitable crack propagation curve be selected. The stress intensity factors, ΔK , should be determined from a detailed finite element modelling of the crack, which is computationally demanding. Alternatively, analytical solutions are provided by standards, which are deduced from semi-elliptical cracks in plates [48]. The crack growth rate can then be determined using a suitable crack propagation curve. The crack propagation curves in the marine environment can be found in design standards and research articles [48,103–105]. The remaining fatigue life can be estimated based on the critical crack growth size.

2.5. Assessment for other limit states and strengthening/inspection for extended life (Block E)

If the remaining fatigue life is found to be satisfactory, it is advisable to check the structure for other limit states (ULS, SLS, ALS) as per Block E of the framework presented in Fig. 1. While the ULS checks are performed to check the structural strength against ultimate load conditions, the SLS checks requires the deflection of structural members within allowable limits. The ALS checks are performed for accidental situations like ship collisions, dropped objects, fire, explosions and seismic actions. For each of these limit states, the structure should be checked for both its current degradation state and considered degradation in the future. These checks should be performed on the same principles as that of the design standards and using the Load Resistance Factor Design philosophy [92,94,101]. The ULS check should be performed for all the load categories (permanent load, variable load, environmental load and deformation load) using the load combination factors in design standards [92,94,101]. The combinations of different environmental loads (wind, waves, current, ice) should be as per the recommended guidelines to obtain ULS combinations with 10^{-2} annual probability of exceedance [101]. The ALS checks for existing structures should also be performed using the design criteria and the load factor is 1.0 for all load categories. The accidental loads and abnormal environmental loads with 10^{-4} as the annual probability of exceedance should be considered [101]. In the assessment of all these limit states, the material factor should be taken from the design standards [92,94,101]. Under the above LRFD approach, an acceptable safety margin is achieved by checking the structure based on characteristic values of load effects and resistances, and appropriate partial safety factors in each of the above limit states [32]. The characteristic values correspond to a confidence level of 95% and a failure probability of 5%.

If all the limit state checks are satisfactory, for both current and future degradation, the extended life of the structure can be proposed. It is advisable to propose a proper inspection and maintenance plan for the structure during its extended life, as per the standards [46,47,92,106]. The intervals for condition monitoring should be adjusted to take into account an increased likelihood of fatigue cracks due to damage accumulation during the initial design life [92]. The Norsok standard N-005 is an important document for the condition monitoring of load bearing structures [106] and should be referred for more information on monitoring intervals, implementation process and selection of inspection methods. However, if the remaining life is not found to be satisfactory for any of the limit state checks, suitable mitigations need to be recommended. These mitigations can consist of possible strengthening, reduction of actions or reduction of operational changes. The strengthening can take the form of grouting of members and joints, adding extra braces at overstressed locations, or adding stiffeners or brackets. Several fatigue life improvement techniques related to the weld can also be used. Examples of these are grinding,

Tungsten Inert Gas (TIG) dressing and hammer peening [58,107]. It is advisable to refurbish the anodes wherever possible. More information on mitigation and strengthening can be found in the design standards [46,92]. The proposed strengthening and mitigation should be checked for feasibility at the offshore site location. On-site inspections are recommended to check the feasibility of proposed strengthening as well as any other feasible alternatives. Mitigations should be planned in case the proposed strengthening is not feasible and alternatives are found. However, in cases where proposed strengthening is not feasible and no alternative mitigations are found, the recommendation is that the structure should not be used beyond its designated service lifetime.

3. Case study: Structural integrity assessment of an existing jacket structure for life extension

A case study is performed on an old existing jacket type of platform in the Gulf of Suez, the Red Sea. The jacket is assessed for its structural integrity, and its remaining life is estimated using the proposed framework. The obtained assessment results are compared with conventional assessment approaches. Hence, the significance of the proposed framework is confirmed.

3.1. Data collection, screening and selection of fatigue assessment approach

The data from the initial design, operational as well as expected extended life, was collected. This includes structural drawings, material properties, loading details and some of the past inspection reports. The inspection reports were screened for all structural degradation information, including the member thickness measurements and fatigue cracks. A suitable fatigue assessment approach was also selected as per the proposed framework. The initial target life of the structure was 25 years and a design fatigue factor of three was taken in the initial design calculations. The design life of the structure is now over and the presented analysis is performed at the end of initial target life.

3.1.1. Structural and material details

The platform, which was installed in 1988, is a four-leg jacket structure. The age of the jacket is 28 years and is well suited for consideration as an aged offshore installation. The jacket has four main legs and is installed in a water depth of 33.5 m. Diagonal braces are present in both the horizontal and vertical planes. All the members have a tubular cross section. The topsides have three levels: the cellar deck, the production deck and the helideck. The material type is A36 with a density of 7850 kg/m³ and a modulus of elasticity of 200 GPa. The yield strength and ultimate tensile strength are 248 MPa and 400 MPa respectively. An image of the structure at the offshore site is shown in Fig. 3(a).

3.1.2. Selection of fatigue assessment method

The structural degradation information was screened for any fatigue cracks; none were found in the inspection records. As the structure is approaching the end of its design life, a detailed fatigue assessment, including simulation of past and future structural degradation, is required for possible life extension. Hence, a safe life approach was used for the fatigue assessment, as described in Block A of the proposed framework presented in Fig. 1.

3.2. Simulation of degradation and development of degraded FE models

The structural degradation information was also screened for any corrosion measurement details. Thickness reduction measurements were not found in the inspection reports. However, recent site inspections have revealed the presence of mild corrosion in the submerged zone and some patch corrosion in the splash zone of the jacket structure, but no significant localized corrosion and no fatigue cracks were found. It is recommended that the uniform corrosion model parameters be selected as per Block B of the proposed framework presented in Fig. 1.

3.2.1. Conventional and framework proposed approaches for selecting model parameters

Conventionally, the degradation is not considered at all in cases of mild corrosion, as the material loss is very low. Also, the model parameters are conventionally taken as per the design standards for simulating patch corrosion [28,42,92,108]. These parameters, as per conventional approach, are shown in Table 4. However, it is advisable not to ignore the degradation effects, even in cases of mild corrosion, and to select the proposed model parameters to represent mild corrosion as per Table 4. It is noteworthy that the model parameters given in the design standards for patch corrosion are very conservative and can result in an underestimation of the remaining fatigue life. It is recommended that patch corrosion be simulated in the splash zone, using the proposed model parameters in the framework for the considered jacket structure. These considered parameters for the proposed approach are shown in Table 4.

3.2.2. Development of degraded finite element models

A finite element model of the structure was developed in FE software SAP 2000 [109], using frame elements. The finite element model and global geometry is shown in Fig. 3(b). The jacket members were degraded, using the conventional and proposed framework approaches. Also, separate model parameters were applied to the members in the splash zone and the submerged zone, as per values mentioned in Table 4. The time-dependent cross-sectional properties were determined using Eqs. (9)–(12), and degraded FE models were developed for the jacket structure.

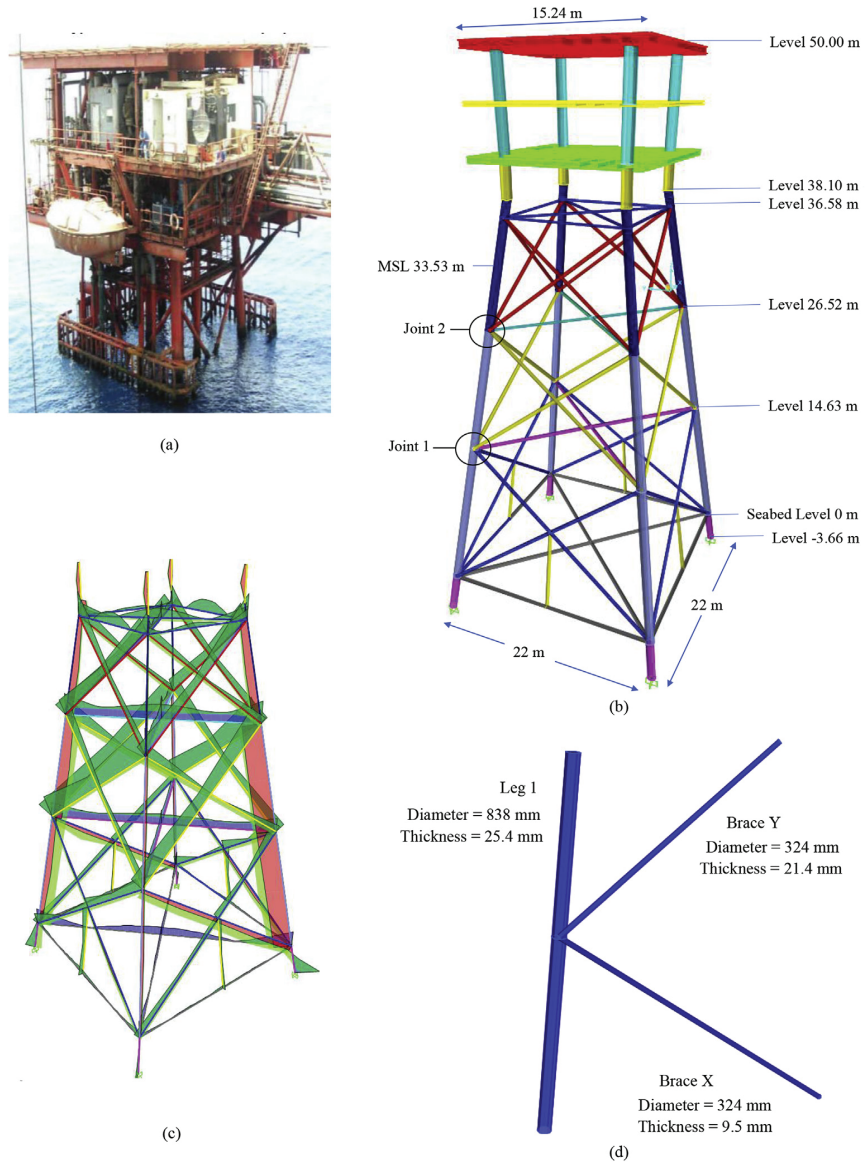


Fig. 3. (a) Considered offshore jacket platform (b) finite element model of the platform and critical joints (c) stress envelope in members for ULS assessment (d) details of critical joint 2.

Table 4
Model parameters for conventional approaches [28,42,92,108] and as per proposed framework.

Model parameters	Splash zone area		Other areas	
	A(mm)	B	A(mm)	B
Conventional approach	0.3	1	0	0
Proposed approach	0.3	0.823	0.084	0.823

3.3. Load simulation and structural analysis

The collected data was screened for loadings over the design life of the structure. This included all permanent loads, variable loads and environmental loads. The loadings considered were the dead load, live load, wave load, current and the wind loads. A nonlinear multistep static structural analysis was performed. The nonlinearities considered were the geometrical nonlinearities in the structure (P- Δ analysis) and the force nonlinearities in the wave loadings.

3.3.1. Loading details and simulation

The permanent and variable loads were defined. The variable load was applied as uniformly distributed loads on the deck. An intensity of 2.4 kN/m² was applied to the helideck, while a 9.6 kN/m² live load was applied to the cellar and production decks. For SLS and ULS checks, a 100-year return period wave, with a wave height of 7.92 m and time period of 8 s, was used. For the FLS check, in the absence of any measured wave heights, the wave loading was simulated using a long-term wave scatter diagram at the installation location, as described in Block C of the proposed framework presented in Fig. 1. The considered wave scatter diagram was derived from actual measurements taken at the site from the period 1992 to 2014. These measurements were carried out and provided by a met ocean consultant company [110]. The current and wind loads were applied in the same direction as that of the wave.

3.3.2. Load cases and load combinations

The dead load and live load were defined as individual load cases. The wave load was defined in seven directions, and seven wave load cases were defined. Since the structure is symmetrical, the directions were chosen from 0 to 180°, spaced at 30° intervals. The wave load was derived using a suitable wave theory as per the applicability criteria of wave theories. A nonlinear 5th order Stoke's wave theory was found to be applicable for the considered jacket. The current and wind loads were defined, along with the wave load. The load cases were combined as per the load combination factors given in the design standards.

3.3.3. Structural analysis

A nonlinear multistep static analysis was performed. For SLS and ULS assessment, a 100-year return period wave was used in the analysis, and a preliminary estimation of overstressed joint locations was made. The stress envelope plot for the ultimate limit state assessment is shown in Fig. 3(c) for the worst load combination. Two critical joint locations were identified from the stress plot, as shown in Fig. 3(b). Detailed geometry of the joint in splash zone (joint 2) is shown in Fig. 3(d). A deterministic fatigue assessment was performed for the critical joints, according to the guidelines mentioned in section 2.3.1. The analysis was also performed separately for each of the degraded models.

3.4. Stress evaluation and estimation of remaining life

Hot spot stress (HSS) approach has been used for fatigue life estimation of considered joints as no localized corrosion was observed. Hence, a global analysis was performed as also mentioned in the proposed framework in Block D and also in Section 2.4.1. However, in cases where localized corrosion is present at the details, it is recommended to perform a notch stress based fatigue analysis where secondary stress state should be determined using detailed thin shell FE analysis.

Forces and moments in the chord and brace members of the considered joint were extracted from the global finite element analysis. The nominal axial and bending stress ranges were subsequently calculated for each of the load combinations under each sea state. The hot spot stress concentration factors for considered joint members were also calculated using the recommended guidelines [58]. The nominal stress ranges were combined using the method of superposition wherein hot spot stress ranges were evaluated at eight locations around the circumference of the intersection for each of the load combinations using formulae given in the guidelines [58]. The maximum value of the geometrical stress ranges is taken as the hot spot stress range value for the most critical member in the considered joint. This was repeated for all the sea states in the wave scatter and for each of the degraded models. The maximum hot spot stress range value and hence the potential crack location is identified at the saddle position of the critical brace member of joint 2. For illustration, the hot spot stress range calculations are shown for the critical brace member of joint 2 in uncorroded model (i.e. model with no degradation) and for one sea state.

Table 5
Forces and moments in the critical brace of Joint 2^a (uncorroded model, one typical sea state).

Load combination	F _{x, max}	F _{x, min}	M _{ip, max}	M _{ip, min}	M _{op, max}	M _{op, min}
DL + LL + wave 0	-1.07E+05	-1.29E+05	3.07E+02	-1.08E+03	-1.48E+04	-2.64E+04
DL + LL + wave 30	-1.08E+05	-1.29E+05	2.59E+03	-2.62E+03	-1.48E+04	-2.63E+04
DL + LL + wave 60	-1.16E+05	-1.26E+05	6.13E+03	-4.37E+03	-1.49E+04	-2.58E+04
DL + LL + wave 90	-1.20E+05	-1.26E+05	8.36E+03	-5.71E+03	-1.40E+04	-2.43E+04
DL + LL + wave 120	-1.21E+05	-1.29E+05	7.75E+03	-5.15E+03	-1.12E+04	-2.38E+04
DL + LL + wave 150	-1.20E+05	-1.32E+05	3.65E+03	-2.96E+03	-8.81E+03	-2.51E+04
DL + LL + wave 180	-1.18E+05	-1.36E+05	-6.50E+01	-1.78E+03	-8.20E+03	-2.53E+04

^a All units are in N, m.

Table 6
Hot spot stress ranges in critical brace of Joint 2³ (un corroded model, one typical sea state).

Load combination	σ_1	σ_2	σ_3	σ_4	σ_5	σ_6	σ_7	σ_8
DL + LL + wave 0	8.26	-7.25	-15.09	-10.67	3.42	18.93	26.77	22.35
DL + LL + wave 30	14.81	-2.51	-15.01	-15.35	-3.35	13.97	26.47	26.81
DL + LL + wave 60	20.95	1.64	-17.08	-24.24	-15.64	3.67	22.39	29.54
DL + LL + wave 90	26.03	5.71	-17.07	-28.96	-23.01	-2.69	20.09	31.98
DL + LL + wave 120	24.69	2.10	-20.43	-29.70	-20.29	2.31	24.84	34.11
DL + LL + wave 150	14.53	-9.62	-26.38	-25.92	-8.52	15.63	32.38	31.92
DL + LL + wave 180	7.91	-14.86	-26.04	-19.08	1.92	24.68	35.87	28.91

^a All units are in MPa.

The forces and moments in the brace member are shown in Table 5 for each load combination and the calculated hot spot stress ranges are shown in Table 6. It was not necessary to perform any detailed local analysis separately, as no localized corrosion was found at the detail or on the members. This is also discussed in the proposed framework in Block D and in Section 2.4.1. The number of cycles to failure, N , was determined using the hot spot stress range for each sea state. In the HSS approach, the T curve should be selected as the relevant fatigue strength curve for tubular joints. The environmental effect on the T curve should be carefully examined, as described in Block D of the proposed framework presented in Fig. 1. The CP protected seawater curve was used in this case, as no severe pitting corrosion was found at the structural detail. The number of stress cycles in a year was determined using the zero up-crossing period (T_z) for the corresponding sea state. The yearly fatigue damage for each sea state was calculated, and the long-term yearly fatigue damage accumulation for all the sea states was calculated as per Eq. (14).

The fatigue damage in the selected joints was determined using both conventional and proposed framework approaches given in Section 2, Fig. 1. The fatigue damage and the thickness reduction versus the age of the jacket was plotted. The damage was plotted only for the most critical brace member of the considered critical joint. The results for the two critical joints are shown in Fig. 4(a) and Fig. 4(b) respectively. A DFF of three was applied in the calculation of the fatigue damage, to account for safety factors [101]. Hence, the DFF is included in the presented fatigue damage values by multiplying the calculated damage by three. The results are also shown for the case where on-site inspections are not possible. The remaining life was estimated using both conventional and proposed framework approaches, and the results are shown in Table 7. It is observed that the conventional approach over estimates the remaining fatigue life for the joint in the submerged zone. This is due to the fact that degradation is not modelled at all in cases of mild corrosion. A low remaining fatigue life is observed for the joint in the splash zone. The remaining life is only one year using the conventional approach; however, using the proposed approach, it is around 10 years and seems more realistic. Recommendations are made to improve the fatigue life of the joints in the splash zone by the use of fatigue improvement techniques.

3.5. Assessment for other limit states and strengthening/inspection plan for extended life

It is intended to extend the life of the considered jacket structure by 20 years. Based on the proposed approach, the remaining fatigue life is 37 years for the critical joint in the submerged zone; this is considered safe for further extension of life. However, the remaining life of the critical joint in the splash zone is found to be only 10 years as per the proposed approach, and mitigations to improve the fatigue life are suggested in the next section. The jacket should also be assessed for other limit state checks, as described in Block E of the proposed framework presented in Fig. 1. A 100-year return period wave, with a wave height of 7.92 m and time period of 8 s, was used for the wave loading. The jacket was analysed as per the design standard [94].

3.5.1. Serviceability limit state (SLS) checks

The free vibration natural time periods and vibration modes for the undamaged model were determined. The values of the natural time periods are 0.90 s, 0.90 s and 0.67 s, respectively, for the first three modes. The first and second modes are sway modes in the two transverse directions. The third mode corresponds to the torsional vibration mode. The variation of the natural period with ageing is shown in Fig. 5(a) and Fig. 5(b) for the conventional and proposed approaches respectively.

The variation of leg displacement in global X direction is also observed with ageing for the worst load combination. The variation of leg displacement with ageing is shown in Fig. 6(a) and Fig. 6(b) for the conventional and proposed approaches respectively. The displacements were found to be within satisfactory limits, and the SLS checks are not found to be critical.

3.5.2. Ultimate limit state (ULS) checks

Variation in the member capacities with ageing is found for critical members. The highly-stressed members were identified as critical members for the ULS checks. These are: one of the main legs (leg 1) and one vertical bracing at each elevation. The variation is shown in Fig. 7(a) and Fig. 7(b) for the conventional and proposed approaches respectively. From Fig. 7(a), it is observed that the bracing members have already violated the ultimate limit state check using the conventional approach and should have given some problems eight years earlier. However, the bracings are still in place and no damage has been reported. This is probably due to higher model parameters used in the conventional approach and hence leading to conservative

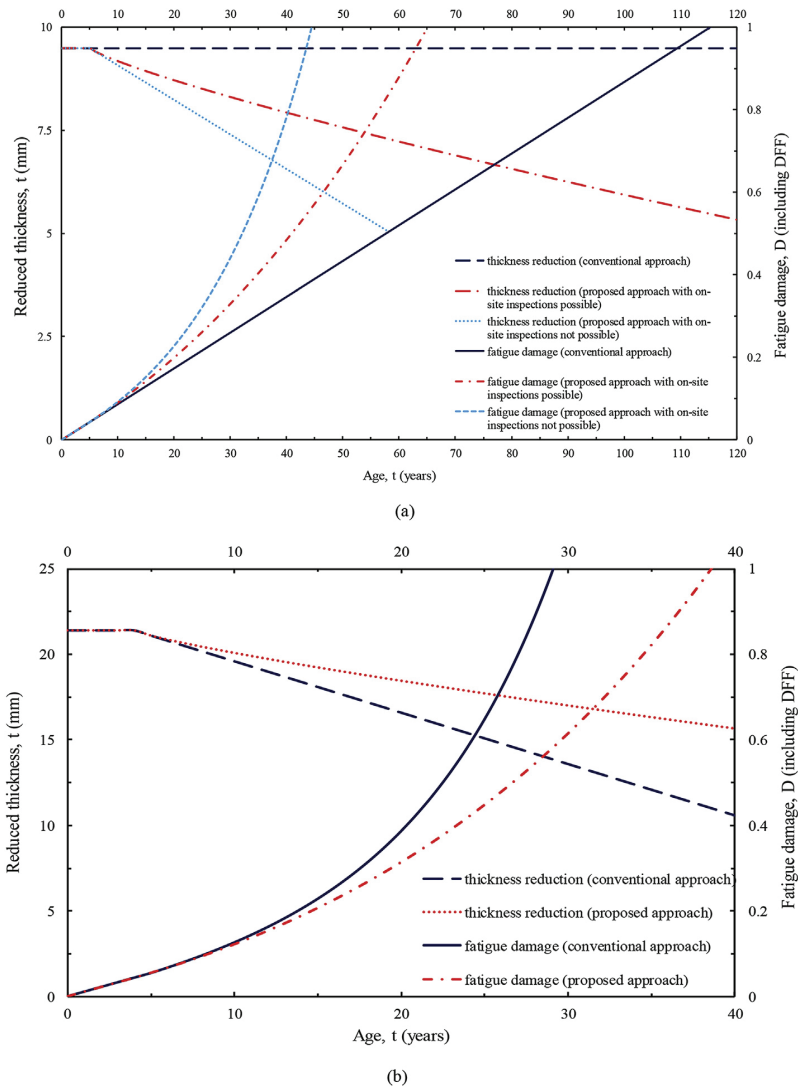


Fig. 4. Fatigue damage (including DFF) and member thickness variation with age in (a) critical joint 1 (b) critical joint 2.

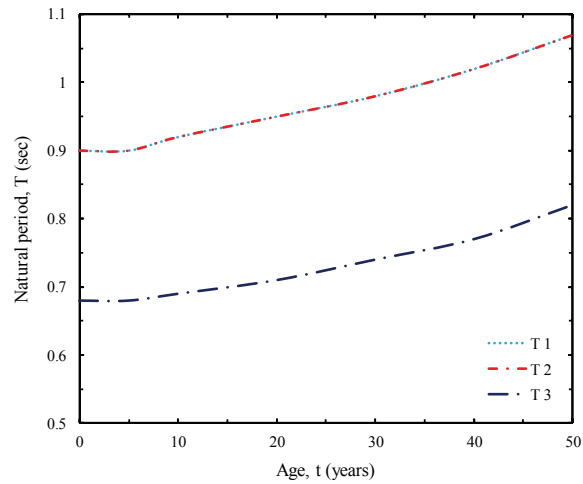
Table 7

Remaining design life of critical joints as per conventional and proposed framework approaches (in years).

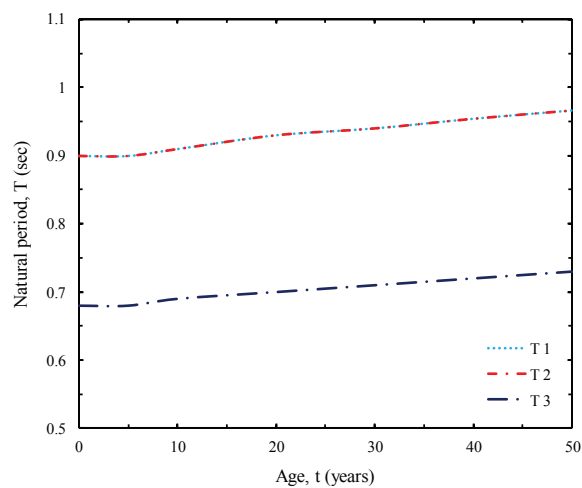
Approaches	Calculated total life from Fig. 4		Remaining life ^a	
	Joint 1	Joint 2	Joint 1	Joint 2
Conventional approach	115	29	87	1
Proposed approach	65	38	37	10

^a Obtained by reducing the current age (i.e. 28 years) from the calculated total life (i.e. when $D = 1$) as per Fig. 4.

results. The utilization ratio results seem more reasonable, using the proposed approach that include more precise model parameters. The expected remaining life of the central and bottom bracings is around four years and 12 years respectively. As the life span of the structure needs to be extended by 20 years, these members require potential strengthening for the safe operation of the structure during the extended life.



(a)



(b)

Fig. 5. Variation of natural periods with age (a) conventional approach (b) proposed approach.

3.5.3. Strengthening/inspection plan for extended life

The considered jacket structure was analysed for various limit states using the proposed framework. It is intended to extend the service life by another 20 years. Although the critical joint in the submerged zone is found safe for extended life as per the proposed approach, the critical joint in the splash zone has a remaining life of only 10 years, as shown in Fig. 5(b). The remaining life needs to be improved by 10 more years and hence a life factor of 2 is desired. It is recommended that the fatigue life of the joints in the splash zone be increased using fatigue improvement techniques such as hammer peening, grinding or TIG dressing. The fatigue life can be improved by up to a factor of 4 for yield strength higher than 350 MPa using these improvement techniques [58]. In case of hammer peening method, this factor depends on the tool used and workmanship. It is therefore recommended to perform fatigue testing of the detail, with and without hammer peening, to decide on a factor. Other mitigations, such as grouting of joints, reduction of operational loads or removal of marine growth, are also possible. More information on the fatigue life improvement techniques can be found in the standards and recent literature [58,106,111,112]. The ultimate limit state assessment was also carried out, with some bracing members found overstressed, as shown in Fig. 7. The proposal of suitable mitigation plans is recommended for these overstressed members. The mitigations

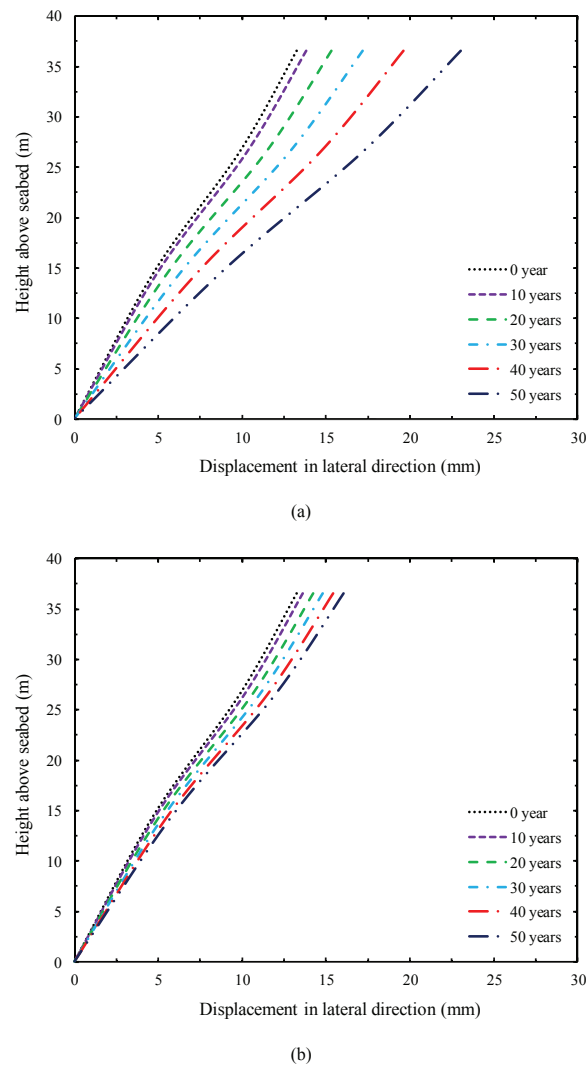
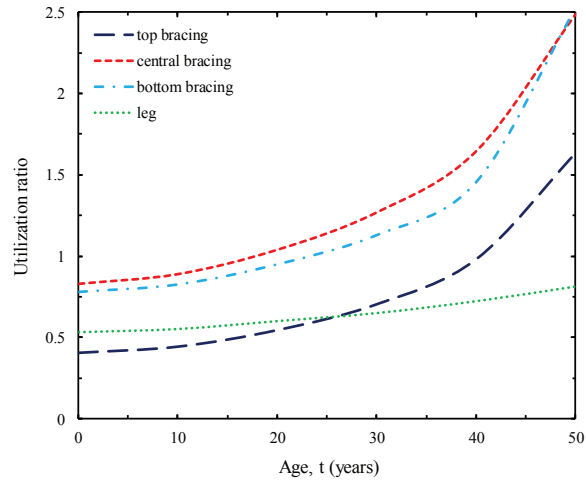
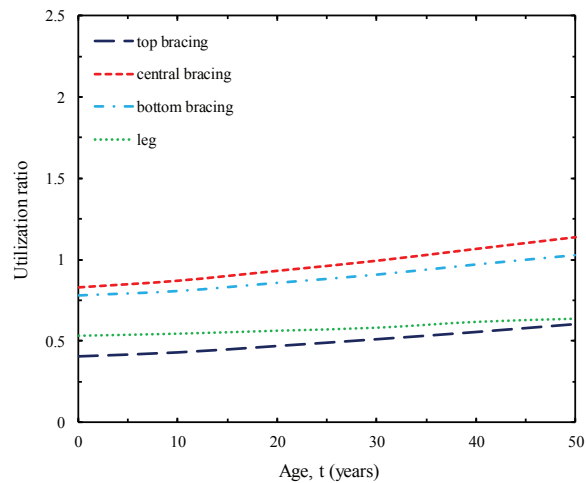


Fig. 6. Variation of leg displacement with age using (a) conventional approach (b) proposed approach.

can consist of possible strengthening, reduction of actions or even reduction of operational changes. The strengthening can be in the form of grouting of overstressed members, adding extra braces at overstressed locations, or adding stiffeners. The reduction of wave action is made possible by the regular removal of marine growth or anti-fouling protection. The structure should be reassessed after carrying out suitable mitigations. The strengthening mitigations are outside the scope of this paper, as they require close coordination with on-site inspection in order to check the feasibility options. The service life of the jacket structure can be extended if the proposed strengthening mitigations are found feasible offshore and the strengthened structure satisfies all limit state checks. It is also advisable to outline an inspection plan for the extended service life. Regular maintenance inspections should be performed, and the inspection intervals should be adjusted to take into account an increased likelihood of fatigue cracks. The time intervals should be as per standard codes and such that potential fatigue cracks are detected with a high level of certainty prior to becoming a threat to overall structural integrity. Refurbishment of the anodes in the CPS is also recommended. Additional CPS clamps can also be provided if necessary. Probabilistic inspection planning methods such as RBI can also be used to plan in-service inspection during the extended life. More details about the probabilistic inspection planning methods can be found in several condition monitoring codes and standards [46,47,92,106].



(a)



(b)

Fig. 7. Variation of ULS utilization ratio in critical members (a) conventional approach (b) proposed approach.

3.6. Comparison and discussion of results

The structural assessment of the considered jacket structure was carried out for various limit states. The time-dependent structural degradation was simulated using both the conventional and proposed framework approaches. In the absence of any thickness reduction measurements, site inspections were carried out, and the presence of mild corrosion was reported in the members of the submerged zone. Also, inspection reports mentioned patch corrosion in the members of the splash zone. Conventionally, these inspection findings have been interpreted in different ways due to the lack of suitable guidelines on simulating structural degradation. Mild corrosion is generally not modelled using conventional approaches. Moreover, patch type of corrosion is conventionally simulated using model parameters, provided by the codes, which are very conservative and can underestimate the remaining fatigue life. To reduce the variability in the interpretation of inspection findings, recommendations are made in the proposed framework on the selection of a suitable corrosion wastage model and its model parameters for members in various zones. The remaining fatigue life of critical joints was determined using both the

conventional and proposed framework approaches. An assessment was also carried out for SLS, by considering lateral displacement and modal vibrations. The ULS checks were also performed for all critical members.

The results shown in Fig. 4(a) and Table 7 demonstrate that the conventional approach overestimates the remaining fatigue life by around 2.3 times for critical joint 1, which is in the submerged zone. This is mainly due to the conventional approach neglecting degradation in cases of mild corrosion. Fig. 4(a) also shows that the proposed approach provides a too conservative remaining life of only 16 years for critical joint 1 when the case of on-site inspection is not possible. Fig. 4(b) and Table 7 show a short remaining life for the joint in the splash zone. The remaining life is found to be only one year using the conventional approach (i.e. model parameters obtained by the design standards). However, the remaining life is found to be around 10 years using the proposed framework approach and seems more reasonable. Recommendations are made to increase the fatigue life of the joints in the splash zone by means of fatigue improvement techniques.

An assessment was also performed for the free vibrations and other limit states. The natural periods of the structure were determined using both the conventional and proposed framework approaches and were found to be away from the wave periods. For SLS assessment, Fig. 6 shows that leg displacement increased by almost 70% at the end of the extended life using the conventional approach, while the increment in leg displacement up to the end of the extended life is around 21% using the proposed framework. Although the displacements are within the allowable limits for both approaches, the results obtained using the proposed approach seem more realistic. For ULS assessment, Fig. 7 shows that the bracing members are overstressed and violate the checks using the conventional approach. According to the conventional approach, the ULS checks of the central and bottom bracings were violated eight years earlier, as shown in Fig. 7. However, damage has still not been found on any of these members. This is probably due to the higher model parameters used in the conventional approach, hence leading to conservative results. However, such high levels of conservativeness are not desirable in life extension studies, and more precise model parameters should be used. The results of ultimate limit state checks seem more reasonable with the employment of the proposed approach, which includes the use of more precise model parameters. The central and bottom bracings are expected to violate the ULS checks after four and 12 years, respectively, using the proposed approach. In order to extend the life of structure by 20 years, strengthening mitigations are desired for these bracings for safe operation during the extended life. Strengthening can be provided as per the recommendations made above in Section 3.5.3.

4. Conclusions

In this paper, a framework is proposed to assess the structural integrity of existing aged offshore structures for possible life extension. The assessment should be carried out for all limit states. The FLS is considered the most critical limit state, and the framework is based on both safe life and damage tolerance approaches. The assessment procedure might involve going through all the paths of the framework, depending on the different degradation states of fatigue critical details in a single structure. The significance of the proposed framework is highlighted through a case study on an existing jacket structure. The framework is an attempt to provide more detailed case-dependent guidelines by adding relevant theories and models, which can capture the time-dependent structural degradation more precisely than currently available assessment guidelines and standards. It caters to the needs of practising engineers by providing recommendations on various issues such as simulation of structural degradation in the absence of any corrosion measurements, precision of loading history, as well as the effect of localized corrosion on stress concentration factors. Suggestions are also made on the determination of stress cycles and the selection of a suitable fatigue strength curve, particularly for severely corroded details. Recently developed precise fatigue damage theories are also included for a more accurate estimation of remaining life.

The simulation of structural degradation using the proposed framework approach is compared with the conventional approach, through the case study. Conventionally, either structural degradation is not modelled for cases of mild corrosion or model parameters are taken on the conservative side to represent patch corrosion. The model parameters recommended in the proposed framework constitute an attempt to reduce such variability in the selection of model parameters. The remaining fatigue life of critical joints is found more accurately using the proposed framework approach, as compared to the conventional approach. The structure can also be assessed for other limit states using the framework. Strengthening/inspection plans for extended life are also recommended. It can be concluded that the proposed framework provides an accurate prediction of remaining life, and the framework is a currently required tool to assess the structural integrity of an ageing jacket structure for possible life extension. The limitations of the proposed framework have been identified. The proposed framework considers only the functional ageing characterised by fatigue and corrosion. Other aspects of functional ageing such as erosion, creep, accumulated plastic deformation have not been considered. Moreover, technological ageing, knowledge based ageing and organisational ageing have been neglected and should be considered wherever applicable. The proposed framework is applied to the considered case study using a deterministic approach but can be used with probabilistic approaches as well. The significance of the proposed framework should be further highlighted on other ageing existing jacket structures using a few more case studies. Thereafter, the proposed framework and given model parameters may be adopted in the assessment standards in future.

Acknowledgements

The funding for this research work is supported by the Norwegian Ministry of Education and Research.

References

- [1] Ersdal G. Assessment of existing offshore structures for life extension. Doctoral thesis. Norway: University of Stavanger; 2005.
- [2] Galbraith D, Sharp JV, Terry E. Managing life extension in aging offshore installations. In: Society of Petroleum engineers international conference; 2005. Aberdeen.
- [3] Stacey A, Birkinshaw M, Sharp JV. Life extension issues for ageing offshore installations. In: Proceedings of the 27th international conference on offshore mechanics and arctic engineering; 2008. Estoril, Portugal.
- [4] Ersdal G, Selnes PO. Life extension of ageing petroleum facilities offshore. In: Society of Petroleum engineers international conference; 2010. Rio de Janeiro, Brazil.
- [5] Zettlemyer N. Life extension of fixed platforms. Tubul Struct XIII 2010;3–13.
- [6] Solland G, Sigurdsson G, Ghosal A. Life extension and assessment of existing offshore structures. In: Society of Petroleum engineers international conference; 2011. Doha, Qatar.
- [7] Nezamian A, Nicolson JR, Iosif D. State of art on life extension of existing offshore structures. In: Proceedings of the 31st international conference on ocean. Rio de Janeiro, Brazil: Offshore and Arctic Engineering; 2012.
- [8] Ersdal G, Sharp JV, Galbraith D. Ageing accidents – suggestions for a definition and examples from damaged platforms. In: Proceedings of the 33rd international conference on offshore mechanics and arctic engineering; 2014. San Francisco, California.
- [9] Galbraith D, Sharp JV. Recommendations for design life extension regulations. Poseidon report for Petroleum Safety Authority, Aberdeen. 2007.
- [10] Ersdal G, Hornlund E. Assessment of offshore structures for life extension. In: Proceedings of the 27th international conference on offshore mechanics and arctic engineering; 2008. Estoril, Portugal.
- [11] Stacey A, Sharp JV. Ageing and life extension considerations in the integrity management of fixed and mobile offshore installations. In: Proceedings of the 30th international conference on ocean. Rotterdam, The Netherlands: Offshore and Arctic Engineering; 2011.
- [12] Rusell J, Keith I. The challenges of extending the life of UK offshore installations. In: International Petroleum technology conference; 2014. Doha, Qatar.
- [13] Nezamian A, Iqbal K. Requalification and extension of service life and integrity requirements for offshore structures in Middle East. In: International Petroleum technology conference; 2015. Doha, Qatar.
- [14] Osmundsen P, Tveteras R. Decommissioning of petroleum installations—major policy issues. Energy Policy 2003;31(15):1579–88.
- [15] Max H, Bernstein B, Swamy S. A multi-attribute decision analysis for decommissioning offshore oil and gas platforms. Integr Environ Assess Manag 2015;11(4):594–609.
- [16] Alveberg LJ, Melberg VE. Facts 2013 Norwegian petroleum sector. Report by the Ministry of Petroleum and the Norwegian Petroleum Directorate, Publication number: Y-0103/14 E, ISSN 1502–5446. 2013.
- [17] Lønvik K, Leinum BH, Heier EB, Serednicki A, Gjørv OE, Myhre T, et al. Material risk – ageing of offshore installations. DNV report for Petroleum Safety Authority Norway, Norway. 2006.
- [18] Wintle J, Sharp J. Requirements for life extension of ageing offshore production installations. For Petroleum Safety Authority, TWI report 17554/1/08. 2008.
- [19] Hokstad P, Håbrekke S, Johnsen R, Sangesland S. Ageing and extension for offshore facilities in general and for specific systems. Norway: SINTEF Technology and Society; 2010.
- [20] Hornlund E, Ersdal G, Hinderaker HR, Johnsen R, Sharp JV. Material issues in ageing and life extension. In: Proceedings of the 30th international conference on ocean. Rotterdam, The Netherlands: Offshore and Arctic Engineering; 2011.
- [21] Stacey A, Sharp JV. Safety factor requirements for the offshore industry. Eng Fail Anal 2007;14(3): 442–258.
- [22] Garbatov Y, Soares CG, Parunov J, Kodvanj J. Tensile strength assessment of corroded small scale specimens. Corros Sci 2014;85:296–303.
- [23] Soares CG, Garbatov Y. Reliability of maintained ship hull girders subjected to corrosion and fatigue. Struct Saf 1998;20(3):201–19.
- [24] Popoola LT, Grema AS, Latinwo GK, Gutti B, Balogun AS. Corrosion problems during oil and gas production and its mitigation. Int J Industrial Chem 2013;4(1):4–35.
- [25] Adasooriya ND, Siriwardane S. Remaining fatigue life estimation of corroded bridge members. Fatigue Fract Eng Material Struct 2014;37(6):603–22.
- [26] Zhang W, Yuan H. Corrosion fatigue effects on life estimation of deteriorated bridges under vehicle impacts. Eng Struct 2014;71:128–36.
- [27] Dong W, Moan T, Gao Z. Fatigue reliability analysis of the jacket support structure for offshore wind turbine considering the effect of corrosion and inspection. Reliab Eng Syst Saf 2012;106:11–27.
- [28] Det Norske Veritas. Design of offshore wind turbine structures. 2014. DNV-OS-J101, May 2014.
- [29] Qin S, Cui W. Effect of corrosion models on the time-dependent reliability of steel plated elements. Mar Struct 2003;16(1):15–34.
- [30] Det Norske Veritas. Cathodic protection design. 2010. DNV-RP-B401, October 2010.
- [31] Moan T. Accidents and near-misses in the offshore oil and gas industry – how and why. Oslo: Norsk Offshore Day; 2007.
- [32] Moan T. Reliability-based management of inspection, maintenance and repair of offshore structures. Struct Infrastructure Eng 2005;1(1):33–62.
- [33] Det Norske Veritas. Probabilistic methods for planning of inspection for fatigue cracks in offshore structures. 2015. DNVGL-RP-0001, May 2015.
- [34] Stacey A, Birkinshaw W. Initiatives on structural integrity management of ageing North Sea installations. In: Proceedings of the 27th international conference on offshore mechanics and arctic engineering; 2008. Estoril, Portugal.
- [35] Stacey A. KP4: ageing and life extension inspection programme for offshore installations. In: Proceedings of the 30th international conference on ocean. Rotterdam, The Netherlands: Offshore and Arctic Engineering; 2011.
- [36] H.S.E. Key programme 4 (KP4) ageing and life extension. An interim report by the offshore division of HSE's hazardous installations directorate, UK. 2012.
- [37] Selnes PO, Ersdal G. Industry developed guidelines and standards for ageing and life extension. In: Proceedings of the 30th international conference on ocean. Rotterdam, The Netherlands: Offshore and Arctic Engineering; 2011.
- [38] American Petroleum Institute. Recommended practice for planning, design and constructing fixed offshore platforms—working stress design. 2000. API RP 2A-WSD, December 2000.
- [39] International Standards Organization. General principles on reliability for structures. 1996. ISO 2394, December 1996.
- [40] International Standards Organization. Bases for design of structures – assessment of existing structures. 2001. ISO 13822, December 2001.
- [41] International Standards Organization. Petroleum and natural gas industries – general requirements for offshore installations. 2002. ISO 19900, December 2002.
- [42] International Standards Organization. Petroleum and natural gas industries – offshore structures, fixed offshore structures. 2007. ISO 19902, December 2007.
- [43] H.S.E. Structural integrity management framework for fixed jacket structures. A report by Atkins Limited for the HSE, UK. 2009.
- [44] Standard NORSOK. Assessment of structural integrity for existing offshore load-bearing structures. 2009. N-006, March 2009.
- [45] Norwegian Oil and Gas Association. Recommended guidelines for the assessment and documentation of service life extension of facilities. 2008. OLF Guideline No. 122, June 2008.
- [46] American Petroleum Institute. Recommended practice for the structural integrity management of fixed offshore structures. 2014. API RP2 SIM, November 2014.
- [47] Det Norske Veritas. Probabilistic methods for planning of inspection for fatigue cracks in offshore structures. 2015. DNVGL-RP-C210, November 2015.
- [48] British Standard Institution. Guide to methods for assessing the acceptability of flaws in metallic structures. 2013. BS 7910, December 2013.
- [49] Nezamian A, Altmann J. An oil field structural integrity assessment for re-qualification and life extension. In: Proceedings of the 32nd international conference on ocean. Nantes, France: Offshore and Arctic Engineering; 2013.

- [50] Sharp JV, Terry EG, Wintle J. A framework for the management of ageing of safety critical elements offshore. In: Proceedings of the 30th international conference on ocean. Rotterdam, The Netherlands: Offshore and Arctic Engineering; 2011.
- [51] Liu H, Shi X, Chen X, Liu Y. Management of life extension for topsides process system of offshore platforms in Chinese Bohai Bay. *J Loss Prev Process Industries* 2015;35:357–65.
- [52] Almar-Naess A. *Fatigue handbook*. Trondheim, Norway: Tapir Publishers; 1985.
- [53] Lotsberg I. *Fatigue design of marine structures*. Cambridge: Cambridge University Press; 2016.
- [54] Haagensen PJ. Fatigue of tubular joints and fatigue improvement methods. *Prog Struct Eng Mater* 1997;1:96–106.
- [55] Gurney TR. *Fatigue of welded structures*. Cambridge: Cambridge University Press; 1979.
- [56] Suresh S. *Fatigue of materials*. Cambridge: Cambridge University Press; 1991.
- [57] Ziegler L, Muskulus M. Comparing a fracture mechanics model to the SN-curve approach for jacket-supported offshore wind turbines: challenges and opportunities for lifetime prediction. In: Proceedings of the 35th international conference on ocean. Busan, South Korea: Offshore and Arctic Engineering; 2016.
- [58] Det Norske Veritas. *Fatigue design of offshore steel structures*. 2016. DNVGL-RP-C-203, April 2016.
- [59] Mesmacque G, Garcia S, Amrouche A, Rubio-Gonzalez C. Sequential law in multiaxial fatigue, a new damage indicator. *Int J Fatigue* 2005;27:461–7.
- [60] Siriwardane S, Ohga M, Dissanayake R, Taniwaki K. Application of new damage indicator-based sequential law for remaining fatigue life estimation of railway bridges. *J Constr Steel Res* 2008;64:228–37.
- [61] Siriwardane S, Ohga M, Dissanayake R, Taniwaki K. Structural appraisal-based different approach to estimate the remaining fatigue life of railway bridges. *Struct Health Monit* 2010;9:323–39.
- [62] Austen IM. An analysis of the applicability of empirical fatigue crack growth relationships. BSC Research Report SH/PT/6795/79/B. London: British Steel Corporation; 1976.
- [63] Irving PE, McCartney LN. Prediction of fatigue crack growth rates: theory, mechanisms and experimental results. *Metal Sci* 1977;11(8/9):351–436.
- [64] Forman RG. Study of fatigue crack initiation from flaws using fracture mechanics theory. *Eng Fract Mech* 2003;4(2):333–45.
- [65] Paris PC, Erdogan FA. A critical analysis of crack propagation laws. *J Basic Eng* 1963;85D(4):528–34.
- [66] King RN. A review of fatigue crack growth rates in air and sea water. Offshore Technology Report, OTH 511. London: H.S.E. Books; 1998.
- [67] Chryssanthopoulos MK, Righiniotis TD. Fatigue reliability of welded steel structures. *J Constr Steel Res* 2006;62(11):1199–209.
- [68] Ayala-Uruga E, Moan T. Fatigue reliability-based assessment of welded joints applying consistent fracture mechanics formulations. *Int J Fatigue* 2007;29(3):444–56.
- [69] Yasser Y, Jeom KM. Ultimate strength reliability analysis of corroded steel-box girder bridges. *Thin Walled Struct* 2011;49:157–66.
- [70] Nguyen KT, Garbatov Y, Soares CG. Spectral fatigue damage assessment of tanker deck structural detail subjected to time-dependent corrosion. *Int J Fatigue* 2013;48:147–55.
- [71] Melchers RE. Modeling and prediction of long-term corrosion of steel in marine environments. *Int J Offshore Polar Eng* 2012;22:257–63.
- [72] Melchers RE. Modelling long term corrosion of steel infrastructure in natural marine environments. *Underst Biocorrosion* 2014:213–41.
- [73] Felii S, Morcillo M, Felii Jr S. The prediction of atmospheric corrosion from meteorological and pollution parameters—II. Long-term forecasts. *Corros Sci* 1993;34(3):415–22.
- [74] Soares CG, Garbatov Y. Reliability of maintained, corrosion protected plate subjected to nonlinear corrosion and compressive loads. *Mar Struct* 1999;12:425–45.
- [75] Soares CG, Garbatov Y, Zayed A, Wang G, Melchers R, Paik J. Non-linear corrosion model for immersed steel plates accounting for environmental factors. *Trans Soc Nav Archit Mar Eng* 2005;113:306–22.
- [76] Melchers RE. Probabilistic modelling of marine corrosion of steel specimens. In: Proceedings of the 5th international offshore and polar engineering conference; 1995. Hague, The Netherlands.
- [77] Melchers RE. Corrosion uncertainty modelling for steel structures. *J Constr Steel Res* 1999;52(1):3–19.
- [78] Bhandari J, Khan F, Abbassi R, Garaniya V, Ojeda R. Modelling of pitting corrosion in marine and offshore steel structures—a technical review. *J Loss Prev Process Industries* 2015;37:39–62.
- [79] Sidharth AAP. Effect of pitting corrosion on ultimate strength and buckling strength of plate—a review. *Dig J Nanomater Biostructures* 2009;4(4):783–8.
- [80] Abdel-Ghany R, Saad-Eldeen S, Leheta H. The effect of pitting corrosion on the strength capacity of steel offshore structures. In: Proceedings of the 27th international conference on offshore mechanics and arctic engineering; 2008. Estoril, Portugal.
- [81] Rokhlin SI, Kim JY, Nagy H, Zoofan H. Effect of pitting corrosion on fatigue crack initiation and fatigue life. *Eng Fract Mech* 1999;62(4):425–44.
- [82] Dolley EJ, Lee B, Wei RP. The effect of pitting corrosion on fatigue life. *Fatigue & Fract Eng Mater Struct* 2000;23(7):555–60.
- [83] Melchers RE. Pitting corrosion of mild steel in marine immersion environment — Part 1: maximum pit depth. *Corrosion* 2004;60(9):824–36.
- [84] Jakubowski M. Influence of pitting corrosion on fatigue and corrosion fatigue of ship structures Part I Pitting corrosion of ship structures. *Pol Marit Res* 2014;21(1):62–9.
- [85] Wang Y, Wang Y, Huang X, Cui W. A simplified maximum pit depth model of mild and low alloy steels in marine immersion environment. *J Ship Mech* 2008;6(1):401–17.
- [86] Linder J, Blom R. Development of a method for corrosion fatigue life prediction of structurally loaded bearing steel. *Corrosion* 2001;57(5):404–12.
- [87] Kumakura Y, Takanashi M, Fuji A, Kitagawa M, Ojima M, Kobayashi Y. Fatigue strength of coated steel plate in seawater. In: Proceedings of the 9th international offshore and polar engineering conference4; 1999. p. 108–13. Brest, France.
- [88] Forsyth DS, Yolken HT, Matzkanin GA. A brief introduction to nondestructive testing. *AMMTIAC* 2006;1(2):7–10.
- [89] Jamali SS, Zhao Y, Gao Z, Li H, Hee AC. In situ evaluation of corrosion damage using non-destructive electrochemical measurements—a case study. *J Industrial Eng Chem* 2016;43:36–43.
- [90] Kawakam Y, Hidesada Kanaji H, Oku K. Study on application of field signature method (FSM) to fatigue crack monitoring on steel bridges. *Procedia Eng* 2011;14:1059–64.
- [91] Li SY, Kim YG, Jung S, Song HS, Lee SM. Application of steel thin film electrical resistance sensor for in situ corrosion monitoring. *Sensors Actuators* 2007;120(2):368–77.
- [92] Standard NORSOK. Assessment of structural integrity for existing offshore load-bearing structures. 2015. N-006, Ed. 2, April 2015.
- [93] Aadedipe O, Brennan F, Kolios A. Review of corrosion fatigue in offshore structures: present status and challenges in the offshore wind sector. *Renew Sustain Energy Rev* 2016;61:141–54.
- [94] Standard NORSOK. Design of steel structures. 2013. N-004, February 2013.
- [95] Chakrabarti SK. *Hydrodynamics of offshore structures*. Boston: Computational Mechanics Publications; 1987.
- [96] Dean RG. *Spec. Rep. 1. Evaluation and development of water wave theories for engineering application, vols. 1 and 2*. Fort Belvoir, USA: U.S. Army, Coastal Engineering Research Center; 1974.
- [97] Budynas RG, Young WC, Sadegh A. *Roark's formulas for stress and strain*. eighth ed. USA: The McGraw-Hill Companies, Inc.; 2001.
- [98] Det Norske Veritas. Position monitoring. 2010. DNV-OS-E301, October 2010.
- [99] Miner MA. Cumulative damage. *J Appl Mech* 1945;12:159–64.
- [100] Det Norske Veritas. Riser fatigue. 2010. DNV-RP-F204, October 2010.
- [101] Det Norske Veritas. Design of offshore steel structures. General. 2016. DNV-OS-C101, April 2016.
- [102] Dattoma V, Giancane S, Nobile R, Panella FW. Fatigue life prediction under variable loading based on a new non-linear continuum damage mechanics model. *Int J Fatigue* 2006;28(2):89–95.

- [103] Huneau B, Mendez J. Evaluation of environmental effects on fatigue crack growth behaviour of a high strength steel in a saline solution with cathodic protection. *Int J Fatigue* 2006;28(2):124–31.
- [104] Adedipe O, Brennan F, Kolios A. Corrosion fatigue load frequency sensitivity analysis. *Mar Struct* 2015;42:115–36.
- [105] Vasudevan AK, Sadananda K. Classification of environmentally assisted fatigue crack growth behavior. *Int J Fatigue* 2009;31(11/12):1696–708.
- [106] NORSOK Standard. Condition monitoring of loadbearing structures. 1997. N-005, December 1997.
- [107] Det Norske Veritas. Fatigue assessment of ship structures. 2014. Classification Notes 30.7, April 2014.
- [108] Det Norske Veritas. Corrosion protection for wind turbines. 2016. DNVGL-RP-0416, March 2016.
- [109] Computers and Structures Inc. SAP2000. Berkeley: California; 1995., Version 17. .
- [110] BMT ARGOSS, Maritime consultancy and weather forecasting company, Amersfoort, 3824 MR, Netherlands.
- [111] Segers JPM. Life extension investigation and repair options for deteriorating marine structures. *From Sea to Shore? Meeting the Challenges of the Sea*, vol. 1. ICE Publishing; 2015. p. 1127–38.
- [112] Martinez LL, Barsoum Z, Paradowska A. State of the art: fatigue life extension of offshore installations. In: *Proceedings of the 31st international conference on ocean. Rio de Janeiro, Brazil: Offshore and Arctic Engineering*; 2012.

Paper IV

**A New Nonlinear Fatigue Damage Model Based Only on
S-N Curve Parameters**

Journal Paper

International Journal of Fatigue

October 2017, Volume 103, Pages 327-341.



Contents lists available at ScienceDirect

International Journal of Fatigue

journal homepage: www.elsevier.com/locate/ijfatigue

A new nonlinear fatigue damage model based only on S-N curve parameters



Ashish Aeran*, Sudath C. Siriwardane, Ove Mikkelsen, Ivar Langen

Department of Mechanical and Structural Engineering and Materials Science, University of Stavanger, P.O. Box 8600 Forus, N-4036 Stavanger, Norway

ARTICLE INFO

Article history:

Received 8 April 2017

Received in revised form 13 June 2017

Accepted 14 June 2017

Available online 16 June 2017

Keywords:

Fatigue life

Nonlinear damage accumulation

Variable amplitude loading

Damage model

ABSTRACT

Several fatigue damage models have been proposed in the past to overcome the shortcomings of the commonly used Miner's rule. However, application of these models requires either the determination of material parameters or modifications to the S-N curve of the material. To overcome these problems, a new fatigue damage model is proposed in this paper. The proposed model is based on the commonly available S-N curve parameters of the material and does not require any additional material parameter determination or S-N curve modification. The validity of the proposed fatigue damage model is confirmed by comparing the experimentally derived damage evolution curves for C 45 and 16 Mn steel. The proposed model gives a better agreement with these experimental results compared to previous models. A new damage transfer concept is also proposed for a more accurate estimation of fatigue life and is verified with experimental results for fatigue lives of six materials. The predicted fatigue lives are in better correlation with experimental results compared to Miner's rule and other recently proposed models. Finally, the application of the proposed model is illustrated by a case of welded joints. The model is applied to butt and fillet welded joints and the predicted fatigue lives show better agreement with experimental results compared to earlier models. The maximum and average deviations from the experimental results are 20% and 9% respectively. It is concluded that the proposed model can be easily applied by practising engineers for an accurate prediction of fatigue life.

© 2017 Elsevier Ltd. All rights reserved.

1. Introduction

Fatigue is one of the main causes of failures in both onshore and offshore steel structures such as bridges, oil platforms, ship structures, etc. [1]. These structures are subjected to variable amplitude loading (VAL) due to traffic loadings and harsh environmental sea conditions [2,3]. Under VAL, the fatigue damage is generally determined using the Palmgren-Miner rule. Palmgren developed a linear fatigue damage model, which was further developed by Miner in 1945 [4]. The model results in simple and reliable life calculations when detailed loading history is unknown. Due to its simplicity and ease of application, it is still widely used in the fatigue design of steel structures. Moreover, the current design codes and standards such as Eurocode [5], Det Norske Veritas [6], etc. also recommend the use of the Palmgren-Miner rule. However, Miner's rule may lead to inaccurate life predictions as it does not consider the damage due to loading sequence accurately [7,8]. Several damage

theories have been proposed since then to overcome these shortcomings.

Among the first improvements are the nonlinear Palmgren-Miner rule [9] and the Marco-Starkey model in 1954 [10]. The models have a constant parameter C that depends on the physical variables of the material and requires fatigue tests [11]. Several other models were proposed subsequently towards the end of the 1950s, but they required the determination of similar material parameters. Manson proposed a double linear damage rule (DLDR) in 1966 by replacing the linear Miner's rule with a set of two lines converging at a knee point [12]. The synergetic effect of the application of this rule in conjunction with a probabilistic approach based on P-S-N curves is recently shown by Correia et al. [13]. The DLDR was further improved and the double damage curve approach (DDCA) was proposed by Manson and Halford in 1981 [14]. Many other damage models were proposed in the 1980s and 1990s such as models by Lemaitre and Plumtree [15] and by Chaboche and Lesne [16]. These models were again based on material parameters p , α , β which can be determined only through extensive material testing. Although some of the above-mentioned models have shown good agreement with the experimental data for specific materials, determination of the knee point

* Corresponding author.

E-mail addresses: ashish.aeran@uis.no (A. Aeran), sasc.siriwardane@uis.no (S.C. Siriwardane), ove.mikkelsen@uis.no (O. Mikkelsen), ivar.langen@uis.no (I. Langen).

<http://dx.doi.org/10.1016/j.ijfatigue.2017.06.017>

0142-1123/© 2017 Elsevier Ltd. All rights reserved.

location and additional material parameters restricted their use in applied engineering problems [17]. A more detailed review of the damage models developed before 1998 can be found in an article by Fatemi and Yang [18]. These damage models are based on crack growth concepts, damage curve modifications and energy based theories, as well as on continuum damage mechanics. However, the application of these models is not found in any of the design standards as they require testing for the determination of material parameters.

Material testing was performed by some researchers to establish fatigue damage behaviour in 1999. These tests were based on the exhaustion of material ductility and estimated the instantaneous damage in material for a given stress amplitude or range [19]. As a result, the damage evolution curves for several materials were established, and these represent the variation in experimental observed damage with number of cycles to failure. Testing was also performed to develop damage models based on hardness increase during the fatigue of material [20]. Subsequently, damage models were proposed to fit such experimental data but were again dependent on material parameters with application to specific materials. In 2005, Mesmacque et al. proposed a sequential law, which does not require any material parameters other than the full-range S-N curve [8]. The application of this model was demonstrated in steel bridges in 2008 [21]. Though the model can capture the loading sequence and predicts the fatigue life accurately, its requirement for a full-range S-N curve restricts industrial application by practising engineers. Also, the design codes given S-N curves are based on detail categories, and the physical meaning of the intercept used for such details is not clear. Moreover, this law cannot be used with the design codes and standards having bilinear and trilinear S-N curves. Some other proposed models do not require material testing and overcome the shortcomings of Miner's rule using load interaction factors [22–24]. However, both the damage evolution curves and the fatigue life predictions differ significantly from experimental results, as will be shown later. Recently, some probabilistic approaches have been proposed by considering a probabilistic S-N field and providing a statistical distribution of the Miner's damage based on log-normal distribution [25,26]. The Miner's damage is related to a normalized variable V , which represents percentile curves in the S-N field unequivocally associated to probability of failure. These models can be applied for fatigue design of structural components subjected to variable amplitude loading and a recent application has been shown on riveted connection made of puddle iron from a bridge [27]. Also, a one parameter fatigue damage model has been proposed based on the concept of iso-damage curves [28]. As mentioned in the discussion of this paper, the model is based on S-N curves with a constant slope and is difficult to apply with bilinear or trilinear S-N curves in the current codes and standards. Also, the model parameter b is verified only for four types of steel and not for any other material. The model has only been compared to two step cyclic loading. Practical applications of the model to structural details have not been presented. Another non-linear fatigue damage model based on strain life curve has been proposed by Huffman and Beckman [29]. However, the applications of this model are not found as the design standards are based on stress life curves (i.e. S-N curves). Many other damage models exist in the literature, based on the concepts of continuum damage mechanics, energy conservation and entropy change. More details about these models can be found in several of the recently reviewed articles regarding fatigue damage theories such as by Santeccchia et al. [30] and by Silitonga et al. [31]. Although many fatigue damage models have been proposed in the literature, the existing codes and standards still use Miner's rule because of its simplicity and ease of application. This indicates the need for an equally simple,

easy to apply and accurate fatigue damage model for engineering applications/structural engineering problems. This becomes even more important for estimating the remaining life of ageing steel structures, where loading histories might be known as well. Such a model will not only predict the remaining life but will also help maintain the existing infrastructure more efficiently. The risk of failure and subsequent consequences will also be reduced using a more accurate model.

To overcome above mentioned problems, an accurate and easy-to-apply fatigue damage model is proposed in this paper. The proposed damage model does not require any material testing and depends only on the commonly available S-N curve of the material or its corresponding detail category. Moreover, it does not require a full-range S-N curve and can be easily applied by practising engineers using the partially known S-N curves given in design standards. These features of the proposed model make it novel compared to other recently proposed model which either require additional material parameters or modifications to the S-N curve. Also, unlike earlier models, the proposed model can be applied to design detail categories using the corresponding S-N curve in the design standards. As a result, the proposed model can be easily implemented by practising engineers for fatigue analysis of several practical problems involving design detail categories. The proposed model considers the loading sequences, along with the interactions between them, and provides better agreement with experimental data compared to previously proposed models. Due to its unique features and better accuracy, the proposed model can provide a platform to design and maintenance communities for an efficient use of existing ageing steel infrastructure by predicting their remaining safe life more accurately. The proposed model and associated damage transfer concept is well illustrated by figures and flowcharts for easy understanding and application by practising engineers. Initially, the paper presents the proposed damage model in detail. The fatigue damage evolution curves are then plotted using the proposed model, and model verification is performed by comparing the results with the experimental data for two materials. Later, a damage transfer concept is proposed for the estimation of fatigue lives under given variable amplitude loading conditions. The proposed model and associated damage transfer concept is further verified with the experimental fatigue life of six materials under block loading conditions. Finally, the proposed model is applied to welded joints, which are used in several engineering applications. Hence, the applicability, validity and significance of the proposed model is confirmed.

2. Proposed fatigue damage model

A new and easy-to-apply fatigue damage model is proposed in this section. The proposed model does not require any material parameters and depends only on commonly available S-N curves. The model can be applied to several engineering applications by practising engineers using the S-N curves in design codes and standards. The proposed model considers the loading sequences, along with the interactions between them.

2.1. Proposed damage index

The new damage index is proposed, as shown in Eq. (1), by understanding the nonlinear fatigue damage evolution of materials under constant amplitude loading conditions. The fatigue damage, D , can be represented by the absolute value of proposed D_i as shown in Eq. (2):

$$D_i = 1 - \left[1 - \frac{n_i}{N_i} \right]^{d_i} \quad (1)$$

$$D = \text{Abs}(D_i) \quad (2)$$

where n_i is the number of cycles for stress amplitude (or range) σ_i , N_f is the corresponding number of cycles to failure which can be obtained from the S-N curve, and Abs represents the absolute value. The model parameter δ_i can be determined using the S-N curve and is discussed in the next section.

2.2. Model parameter, δ_i

The proposed model has a single parameter δ_i and is given in Table 1. The proposed model also represents some of the earlier proposed damage models for specific values of δ_i . The value of δ_i is determined by studying the work by past researchers and understanding the fatigue damage behaviour of the materials under constant amplitude loading.

The proposed new formulation of model parameter δ_i can be determined using the partially known S-N curves in design standards as shown in Table 1. The parameter can also be determined for any design detail category (i.e. constructional discontinuities where stress concentration is induced) and does not require any additional material testing or modification to the S-N curve. The earlier proposed models require detailed material testing for the determination of material parameters such as p , α as shown in Table 1. This not only restricts the application of such models for a different material, but is also a hindrance in their practical application for design detail categories. Due to these limitations in earlier proposed models, the Miner's rule is still widely used and recommended by the design standards. The proposed model not only overcomes the shortcomings of the Miner's rule and can also be applied by practicing engineers using only the S-N curve of the material or the considered detail category. In the following sections, verification of the proposed model is performed for both the damage evolution curves and fatigue life estimations of several materials.

3. Verification of proposed model with experimental damage evolution

The proposed fatigue damage model is verified by comparing the experimental results for damage evolution curves. C 45 and 16 Mn steels are used for this verification [19].

3.1. Comparison of predicted fatigue damage evolution curves with experimental results of C 45 steel

This material is of interest to the authors due to its currently increasing use in offshore structures [32]. The yield strength and ultimate tensile strength for this material are 371.7 MPa and 598.2 MPa, respectively [19]. In the past, experiments were conducted on this material for constant amplitude stresses, and the fatigue damage was determined by measuring the static relative ductility change in the material [19]. The experiments were conducted at 330.9 MPa and 405.8 MPa stress amplitudes (with zero mean stress); the results are shown in Fig. 1(a) and (b), respectively. Fatigue damage curves are also plotted for each of the stress amplitudes using the proposed model. The proposed model is also

compared with some of the recently developed models which do not require additional material testing, other than their S-N curve.

3.2. Comparison of predicted fatigue damage evolution curves with experimental results of 16 Mn steel

The damage evolution curves were also determined experimentally for 16 Mn steel by measuring the static relative ductility change in material [19]. For this material, the yield strength is 382.5 MPa, and the ultimate tensile strength is 570.7 MPa. The experiments were conducted at 337.1 MPa and 373.5 MPa stress amplitudes (with zero mean stress); the damage evolution curves are shown in Fig. 2(a) and (b), respectively. Fatigue damage curves are also plotted for each of the stress amplitudes using the proposed model. The proposed model is also compared with some of the recently developed models which do not require additional material testing, other than their S-N curve.

3.3. Discussion of comparison of damage evolution curves with experimental data

From Fig. 1(a) and (b), it is seen that the proposed model gives good prediction of the damage curves for material C 45 and is in good agreement with the experimental results. The damage evolution curves for 16 Mn steel are shown in Fig. 2(a) and (b) for the two stress amplitudes. Again, it is seen that the proposed model is in good agreement with the experimental results and can predict the damage behaviour more accurately. The proposed model is also compared with some of the other recently developed models which do not require additional material testing, other than their S-N curve. It is seen that the model developed by Kwofie and Rahbar [22] is not in good agreement with the experimental data and is equivalent to Miner's rule while predicting the damage behaviour. The models proposed by Liakat and Khonsari [23] and Lv et al. [24] seem to give the same damage evolution curves for both of the considered materials. The sequential law proposed by Mesmacque et al. [8] is also compared with the experimental data. It is seen that the model gives good agreement with the experimental results. However, the model requires the determination of the full-range S-N curve, thereby restricting its use by practising engineers. After comparing all the curves shown in Figs. 1 and 2, it is concluded that the proposed model predicts the real damage evolution behaviour quite accurately for the two materials considered, when compared to previous models. The damage curves can be plotted using the proposed model without determining additional material parameters and using only code-given S-N curves. A new damage transfer concept is proposed in the next section for the prediction of fatigue life using the proposed model.

4. Damage transfer concept

A new damage transfer concept is proposed for a more reliable estimation of the fatigue life under variable amplitude loading. This concept is based on the use of fatigue damage evolution curves and a proposed load interaction factor. The proposed interaction factor considers the loading sequences along with the inter-

Table 1
Parameters of the proposed model and its special cases [4,15,19].

δ_i	Damage model	Remarks
$-1.25/\ln N_f$	Proposed model	Only based on commonly available S-N curves
1	Miner's rule, 1945 [4]	Most commonly used, but is inaccurate under VAL
$1/p + 1$	Lemaitre and Plumtree, 1979 [15]	p is a material constant determined by damage evolution curves based on cyclic stress ranges
$1/1 - \alpha$	Shang and Yao, 1999 [19]	α is a material constant determined by damage evolution curves based on static relative ductility change of material

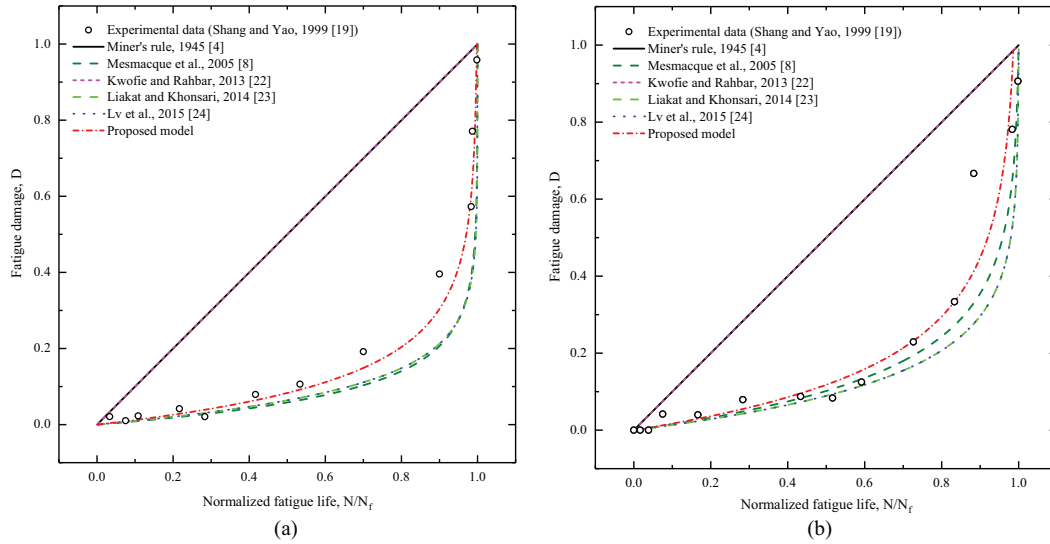


Fig. 1. Comparison of theoretically predicted fatigue damage evolution with experimental damage of C 45 steel for stress amplitude (a) $\sigma_a = 330.9$ MPa (b) $\sigma_a = 405.8$ MPa.

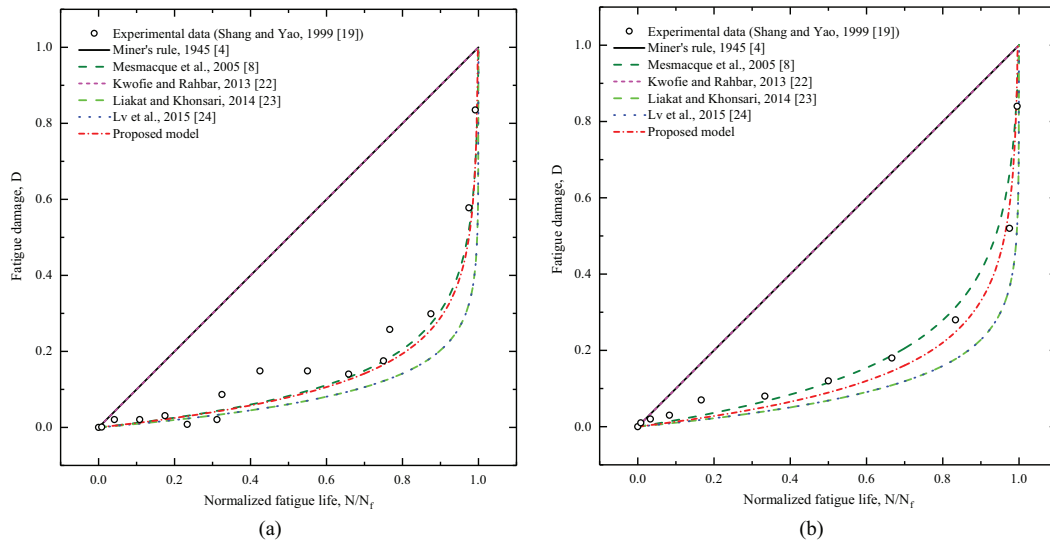


Fig. 2. Comparison of theoretically predicted fatigue damage evolution with experimental damage of 16 Mn steel for stress amplitude (a) $\sigma_a = 337.1$ MPa (b) $\sigma_a = 373.5$ MPa.

actions between them. The interaction factor is first explained in detail, followed by the damage transfer concept.

4.1. Proposed load interaction factor

A load interaction factor is proposed while transferring the damage from one stress level to the next. This factor considers the loading sequence along with the interaction effects and leads to a more precise estimation of fatigue life under variable amplitude loading. The load sequence represents the sequence of stress ranges in a

random stress-time history, whereas the load interactions represent the interface between adjoining stress ranges and their magnitudes. The proposed interaction factor is given by Eq. (3):

$$\mu_{i+1} = \left(\frac{\sigma_i}{\sigma_{i+1}} \right)^2 \tag{3}$$

where σ_i and σ_{i+1} are the two adjoining stress levels and μ_{i+1} represents the load interaction between these stress levels.

For high-low amplitude loading, the interaction factor is more than one, and the predicted fatigue lives are shorter than that pro-

posed by Miner’s rule. Similarly, for low-high amplitude loading, the interaction factor is less than one, and the predicted life is longer than Miner’s prediction. In both these cases, it has been seen that the predicted life is closer to the experimental results than is the case with Miner’s prediction. The proposed model is the square of the ratio between the adjoining stress levels. This is determined based on the observed experimental behaviour of several materials under cyclic loading. It is seen that the damaging effects are much worse than expected in the case of high-low loading and vice versa in the case of low-high loading. Under the high-low loading, initial microcracks start appearing at an early stage as a result of initial large strains (high stress). Subsequently, these microcracks start propagating even under small strains (low stress) and result in more material damage sooner than that predicted by Miner’s rule. Moreover, the initial large strains will cause a roughening of the surface and will lead to the creation of more potential crack initiation sites under the subsequent small strains [33]. On the other hand, under the low-high amplitude loading, the microcracks start developing at a very late stage and result in less damage compared to Miner’s rule and, hence, a longer fatigue life. The proposed load interaction factor is a novel contribution to the field of fatigue damage theories and leads to a more precise estimation of fatigue life under variable amplitude loading compared to other recently proposed models.

4.2. Proposed damage transfer concept

The proposed damage transfer concept is based on the use of fatigue damage evolution curves and a proposed load interaction factor. The damage for a given stress level can be determined using the damage evolution curve of the considered material. This damage is then transferred to the next stress level by determining the effective number of cycles using the proposed load interaction factor. The physical meaning of the concept is to assume the same damage state of the material, while transferring the loading state from one stress level to the next and determining the effective number of cycles required to cause this damage.

Suppose a material is subjected to a certain stress amplitude (or range) σ_i for n_i number of cycles at load level i . The number of cycles to failure for this stress state is N_i and can be determined from the S-N curve of the material. The fatigue damage from this stress range can be determined using the proposed damage model and can be written as shown in Eqs. (4) and (5):

$$D_i = 1 - \left[1 - \frac{n_i}{N_i} \right]^{\delta_i} \tag{4}$$

$$\delta_i = \frac{-1.25}{\ln N_i} \tag{5}$$

In the proposed damage transfer concept, it is required to transfer the same damage to the next stress amplitude (or range) σ_{i+1} , using the proposed load interaction factor, μ_i . By doing so, the effective number of cycles $n_{(i+1),eff}$ can be determined corresponding to the stress range σ_{i+1} , using Eqs. (6) and (7). This effective number of cycles for stress range σ_{i+1} would give the same damage D_i , had it been present right from the start:

$$D_i = 1 - \left[1 - \frac{n_{(i+1),eff}}{N_{i+1}} \right]^{\delta_{i+1}} \tag{6}$$

$$n_{(i+1),eff} = \left[1 - (1 - D_i)^{\frac{N_{i+1}}{\delta_{i+1}}} \right] \cdot N_{i+1} \tag{7}$$

Considering n_{i+1} as the number of cycles for stress state σ_{i+1} , the total number of cycles for loading step $i + 1$ can be written using the Eq. (8):

$$n_{(i+1),total} = n_{(i+1),eff} + n_{(i+1)} \tag{8}$$

Subsequently, the cumulative damage at loading step $i + 1$ is written as

$$D_{i+1} = 1 - \left[1 - \frac{n_{(i+1),total}}{N_{i+1}} \right]^{\delta_{i+1}} \tag{9}$$

The corresponding fatigue damage can be determined using the Eq. (10):

$$D = Abs(D_{i+1}) \tag{10}$$

This damage transfer technique is continued until the fatigue damage D becomes one, denoting fatigue failure. The proposed damage transfer concept is explained graphically, as shown in Fig. 3. For ease of understanding and application, the concept is also explained using a simple flowchart in Fig. 4.

5. Verification of proposed model with experimental results for fatigue life

The proposed damage model and the associated damage transfer concept is applied to predict the fatigue life of several materials subjected to multilevel block loadings. The results are compared with experimentally obtained fatigue lives to demonstrate the accuracy of the proposed model. The fatigue lives predicted by the proposed model are also compared with those predicted by other models. The fatigue life comparison under two-block loading is firstly discussed, followed by those under four and five-block loading. The six materials are selected based on their practical applicability to the structural engineering field.

5.1. Comparison of calculated fatigue life with experimental life for C 45 steel

C 45 steel is known for its wear resistance and capability for quenching and tempering. It is mainly used for manufacturing tools, machines, or structures that sustain impact loading, sharp cutting edges, corrosion and brittle fracture, and to provide high

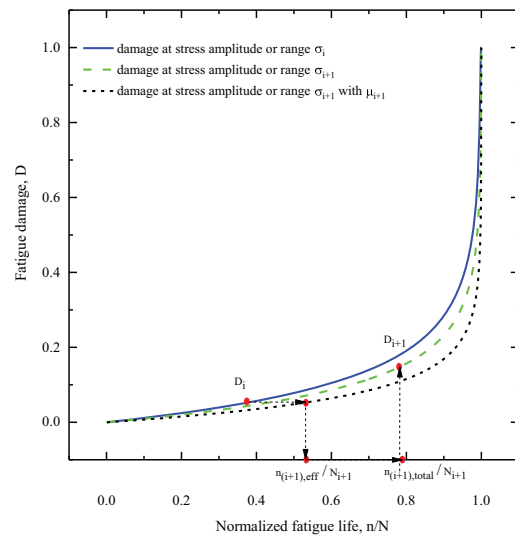


Fig. 3. Graphical representation of the proposed damage transfer concept.

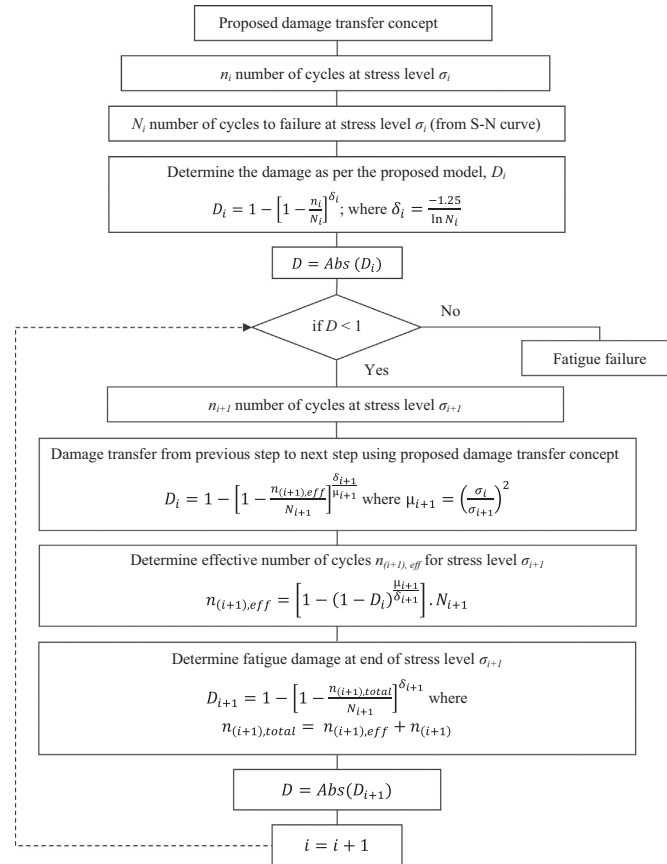


Fig. 4. Flow chart of the proposed damage transfer concept.

performance and weldability. This material is also widely used in the oil and gas industry and is used in the manufacture of several structural elements for offshore structures [32].

Uniaxial fatigue tests were performed under stress controlled and fully reversed loading conditions by past researchers [19]. Two sets of tests were performed corresponding to high-low and low-high loading patterns. The stress amplitudes for the two sets are 331.5 MPa and 284.4 MPa. The loading spectrum for low-high loading is 284.4–331.5 MPa, and the observed fatigue lives are shown in Fig. 5(a). The high-low loading spectrum is 331.5–284.4 MPa, and the observed fatigue lives are shown in Fig. 5(b). The solid line refers to ideal conformity of the results. The dotted lines represent a scatter band with a coefficient of two. The proposed model satisfies the ideal conformity for most of the tests as compared to other models. Also, all the predicted fatigue lives are within the scatter band unlike some of the other models.

5.2. Comparison of calculated fatigue life with experimental life for 16 Mn steel

The 16 Mn steel is a high-strength low-alloy structural steel with carbon as the main element. It has excellent mechanical and welding properties and is widely used in many industries [34]. It finds a

wide range of applications in petrochemical plants and in the nuclear industry [35]. Moreover, it is widely used for welding structural parts in the manufacture of ships, railways, vehicles, bridges, boilers, pressure vessel containers, steel oil tanks, etc.

Uniaxial fatigue tests were performed on this material under similar test conditions as those of C 45 [19]. Two sets of tests were performed corresponding to high-low and low-high loading patterns. The stress amplitudes used in the testing are 372.65 MPa, 392.3 MPa and 562.9 MPa. The loading spectrum for low-high loading is 372.65–392.3 MPa; the observed fatigue lives are shown in Fig. 6(a). The low-high loading spectrum is 562.9–392.3 MPa, and the observed fatigue lives are shown in Fig. 6(b). The solid line refers to ideal conformity of the results. The dotted lines represent a scatter band with a coefficient of two. The proposed model satisfies the ideal conformity for majority of tests and some of the predicted fatigue lives are outside the scatter band for two tests as also discussed in later section.

5.3. Comparison of calculated fatigue life with experimental life for Al 2024-T42

The Al 2024-T42 material is one of the best known high-strength aluminum alloys, with copper as a primary element. It

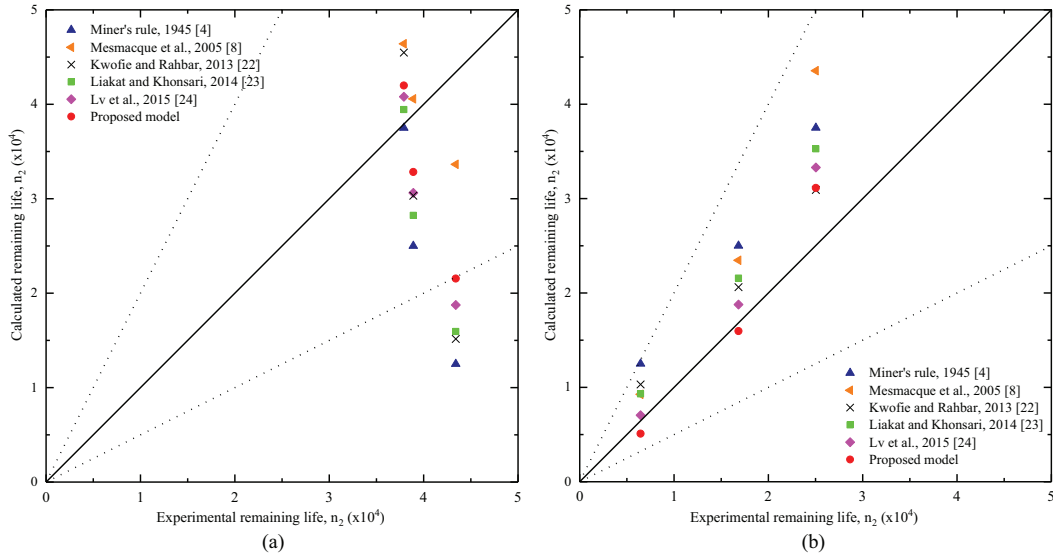


Fig. 5. Comparison of calculated fatigue life with experimental life for C 45 steel under (a) low-high loading (b) high-low loading.

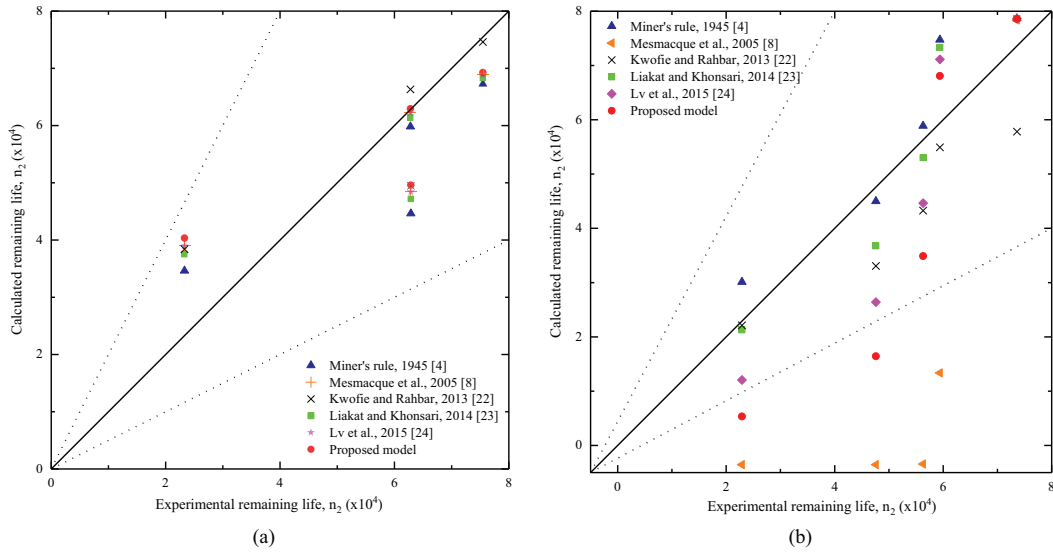


Fig. 6. Comparison of calculated fatigue life with experimental life for 16 Mn steel under (a) low-high loading (b) high-low loading.

is widely used in engineering applications where high strength-to-weight ratio, as well as high fatigue strength, is required. It is one of the best materials for the aircraft industry, owing to its light weight and corrosion-resistant properties, and it is used to make structural components for aircraft, such as wing and fuselage structures. In sheet form, it is used in commercial and military aircraft for fuselage skins. In addition to the aircraft industry, the material finds several other applications in hardware, truck wheels and several appliances for the transportation industry.

The tests were performed on this material under two-stage loading up to the failure point [20]. The stress amplitudes under two-stage loading are 150 MPa and 200 MPa. The loading spectrum for low-high loading is 150–200 MPa, and the observed fatigue lives are shown in Fig. 7(a). The high-low loading spectrum is 200–150 MPa; the observed fatigue lives are shown in Fig. 7(b). The solid line refers to ideal conformity of the results. The dotted lines represent a scatter band with a coefficient of two. The proposed model satisfies the ideal conformity for almost all the tests

as compared to other models. Also, all the predicted fatigue lives are within the scatter band unlike some of the other models.

5.4. Comparison of calculated fatigue life with experimental life for 30CrMnSiA

Th 30CrMnSiA is a type of steel with excellent mechanical properties such as high strength and toughness after quenching and tempering [36]. It is typically used for mechanical parts in equipment manufacturing industries [37]. It is also a very important steel for the aerospace industry and is used in the manufacture of many parts such as motor frames, actuating cylinder piston rods, pump plungers, etc. [38]. It is also employed for making shafts, piston type parts, automobiles and other kinds of special wear-resistant parts.

Uniaxial two-level fatigue tests have been performed on this material by past researchers [39]. The tests were performed for three sets of loadings and for both high-low and low-high loading sequences in each set. The stress levels in the three sets are 732–836 MPa, 850–940 MPa and 797–9440 MPa. The remaining fatigue life is determined using the proposed model, and the observed fatigue lives are shown in Fig. 8 for all loading sets. The comparison of fatigue life with experimental data and other models is shown in Figs. 9–11 for each of the three loading sets. The observed fatigue lives cannot be determined using the Mesmacque model, as the full-range S-N curve data is not available for this material. In all the figures, the solid line refers to ideal conformity of the results and the dotted lines represent a scatter band with a coefficient of two. The proposed model satisfies the ideal conformity for majority of the tests as compared to other models. Also, all the predicted fatigue lives are within the scatter band unlike some of the other models.

5.5. Comparison of calculated fatigue life with experimental life for Al 6082-T6

The Al 6082-T6 alloy is a medium-strength alloy with excellent corrosion-resistant properties. It has the highest strength among

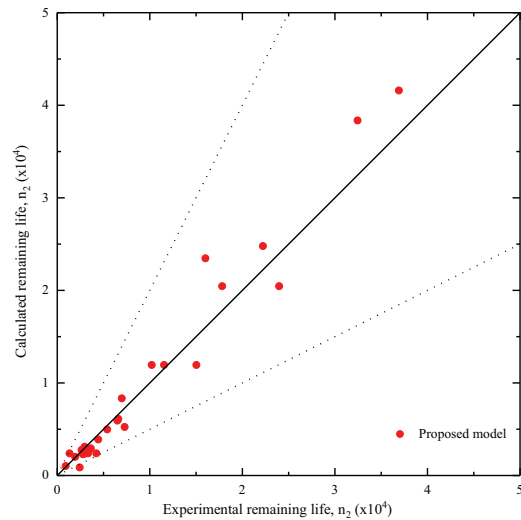


Fig. 8. Comparison of calculated fatigue life with experimental life for 30CrMnSiA under all loading sets.

the 6000 series alloys, due to its higher percentage of manganese. Therefore, it has replaced alloy Al 6061 in many applications. This material is typically used in highly stressed applications, trusses, bridges, cranes and in several other transport applications. In plated form, it is the most commonly used aluminum alloy for machining.

The verification of the proposed model is performed for this material under multilevel staged loading. The experiments were performed by Chaboche and Lesne in 1988, and three different loading sequences were applied [16]. The different stress ampli-

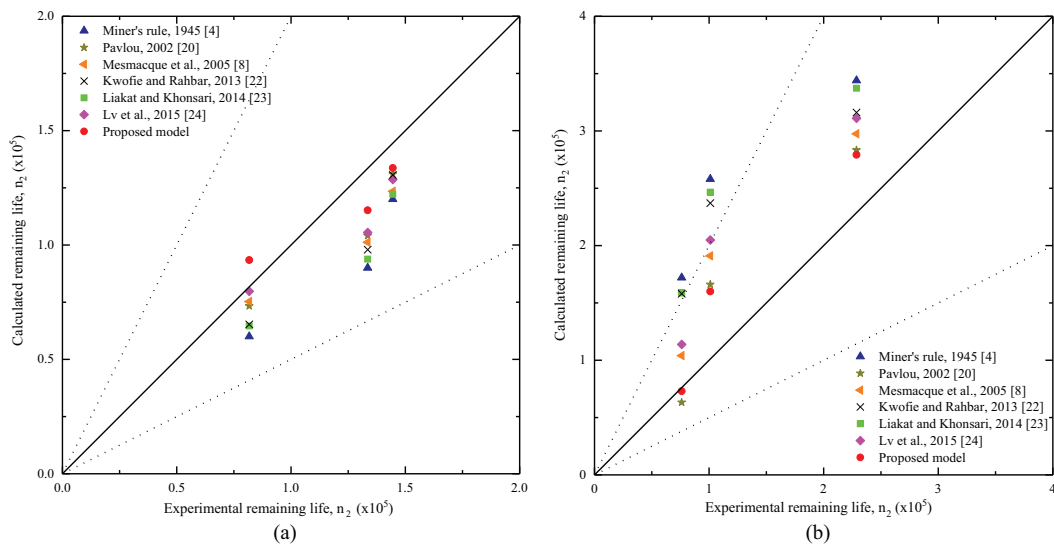


Fig. 7. Comparison of calculated fatigue life with experimental life for Al 2024-T42 under (a) low-high loading (b) high-low loading.

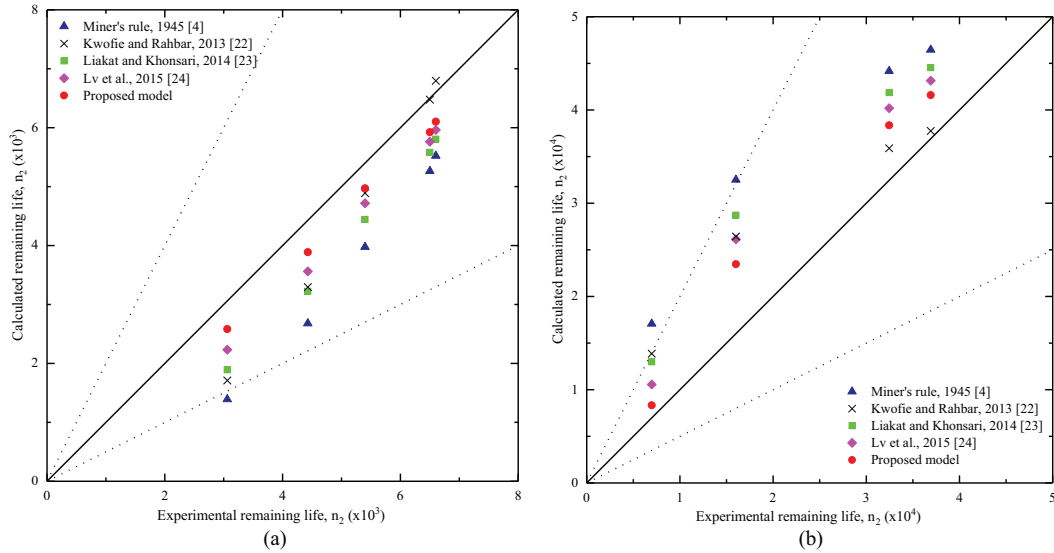


Fig. 9. Comparison of calculated fatigue life with experimental life for 30CrMnSiA under the loading (a) low high i.e. $\sigma_1 = 732$, $\sigma_2 = 836$ (b) high low i.e. $\sigma_1 = 836$, $\sigma_2 = 732$.

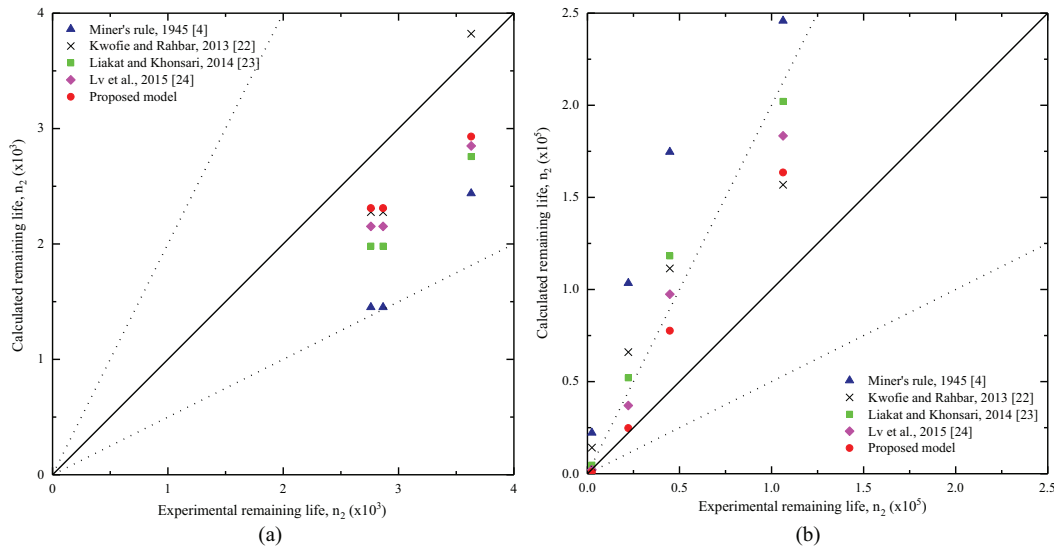


Fig. 10. Comparison of calculated fatigue life with experimental life for 30CrMnSiA under the loading (a) low high i.e. $\sigma_1 = 797$, $\sigma_2 = 940$ (b) high low i.e. $\sigma_1 = 940$, $\sigma_2 = 797$.

tudes and corresponding number of cycles to failure are shown in Table 2. The loading sequences are shown in Table 3.

The remaining life (n_4) under each loading sequence is estimated using the proposed model and shown in Fig. 12. The solid line refers to ideal conformity of the results. The dotted lines represent a scatter band with a coefficient of two. The proposed model satisfies the ideal conformity for majority of the tests as compared to other models. Also, all the predicted fatigue lives are within the scatter band unlike some of the other models.

5.6. Comparison of calculated fatigue life with experimental life for Al alloy

The proposed model is also verified under multilevel staged loading for this material. The tests were performed in the high cycle fatigue region under variable amplitude block loading [8]. The stress amplitudes and corresponding number of cycles to failure are shown in Table 4, while the loading sequences can be seen in Table 5.

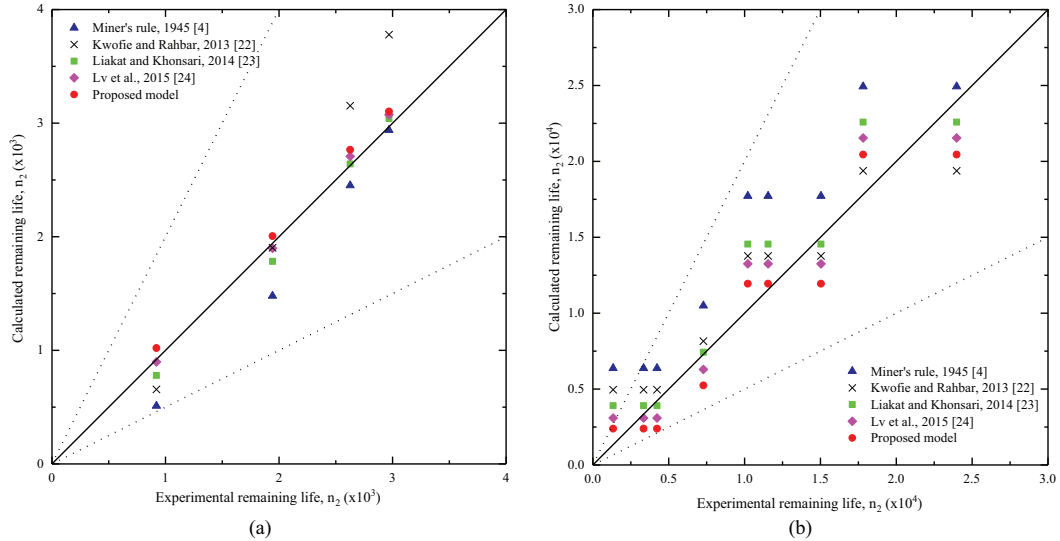


Fig. 11. Comparison of calculated fatigue life with experimental life for 30CrMnSiA under the loading (a) low high i.e. $\sigma_1 = 850, \sigma_2 = 940$ (b) high low i.e. $\sigma_1 = 940, \sigma_2 = 850$.

Table 2
Stress amplitudes and cycles to failure for Al 6082-T6 [16].

Block	1	2	3	4
Stress amplitude	240	260	280	305
N_f	394,765	180,660	87,612	38,000

The remaining life (n_4 for the first two sets and n_5 for the third set) is estimated using the proposed model; the results are presented in Fig. 13. The solid line refers to ideal conformity of the results. The dotted lines represent a scatter band with a coefficient of two. The proposed model satisfies the ideal conformity for few tests only. Also, the predicted fatigue life is outside the scatter band for one test.

6. Application and verification of proposed model for fatigue life estimation of welded joints

The proposed model is applied and further verified for estimating the fatigue life of welded joints. These welded joints are used in a number of engineering applications such as vehicles, electrical mobile units (EMUs), etc., and an accurate prediction of life is necessary for the safety of both passengers and vehicles. There has been a significant advancement in technology over the past couple of decades. As a result, conventional diesel locomotives are increasingly being replaced by faster electrical mobile units (EMUs). These EMUs can reach speeds of 250 km/h and above, as

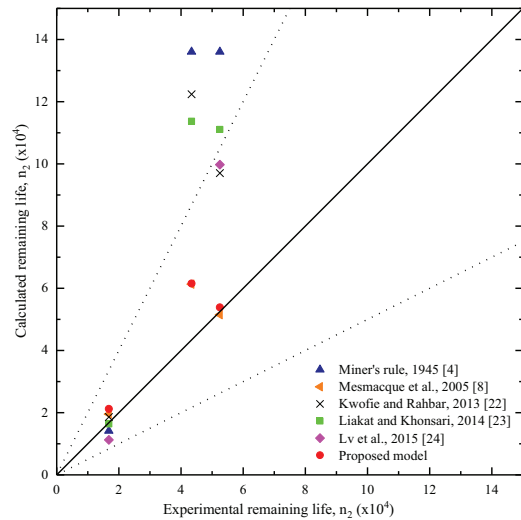


Fig. 12. Comparison of calculated fatigue life with experimental life for Al 6082-T6 under multilevel block loading.

compared to the diesel locomotives which used to have typical speeds of 160 km/h [40]. While the advancement of the vehicle

Table 3
Experimental results under four steps block loading for Al 6082-T6 [16].

Load sequence	n_1	n_2	n_3	n_4
Increasing load sequence (1-2-3-4)	103,000	26,258	19,427	16,800
Decreasing load sequence (4-3-2-1)	10,950	19,427	26,258	52,500
Random load sequence (3-4-2-1)	19,427	10,950	26,258	43,400

Table 4
Stress amplitudes and cycles to failure for Al alloy [8].

Block	1	2	3	4
Stress amplitude	260	275	290	305
N_f	840,000	442,000	240,000	135,000

technology is good for the fast commuting of passengers, it also puts vehicle safety, as well as the safety of people, at huge risk. Such risks arise from the increasingly daily passenger loads, inefficient maintenance of vehicles, as well as ageing of the car bodies, which, in these high-speed trains are generally made from aluminum alloy due to its light weight, security and comfort [41]. However, as a result of the high thermal conductivity coefficient and high linear expansion coefficient, aluminum alloys can have complex welding deformations and stresses at the welded joints. The softening and embrittlement of these welded joints can have a serious effect on the structural strength of the car body. It is reported that the failure of the car body usually occurs in the welded joint, and the major cause is fatigue loading [41,42], which is most critical for the welded connections; it is therefore important to estimate the fatigue life accurately to minimize the risks.

Much research has been carried out in the past on the fatigue properties of welded aluminum joints. Recently, a group of researchers performed fatigue tests on such aluminum joints to thoroughly understand the fatigue properties and predict the life more accurately [41,42]. Firstly, the experimental setup and considered joints are explained in detail, followed by the P-S-N curves of the selected critical joints. The P-S-N curves represent the standard S-N curves together with a given survivability percentage [43]. Recently, some advanced statistical models have been proposed to obtain P-S-N curves more accurately [44]. A generalization of the Castillo and Fernández-Canteli probabilistic model is presented in this paper by considering a generic fatigue damage parameter ψ and obtaining a family of Weibull percentile curves, $p-\psi-N_f$. The applications of this model have been shown on shear splice extracted from a railway bridge [45] and on double shear riveted connections [46]. The P-S-N curves can also be obtained using statistical models recommended by the design standards. The American Standard ASTM E739-91 [47] is used in this study to obtain the survival probabilities of 0.5, 0.90 and 0.99. Finally, using these curves, the experimental results of the fatigue life are compared with the proposed damage model. Hence, the significance and applicability of the proposed model has been highlighted.

6.1. Experimental setup and considered welded joint details

The fatigue tests were performed for both butt and fillet welded joints by using the PLG-200 fatigue testing machine. The test specimens are shown in Fig. 14. The base material of the specimen is aluminum alloy ENAW6005 having the main chemical composition in mass percentage as: 0.35Fe, 0.6–0.9Si, 0.1Mn, 0.1Ti, 0.4–0.6Mg, 0.1Cu, 0.1Zn and 0.1 Cr [41,42]. The tensile strength and yielding strength of the base material are 270 and 225 MPa, respectively. The specimens were tested under a four-point bending load cycle with cyclic stress ratio $R = -1$. The load-time history follows

Table 5
Experimental results under four and five steps block loading for Al alloy [8].

Load sequence	n_1	n_2	n_3	n_4	n_5
Increasing sequence 1-2-3-4	210,000	110,500	60,000	54,000	–
Decreasing sequence 4-3-2-1	33,750	60,000	110,500	32,250	–
Random sequence 1-2-3-4-1	168,000	88,400	48,000	27,000	199,600

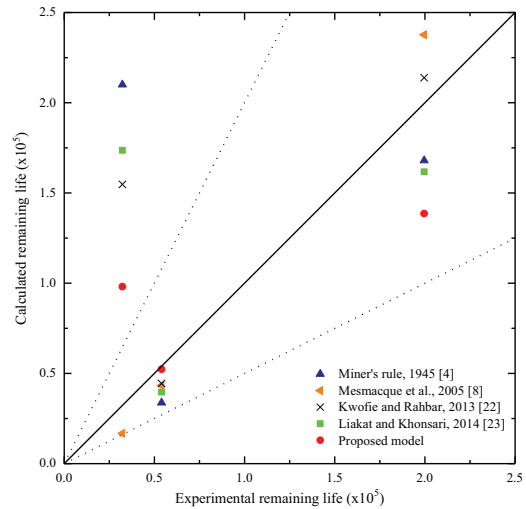


Fig. 13. Comparison of calculated fatigue life with experimental life for Al alloy under multilevel block loading.

the sine function. The loading frequency is 110 Hz, and room temperature is 20–30 °C [41,42].

Based on the conducted experiments on the two welded joints, P-S-N curves were derived as shown in Figs. 23 and 24 for the butt and fillet welded joint, respectively [41,42]. The yellow, pink and black colour data points in Figs. 15 and 16 represent the 99%, 90% and 50% survivability percentages of the test specimens, respectively.

6.2. Experimental results for fatigue life of considered welded joints

Experiments were also conducted under two-stage block loading for each of the considered welded joints. The load sequence considered for the butt-welded joint are 104–74 MPa and 89–74 MPa for high-low loading sequence, and 74–89 MPa and 74–104 MPa for low-high loading sequences. The load sequences considered for the fillet welded joint are 93–73 MPa and 83–73 MPa under high-low loading, and 73–83 MPa and 73–93 MPa under low-high loading, respectively. The experimentally obtained fatigue lives for the butt and fillet welded joint are shown in Tables 6 and 7, respectively [41,48].

6.3. Verification of proposed model with experimental results

The proposed damage model is compared with experimentally obtained fatigue lives for the considered welded joints. The loading sequences are given in Tables 6 and 7. Some of the recently proposed models have also been included in the comparison. The comparison of fatigue life is shown in Figs. 17 and 18 for the butt and fillet welded joints, respectively. The maximum and average devi-

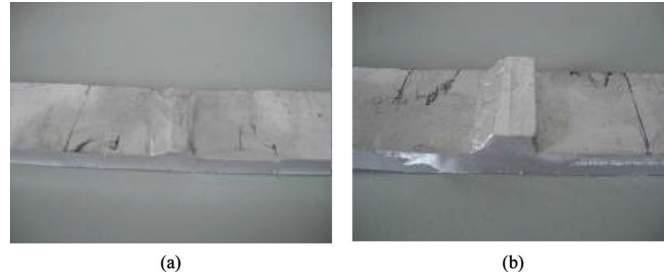


Fig. 14. (a) Butt welded joint test specimen (b) Fillet welded joint test specimen [41,42].

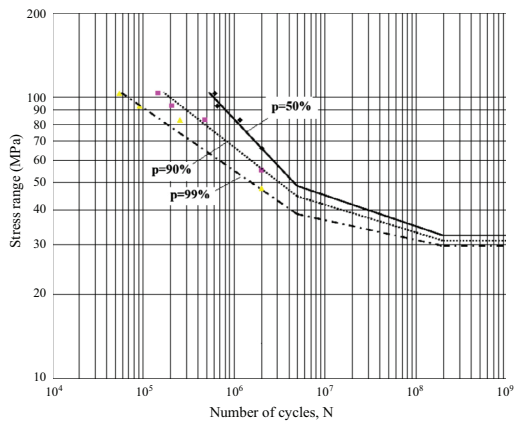


Fig. 15. P-S-N curves for butt welded joint [41,48].

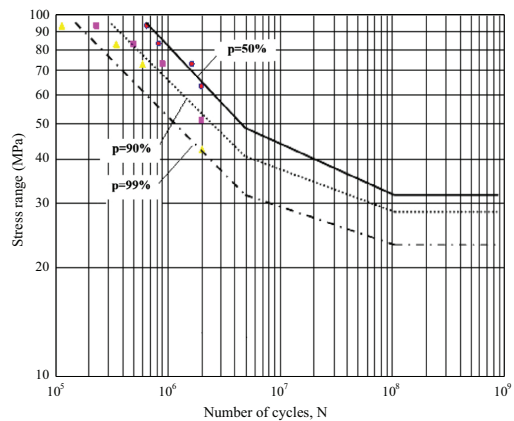


Fig. 16. P-S-N curves for fillet welded joint [41,48].

ations from the experimental results are 20% and 9% respectively. The solid line refers to ideal conformity of the results. The dotted lines represent a scatter band with a coefficient of two.

7. Discussion of the comparison of predicted fatigue lives using proposed model with experimental fatigue lives

The predicted fatigue lives using proposed model is verified with experimental fatigue lives under two, four and five steps block loadings for six materials. The model is further verified with the experimental data for butt and fillet welded joints. The fatigue lives obtained using proposed model are found in good agreement with experimental values as shown in Section 6 and Fig. 19. The comparison of fatigue lives for C 45 steel is shown in Fig. 5 (a) and (b) for low-high and high-low loadings respectively. It is seen that there is some variability in the results for low-high loading condition. However, the proposed model is in good agreement with experimental results for high-low loading compared to Miner’s rule and earlier models. The comparison of fatigue lives for 16 Mn steel is shown in Fig. 6(a) and (b). Though the proposed model shows good agreement with experimental results under low-high loading, there is a large scatter in the predicted lives under high-low loading. The probable reason for this large scatter in the proposed model and in all other models can be the stress levels being very near to the ultimate stress of the material during the high-low loading tests. The predicted lives using proposed model is also compared with experimental data for Al 2024-T42 material. The model gives good agreement with experimental results under both low-high and high-low loading conditions as shown in Fig. 7(a) and (b) respectively. Hence, the proposed model can predict the fatigue life for this material accurately without the need of full-range S-N curve or hardness measurements, as used by Mesmacque et al. [8] and Pavlou [20]. The model can therefore be easily applied by practicing engineers for predicting fatigue lives using only the commonly available S-N curve of this material. The proposed model is further verified for 30CrMnSiA steel under different loading conditions and shows a good agreement with experimental results as shown in Fig. 8.

The proposed model is also verified with experimental data for two materials under multi step block loadings. The comparison for Al 6082-T6 alloy is shown in Fig. 12. The proposed model gives better agreement with experimental results compared to Miner’s and other models. The comparison for Al alloy is shown in Fig. 13 under five step block loading conditions. Though there is some variability and scatter in the results, the proposed model is better than other models for most of the cases. The sequential law proposed by Mesmacque et al. [8] also gives a good agreement with experimental results for few cases. However, the requirement of full-range S-N curve and complex calculations are some challenges in its practical application in the industry. Finally, the proposed model is used to predict the fatigue lives of welded joints used in several engineering applications. The predicted lives using the proposed model are in good agreement with the experimental lives compared to Miner’s rule and other models. The maximum and average devia-

Table 6
Experimental fatigue lives for fatigue testing on butt welded joint [41,48].

Load set	σ_1 (MPa)	σ_2 (MPa)	n_1 (*1000)	n_2 (*1000)	N_{f1}	N_{f2}
Set 1	104	74	109.9	797.6	549,300	1,540,100
Set 2	89	74	176.1	1029.2	880,500	1,540,100
Set 3	74	89	770.1	545.6	1,540,100	880,500
Set 4	74	104	770.1	418.9	1,540,100	549,300

Table 7
Experimental fatigue lives for fatigue testing on fillet welded joint [41,48].

Load set	σ_1 (MPa)	σ_2 (MPa)	n_1 (*1000)	n_2 (*1000)	N_{f1}	N_{f2}
Set 1	93	73	309.9	587.5	619,800	1,546,100
Set 2	83	73	476.1	681.1	9,523,00	1,546,100
Set 3	73	83	509.2	708.2	1,546,100	952,300
Set 4	73	93	773.0	426.4	1,546,100	619,800

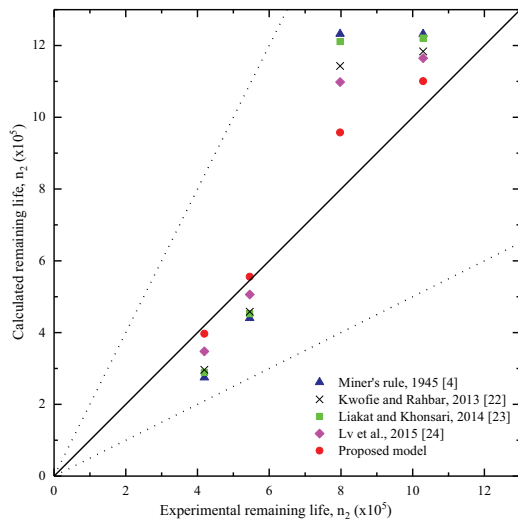


Fig. 17. Comparison of calculated fatigue life with experimental life for butt welded joint.

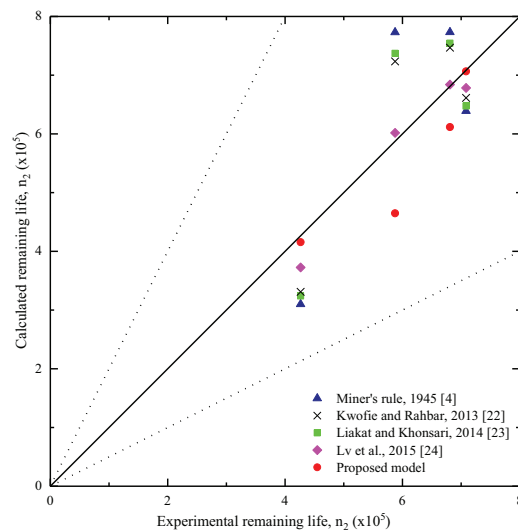


Fig. 18. Comparison of calculated fatigue life with experimental life for fillet welded joint.

tions from the experimental results are 20% and 9% respectively for these joints as shown in Fig. 17 and 18. The scatter bands having a coefficient two is also plotted in all the figures where experimental fatigue life is compared with predicted life. The predicted fatigue lives are lying within the scatter band for 97% of the total tests considered except for two tests out of 62 experimental tests, one each in Figs. 6(b) and 13. The possible reasons for these couple of tests could be uncertainties in experimental setup and/or material defects or possible fabrication errors. The proposed model gives better agreement with experimental results for most of the cases compared to other models and hence the proposed model can be used by practicing engineers for better life predictions of many engineering applications.

8. Conclusions

The paper presents a new fatigue damage model. The proposed model considers the loading sequences along with the interactions between them. The model does not require any material parameters, other than the commonly available S-N curve parameters,

which are generally used with Miner's rule. The proposed model is novel as it consists of a new damage index and a load interaction factor. The major advantage of proposed model is that it does not require detail material testing or modifications to the S-N curve. Also, unlike earlier models, the proposed model can be applied to design detail categories using the corresponding partially known S-N curve in the design standards. Therefore, the proposed model can be easily implemented by practicing engineers for fatigue analysis of several engineering problems. The model is verified with both the damage evolution curves and fatigue life estimations. It is concluded that the damage curves plotted using the proposed model are in good agreement with the available experimental data for two considered materials. The model is further verified with fatigue life predictions under two-level and multilevel block loading for six materials. It is concluded that, using the proposed model, the life predictions are better than the widely used Miner's rule as well as some of the recently developed models. The applicability, validity and significance of the proposed model is also highlighted, by comparing its predicted fatigue lives with the experimentally observed fatigue lives of welded joints used in sev-

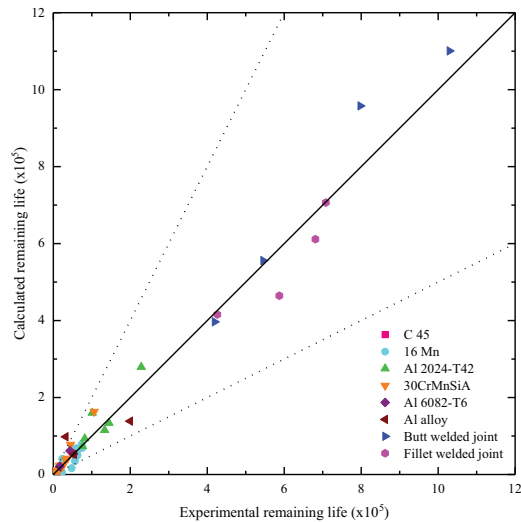


Fig. 19. Comparison of fatigue lives predicted by proposed model with experimental lives for all material and welded joints.

eral engineering applications. The predicted fatigue lives of these joints are found to be in good agreement with the experimental results. The significant differences between the fatigue lives calculated by both the proposed model and Miner's rule underline the significance of having accurate fatigue damage models for structural detail categories. It is concluded that the proposed model can be used for better fatigue life predictions and can be easily applied by practising engineers using only the code-given S-N curves. The applicability, significance and validity of the proposed fatigue damage model should be further verified in the future by applying the model to real case studies. Also, the implementation of the proposed model in conjunction with the probabilistic models proposed by Castillo and Fernandez-Canteli will be investigated in the future studies.

Acknowledgements

The funding for this research work is supported by the Norwegian Ministry of Education and Research.

References

- [1] Almar-Naess A. Fatigue handbook. Trondheim (Norway): Tapir Publishers; 1985.
- [2] Imam B, Righiniotis TD, Chryssanthopoulos MK. Fatigue assessment of riveted railway bridges. *Int J Steel Struct* 2005;5(5):485–94.
- [3] Lotsberg I. Fatigue design of marine structures. Cambridge (UK): Cambridge University Press; 2016.
- [4] Miner MA. Cumulative damage in fatigue. *J Appl Mech* 1945;A159–64.
- [5] Eurocode 3: design of steel structures – Part 1–9: fatigue. NS-EN 1993-1-9:2005+NA:2010, 2010.
- [6] Det Norske Veritas Fatigue design of offshore steel structures; 2016. DNVGL-RP-C203; 2016.
- [7] Suresh S. Fatigue of materials. Cambridge (UK): Cambridge University Press; 1998.
- [8] Mesmacque G, Garcia S, Amrouche A, Rubio-Gonzalez C. Sequential law in multiaxial fatigue, a new damage indicator. *Int J Fatigue* 2005;27(4):461–7.
- [9] Leve HL. Cumulative damage theories. In: Madayag AF, editor. Metal fatigue: theory and design; 1960. p. 170–203.
- [10] Marco SM, Starkey WL. A concept of fatigue damage. *Trans ASME* 1954;76(6):626–62.
- [11] Hwang W, Han KS. Cumulative damage models and multi-stress fatigue life prediction. *J Compos Mater* 1986;20(2):125–53.
- [12] Manson SS, Freche JC, Ensign CR. Application of a double linear damage rule to cumulative fatigue. In: Fatigue crack propagation. ASTM STP 415. p. 384–412.
- [13] Correia JAF, De Jesus AMP, Balsón S, Calvente M, Fernandez-Canteli A. Probabilistic non-linear cumulative fatigue damage of the P355NL1 pressure vessel steel. In: Pressure vessels and piping conference: materials and fabrication, paper no. PVP2016-63920, vol. 6A. ASME; 2016.
- [14] Manson SS, Halford GR. Practical implementation of the double linear damage rule and damage curve approach for treating cumulative fatigue damage. *Int J Fract* 1981;7:169–92.
- [15] Lemaitre J, Plumtree A. Application of damage concepts to predict creep-fatigue failures. *J Eng Mater Technol* 1979;101(3):284–92.
- [16] Chaboche JL, Lesne PM. A non-linear continuous fatigue damage model. *Fatig Fract Eng Mater Struct* 1988;11(1):1–17.
- [17] Goodin E, Kallmeyer A, Kurath P. Evaluation of nonlinear cumulative damage models for assessing HCF/LCF interactions in multiaxial loadings. In: Proceedings of the 9th national turbine engine high cycle fatigue (HCF) Conference; 2004 March 16–19; Pinehurst, North Carolina, US; 2004.
- [18] Fatemi A, Yang L. Cumulative fatigue damage and life prediction theories: a survey of the state of the art for homogeneous materials. *Int J Fatigue* 1998;20(1):9–34.
- [19] Shang DG, Yao WX. A nonlinear damage cumulative model for uniaxial fatigue. *Int J Fatigue* 1999;21(2):187–94.
- [20] Pavlou DG. A phenomenological fatigue damage accumulation rule based on hardness increasing, for the 2024-T42 aluminum. *Eng Struct* 2002;24(11):1363–8.
- [21] Siriwardane S, Ohga M, Dissanayake R, Taniwaki K. Application of new damage indicator-based sequential law for remaining fatigue life estimation of railway bridges. *J Construct Steel Res* 2008;64:228–37.
- [22] Kwofie S, Rahbar N. A fatigue driving stress approach to damage and life prediction under variable amplitude loading. *Int J Damage Mech* 2013;22(3):393–404.
- [23] Liakat M, Khonsari MM. An experimental approach to estimate damage and remaining life of metals under uniaxial fatigue loading. *Mater Des* 2014;57:289–97.
- [24] Lv Z, Huang HZ, Zhu SP, Gao H, Zuo F. A modified nonlinear fatigue damage accumulation model. *Int J Damage Mech* 2015;24(2):168–81.
- [25] Fernández-Canteli A, Blasón S, Correia JAF, De Jesus AMP. A probabilistic interpretation of the Miner number for fatigue life prediction. *Frattura ed Integrità Strutturale* 2014;30:327–39.
- [26] Balsón S, Correia JAF, De Jesus AMP, Calçada RAB, Fernandez-Canteli A. A probabilistic analysis of Miner's law for different loading conditions. *Struct Eng Mech* 2016;60:71–90.
- [27] Correia JAF, De Jesus AMP, Fernández-Canteli A, Calçada RAB. Fatigue damage assessment of a riveted connection made of puddle iron from the Fão bridge using the modified probabilistic interpretation technique. *Procedia Eng* 2015;114:760–7.
- [28] Rege K, Pavlou DG. A one-parameter nonlinear fatigue damage accumulation model. *Int J Fatigue* 2017;98:234–46.
- [29] Huffman PJ, Beckman SP. A non-linear damage accumulation fatigue model for predicting strain life at variable amplitude loadings based on constant amplitude fatigue data. *Int J Fatigue* 2013;48:165–9.
- [30] Santeccchia E, Hamouda AMS, Musharavati F, Zalnezhad E, Cabibbo M, El Mehtedi M, et al. A review on fatigue life prediction methods for metals. *Adv Mater Sci Eng* 2016;9573524:1–26.
- [31] Silitonga S, Maljaars J, Soetens F, Snijder HH. Survey on damage mechanics models for fatigue life prediction. *Heron* 2013;58(1):25–60.
- [32] Abed FH, Saffarini MH, Abdul-Latif A, Voyiadjis GZ. Flow stress and damage behavior of C45 steel over a range of temperatures and loading rates. *J Eng Mater Technol* 2017;139(2). 021012–021012-8.
- [33] Watson P, Hoddinott DS, Norman JP. Periodic overloads and random fatigue behavior. Cyclic stress-strain behavior-analysis, experimentation, and prediction. ASTM STP 519. Philadelphia; 1973. p. 271–84.
- [34] Baotung L, Xiaoyan L, Xiulin Z. Effects of microstructure on fatigue crack initiation and propagation of 16Mn steel. *Metal Mater Trans* 1989;20(3):413–9.
- [35] Xiong Y, Hu XX. The effect of microstructures on fatigue crack growth in Q345 steel welded joint. *Fatig Fract Eng Mater Struct* 2012;35(6):500–12.
- [36] Chen S, Huang C, Wang C, Duan Z. Mechanical properties and constitutive relationships of 30CrMnSiA steel heated at high rate. *Mater Sci Eng* 2008;483:105–8.
- [37] Qu SG, Lai FQ, Wang GH, Yuan ZM, Li XQ, Guo H. Friction and wear behavior of 30CrMnSiA steel at elevated temperatures. *J Mater Eng Perform* 2016;25(4):1407–15.
- [38] Ge WJ, Li ZH, Lv QY. Restoration technology of 30CrMnSiA steel parts on airplane by electroless Ni-plating. *Adv Mater Res* 2011;154:1508–12.
- [39] YanLi F. New continuous fatigue damage model based on whole damage field measurement. *J Mech Strength* 2006;28(4):582–6.
- [40] Fang J, Zhao WZ, Zhang J. Fatigue life prediction of CRH3 carbody based on rigid-flexible coupling model and the master S-N curve. In: Proceedings of the 1st international workshop on high-speed and intercity railways. Berlin, Heidelberg: Springer; 2012. p. 403–12.
- [41] Wang W, Li Q, Liu Z, Wang B. Experimental study on fatigue performance and damage model of aluminum alloy welding joints for high-speed train car body.

- In: Fourth international conference on experimental mechanics. International Society for Optics and Photonics; 2009. p. 752251–752251.
- [42] Zou H, Li W, Li Q, Wang P. Probabilistic fatigue property of aluminum alloy welded joint for high-speed train. *Adv Mater Res* 2010;118:527–31.
- [43] Zheng XL, Lu B, Jiang H. Determination of probability distribution of fatigue strength and expressions of P-S-N curves. *Eng Fract Mech* 1995;50(4):483–91.
- [44] Correia J, Apetre N, Arcari A, De Jesus AMP, Muñiz-Calvente M, Calçada R, et al. Generalized probabilistic model allowing for various fatigue damage variables. *Int J Fatigue* 2017;100:187–94.
- [45] De Jesus AMP, Pinto H, Fernández-Canteli A, Castillo E, Correia JAFO. Fatigue assessment of a riveted shear splice based on a probabilistic model. *Int J Fatigue* 2010;32(2):453–62.
- [46] Gallegos Mayorga L, Sire S, Correia JAFO, De Jesus AMP, Rebelo C, Fernández-Canteli A, et al. Statistical evaluation of fatigue strength of double shear riveted connections and crack growth rates of materials from old bridges. *Eng Fract Mech* 2017. <http://dx.doi.org/10.1016/j.engfracmech.2017.05.039>.
- [47] ASTM E 739-91: Standard practice for statistical analysis of linear or linearized stress-life (S-N) and strain life (e-N) fatigue data. *Annual Book of ASTM Standards*, American Society for Testing and Materials; 1991. p. 597–603.
- [48] Tian J, Liu ZM, He R. Nonlinear fatigue-cumulative damage model for welded aluminum alloy joint of EMU. *J Chin Railw Soc* 2012;34(3):40–3.

Paper V

**An Accurate Fatigue Damage Model for Welded Joints
Subjected to Variable Amplitude Loading**

Conference Paper

*Conference of Computational Methods in Offshore Technology,
COTech 2017*

Stavanger, Norway.

Not yet available in Brage due to copyright

PAPER • OPEN ACCESS

An accurate fatigue damage model for welded joints subjected to variable amplitude loading

To cite this article: A Aeran *et al* 2017 *IOP Conf. Ser.: Mater. Sci. Eng.* **276** 012038

View the [article online](#) for updates and enhancements.

Related content

- [Vibration-induced fatigue life estimation of ball grid array packaging](#)
Mei-Ling Wu
- [Gigacycle fatigue data sheets for advanced engineering materials](#)
Koji Yamaguchi, Takayuki Abe, Kazuo Kobayashi et al.
- [Experimental and numerical evaluation of the fatigue behaviour in a welded joint](#)
P Almaguer and R Estrada



IOP | ebooks™

Bringing you innovative digital publishing with leading voices to create your essential collection of books in STEM research.

Start exploring the collection - download the first chapter of every title for free.

An accurate fatigue damage model for welded joints subjected to variable amplitude loading

A Aeran*, S C Siriwardane, O Mikkelsen and I Langen

Department of Mechanical and Structural Engineering and Materials Science,
University of Stavanger, Norway

*Contact author: ashish.aeran@uis.no

Abstract. Researchers in the past have proposed several fatigue damage models to overcome the shortcomings of the commonly used Miner's rule. However, requirements of material parameters or S-N curve modifications restricts their practical applications. Also, application of most of these models under variable amplitude loading conditions have not been found. To overcome these restrictions, a new fatigue damage model is proposed in this paper. The proposed model can be applied by practicing engineers using only the S-N curve given in the standard codes of practice. The model is verified with experimentally derived damage evolution curves for C 45 and 16 Mn and gives better agreement compared to previous models. The model predicted fatigue lives are also in better correlation with experimental results compared to previous models as shown in earlier published work by the authors. The proposed model is applied to welded joints subjected to variable amplitude loadings in this paper. The model given around 8% shorter fatigue lives compared to Eurocode given Miner's rule. This shows the importance of applying accurate fatigue damage models for welded joints.

1. Introduction

Fatigue is one of the main causes of failures in both onshore and offshore steel structures subjected to variable amplitude loading (VAL) [1]. The fatigue damage is generally determined using the Miner's rule due to its simplicity and ease of application [2]. Moreover, the current design codes and standards such as Eurocode [3], Det Norske Veritas [4] etc. also recommend its use in the design practice. However, Miner's rule may lead to inaccurate life predictions as it does not consider the damage due to loading sequence accurately [5][6]. Several damage theories have been proposed since then to overcome these shortcomings.

Among the first improvements are the nonlinear Palmgren-Miner rule [7] and the Marco-Starkey model in 1954 [8]. The models have a constant parameter C that depends on the physical variables of the material and requires fatigue tests [9]. Several other models were proposed subsequently towards the end of the 1950s, but they required the determination of similar material parameters. Manson proposed a double linear damage rule (DLDR) in 1966 by replacing the linear Miner's rule with a set of two lines converging at a knee point [10]. The synergetic effect of the application of this rule in conjunction with a probabilistic approach based on P-S-N curves is recently shown by Correia et al.



[11]. The DLDR was further improved and the double damage curve approach (DDCA) was proposed by Manson and Halford in 1981 [12]. Many other damage models were proposed in the 1980s and 1990s such as models by Lemaitre and Plumtree [13] and by Chaboche and Lesne [14]. These models were again based on material parameters p , α , β which can be determined only through extensive material testing. Although some of the above-mentioned models have shown good agreement with the experimental data for specific materials, determination of the knee point location and additional material parameters restricted their use in applied engineering problems [15]. A more detailed review of the damage models developed before 1998 can be found in an article by Fatemi and Yang [16]. These damage models are based on crack growth concepts, damage curve modifications and energy based theories, as well as on continuum damage mechanics. However, the application of these models is not found in any of the design standards as they require testing for the determination of material parameters.

Material testing was performed by some researchers to establish fatigue damage behaviour in 1999. These tests were based on the exhaustion of material ductility and estimated the instantaneous damage in material for a given stress amplitude or range [17]. As a result, the damage evolution curves for several materials were established, and these represent the variation in experimental observed damage with number of cycles to failure. Testing was also performed to develop damage models based on hardness increase during the fatigue of material [18]. Subsequently, damage models were proposed to fit such experimental data but were again dependent on material parameters with application to specific materials. In 2005, Mesmacque et al. proposed a sequential law, which does not require any material parameters other than the full-range S-N curve [6]. The application of this model was demonstrated in steel bridges in 2008 [19]. Though the model can capture the loading sequence and predicts the fatigue life accurately, its requirement for a full-range S-N curve restricts industrial application by practicing engineers. Also, the design codes given S-N curves are based on detail categories, and the physical meaning of the intercept used for such details is not clear. Moreover, this law cannot be used with the design codes and standards having bilinear and trilinear S-N curves. Some other proposed models do not require material testing and overcome the shortcomings of Miner's rule using load interaction factors [20-22]. However, both the damage evolution curves and the fatigue life predictions differ significantly from experimental results, as will be shown later.

Recently, some probabilistic approaches have been proposed by considering a probabilistic S-N field and providing a statistical distribution of the Miner's damage based on log-normal distribution [23] [24]. The Miner's damage is related to a normalized variable V , which represents percentile curves in the S-N field unequivocally associated to probability of failure. These models can be applied for fatigue design of structural components subjected to variable amplitude loading and a recent application has been shown on riveted connection made of puddle iron from a bridge [25]. Also, a one parameter fatigue damage model has been proposed based on the concept of iso-damage curves [26]. As mentioned in the discussion of this paper, the model is based on S-N curves with a constant slope and is difficult to apply with bilinear or trilinear S-N curves in the current codes and standards. Also, the model parameter b is verified only for four types of steel and not for any other material. The model has only been compared to two step cyclic loading. Practical applications of the model to structural details subjected to variable amplitude loading have not been presented. Another non-linear fatigue damage model based on strain life curve has been proposed by Huffman and Beckman [27]. However, the applications of this model are not found as the design standards are based on stress life curves (i.e. S-N curves). Many other damage models exist in the literature, based on the concepts of continuum damage mechanics, energy conservation and entropy change. More details about these models can be found in several of the recently reviewed articles regarding fatigue damage theories such as by Santecchia et al. [28] and by Silitonga et al. [29].

Although many fatigue damage models have been proposed in the literature, the existing codes and standards still use Miner's rule because of its simplicity and ease of application. This indicates the need for an equally simple, easy to apply and accurate fatigue damage model for engineering applications/structural engineering problems. This becomes even more important for estimating the

remaining life of ageing steel structures, where loading histories might be known as well. Such a model will not only predict the remaining life but will also help maintain the existing infrastructure more efficiently. The risk of failure and subsequent consequences will also be reduced using a more accurate model.

To overcome above mentioned problems, an accurate and easy-to-apply fatigue damage model is proposed in this paper. The proposed damage model does not require any material testing and depends only on the commonly available S-N curve of the material or its corresponding detail category. Moreover, it does not require a full-range S-N curve and can be easily applied by practicing engineers using the partially known S-N curves given in design standards. The proposed model can be applied to structural details subjected to variable amplitude loading conditions unlike most of the earlier models applied only to block loading cases. As a result, the proposed model can be easily implemented by practicing engineers for fatigue analysis of several practical problems involving design detail categories subjected to variable amplitude loadings. The proposed model considers the loading sequences, along with the interactions between them, and provides better agreement with experimental data compared to previously proposed models. Due to its unique features and better accuracy, the proposed model can provide a platform to design and maintenance communities for an efficient use of existing ageing steel infrastructure by predicting their remaining safe life more accurately. Initially, the paper presents the proposed damage model in detail. The model is verified with experimentally derived damage evolution curves for C 45 and 16 Mn and gives better agreement compared to previous models. The practical application of the proposed model is shown on welded joints used in several engineering applications. The model is applied to butt and fillet welded joints subjected to block loading and predicted lives are compared with experimental results. The application of the model under variable amplitude loading is also shown on these joints and the results are compared with Eurocode predicted lives. Hence, the applicability, validity and significance of the proposed model is confirmed.

2. Proposed fatigue damage model

A new and easy-to-apply fatigue damage model is proposed as shown in equation (1). The damage for a given stress level is determined using the damage evolution curve of the considered material. This damage is then transferred to the next stress level by determining the effective number of cycles using the proposed load interaction factor. The physical meaning of the concept is to assume the same damage state of the material, while transferring the loading state from one stress level to the next and determining the effective number of cycles required to cause this damage.

$$D_i = 1 - \left[1 - \frac{n_i}{N_i} \right]^{\delta_i} = 1 - \left[1 - \frac{n_{(i+1),eff}}{N_{i+1}} \right]^{\frac{\delta_{i+1}}{\mu_{i+1}}} \quad (1)$$

where D_i is the damage at load level i when member is subjected to a certain stress amplitude (or range) σ_i for n_i number of cycles and $n_{(i+1),eff}$ is the effective number of cycles corresponding to the stress range σ_{i+1} at level $i+1$. N_i and N_{i+1} are the corresponding number of cycles to failure and can be determined from the S-N curve given in design standards and codes. δ_i and μ_i are the model parameters and depends only on N and given stress levels as shown in equation (2) and equation (3). The proposed model also represents some of the earlier proposed damage models for specific values of δ_i as shown in Table 1.

$$\delta_i = \frac{-1.25}{\ln N_i} \quad (2)$$

$$\mu_i = \left(\frac{\sigma_{i-1}}{\sigma_i} \right)^2 \quad (3)$$

The damage at load level $i+1$ can be determined using equation (4) and equation (5).

$$D_{i+1} = 1 - \left[1 - \frac{n_{(i+1),total}}{N_{i+1}} \right]^{\delta_{i+1}} \quad (4)$$

where

$$n_{(i+1),total} = n_{(i+1),eff} + n_{(i+1)} \quad (5)$$

where n_{i+1} is the number of cycles for stress state σ_{i+1} . Also, $n_{(i+1),total}$ is the total number of cycles for stress state σ_{i+1} obtained using the proposed concept.

Table 1. Parameters of the proposed model and its special cases [2] [3] [17].

δ_i	Damage model	Remarks
$-1.25/\ln N_i$	Proposed model	only based on commonly available S-N curves
1	Miner's rule, 1945 [2]	most commonly used, but is inaccurate under VAL
$1/p+1$	Lemaitre and Plumtree, 1979 [13]	p is a material constant determined by damage evolution curves based on cyclic stress ranges
$1/1-\alpha$	Shang and Yao, 1999 [17]	α is a material constant determined by damage evolution curves based on static ductility change

This damage transfer technique is continued until the fatigue damage D becomes one, denoting fatigue failure. The proposed damage transfer concept is explained graphically, as shown in Figure 1. More details of the proposed model and associated parameters can be found in recently published work by the authors [30].

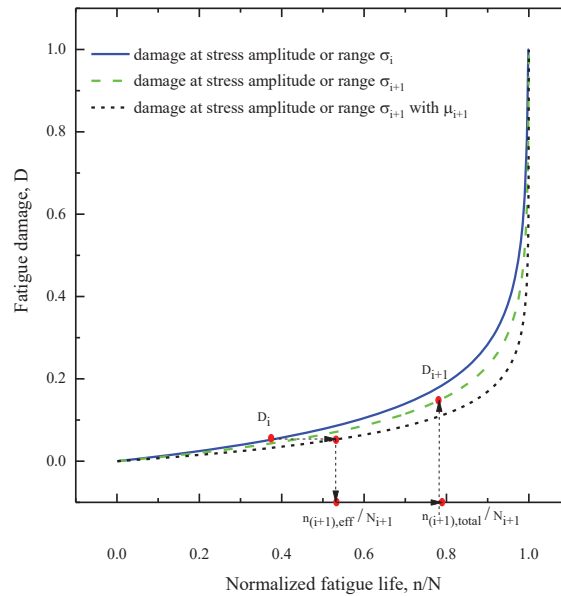


Figure 1. Graphical representation of the proposed damage transfer concept

2.1. Verification of proposed model with experimental damage evolution

The proposed fatigue damage model is verified by comparing the experimental results for damage evolution curves. C 45 and 16 Mn steels are used for this verification [17].

2.1.1. C 45 steel. This material is of interest to the authors due to its currently increasing use in offshore structures [31]. The yield strength and ultimate tensile strength for this material are 371.7 MPa and 598.2 MPa, respectively [17]. In the past, experiments were conducted on this material for constant amplitude stresses, and the fatigue damage was determined by measuring the static relative ductility change in the material [17]. The experiments were conducted at 330.9 MPa and 405.8 MPa stress amplitudes (with zero mean stress); the results are shown in Figure 2 (a) and Figure 2 (b), respectively. Fatigue damage curves are also plotted for each of the stress amplitudes using the proposed model. The proposed model is also compared with some of the recently developed models which do not require additional material testing, other than their S-N curve.

2.1.2. 16 Mn steel. The damage evolution curves were also determined experimentally for 16 Mn steel by measuring the static relative ductility change in material [17]. For this material, the yield strength is 382.5 MPa, and the ultimate tensile strength is 570.7 MPa. The experiments were conducted at 337.1 MPa and 373.5 MPa stress amplitudes (with zero mean stress); the damage evolution curves are shown in Figure 3 (a) and Figure 3 (b), respectively. Fatigue damage curves are also plotted for each of the stress amplitudes using the proposed model. The proposed model is also compared with some of the recently developed models which do not require additional material testing, other than their S-N curve.

2.1.3. Discussion of verification study. From Figure 2 (a) and Figure 2 (b), it is seen that the proposed model gives good prediction of the damage curves for material C 45 and is in good agreement with the experimental results. The damage evolution curves for 16 Mn steel are shown in Figure 3 (a) and Figure 3 (b) for the two stress amplitudes. Again, it is seen that the proposed model is in good agreement with the experimental results and can predict the damage behaviour more accurately. The proposed model is also compared with some of the other recently developed models which do not require additional material testing, other than their S-N curve. It is seen that the model developed by Kwofie and Rahbar [20] is not in good agreement with the experimental data and is equivalent to Miner's rule while predicting the damage behaviour. The models proposed by Liakat and Khonsari [21] and Lv et al. [22] seem to give the same damage evolution curves for both considered materials. The sequential law proposed by Mesmacque et al. [6] is also compared with the experimental data. It is seen that the model gives good agreement with the experimental results. However, the model requires the determination of the full-range S-N curve, thereby restricting its use by practicing engineers. After comparing all the curves shown in Figure 2 and Figure 3, it is concluded that the proposed model predicts the real damage evolution behaviour quite accurately for the two materials considered, when compared to previous models. The damage curves can be plotted using the proposed model without determining additional material parameters and using only code-given S-N curves.

3. Application of proposed model to welded joints

The proposed model is applied on welded joints subjected to both block loading as well as variable amplitude loading. These welded joints are used in several engineering applications such as vehicles, electrical mobile units (EMUs), etc., and an accurate prediction of life is necessary for the safety of both passengers and vehicles. There has been a significant advancement in technology over the past couple of decades. As a result, conventional diesel locomotives are increasingly being replaced by faster electrical mobile units (EMUs). These EMUs can reach speeds of 250 km/h and above, as compared to the diesel locomotives which used to have typical speeds of 160 km/hr [32]. While the advancement of the vehicle technology is good for the fast commuting of passengers, it also puts vehicle safety, as well as the safety of people, at huge risk. Such risks arise from the increasingly daily passenger loads, inefficient maintenance of vehicles, as well as ageing of the car bodies, which, in these high-speed trains are generally made from aluminium alloy due to its light weight, security and comfort [33].

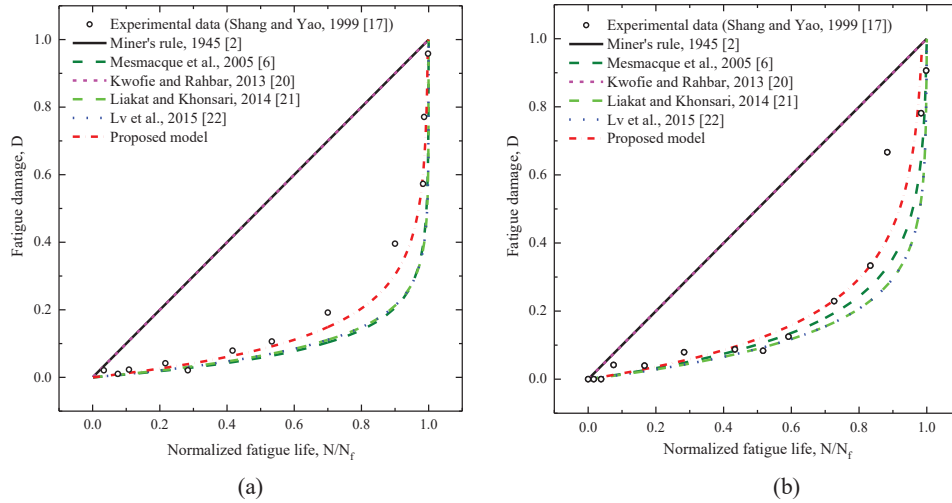


Figure 2. Comparison of theoretically predicted fatigue damage evolution with experimental damage of C 45 steel for stress (a) $\sigma_a = 330.9$ MPa (b) $\sigma_a = 405.8$ MPa

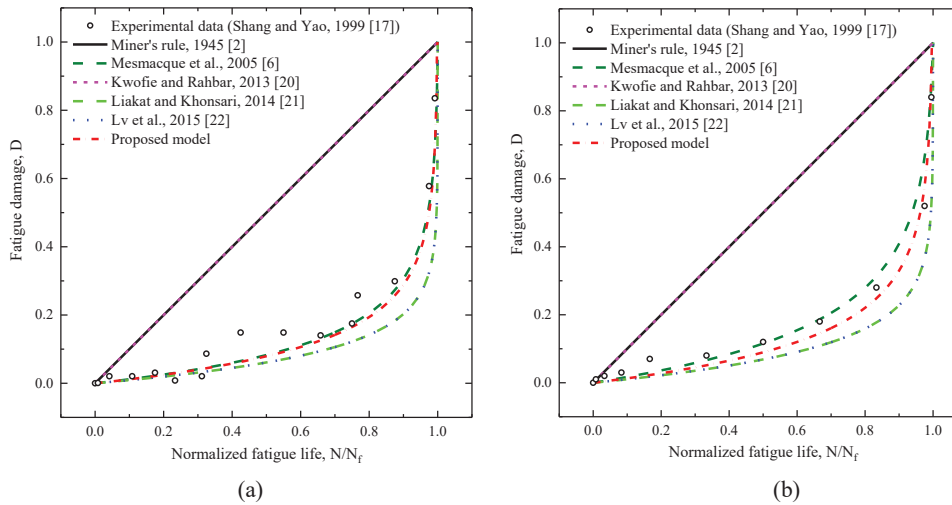


Figure 3. Comparison of theoretically predicted fatigue damage evolution with experimental damage of 16 Mn steel for stress (a) $\sigma_a = 337.1$ MPa (b) $\sigma_a = 373.5$ MPa

However, as a result of the high thermal conductivity coefficient and high linear expansion coefficient, aluminum alloys can have complex welding deformations and stresses at the welded joints. The softening and embrittlement of these welded joints can have a serious effect on the structural strength of the car body. It is reported that the failure of the car body usually occurs in the welded joint,

and the major cause is fatigue loading [33] [34], which is most critical for the welded connections; it is therefore important to estimate the fatigue life accurately to minimize the risks.

Much research has been carried out in the past on the fatigue properties of welded aluminum joints. Recently, a group of researchers performed fatigue tests on such aluminum joints to thoroughly understand the fatigue properties and predict the life more accurately under the block loading conditions [33] [34]. Firstly, the experimental setup and considered welded joints are explained in detail in this section. The proposed model is then applied to these joints under the given block loading conditions and predicted lives are compared with experimental results. The applicability and accuracy of proposed model under block conditions is henceforth confirmed. The application of the proposed model is also shown on these welded joints subjected to random variable amplitude loadings (VAL). An in-situ measured VAL is considered for this study. The results are compared with Eurocode recommended Miner's rule. Hence, the applicability of the proposed model under VAL is also confirmed in this study.

3.1. Considered welded joint details

The fatigue tests were performed for both butt and fillet welded joints by using the PLG-200 fatigue testing machine. The test specimens are shown in Figure 4 (a) and Figure 4 (b) respectively. The base material of the specimen is aluminum alloy ENAW6005 having the main chemical composition in mass percentage as: 0.35Fe, 0.6-0.9Si, 0.1Mn, 0.1Ti, 0.4-0.6Mg, 0.1Cu, 0.1Zn and 0.1 Cr [33] [34]. The tensile strength and yielding strength of the base material are 270 and 225 MPa, respectively. The specimens were tested under a four-point bending load cycle with cyclic stress ratio $R = -1$. The load-time history follows the sine function. The loading frequency is 110 Hz, and room temperature is 20~30°C [33] [34].



Figure 4. Welded joint test specimens (a) Butt welded joint (b) Fillet welded joint [33] [34]

3.2. Application of proposed model under block loading

The proposed model is applied to welded joints under block loading conditions and the predicted lives are compared with experimental lives. The experiments were conducted by previous researchers under two-stage block loading for each of the considered welded joints [33] [35]. The load sequence considered for the butt-welded joint are 104–74 MPa and 89–74 MPa for high-low loading sequence, and 74–89 MPa and 74–104 MPa for low-high loading sequences. The load sequences considered for the fillet welded joint are 93–73 MPa and 83–73 MPa under high-low loading, and 73–83 MPa and 73–93 MPa under low-high loading, respectively. The experimentally obtained fatigue lives for the butt and fillet welded joint are shown in Table 2 and Table 3, respectively [33] [35].

The proposed damage model is compared with experimentally obtained fatigue lives for the considered welded joints. The loading sequences are given in Table 2 and Table 3. Some of the recently proposed models have also been included in the comparison. The comparison of fatigue life is shown in Figure 5 (a) and Figure 5 (b) for the butt and fillet welded joints, respectively. The maximum and average deviations from the experimental results are 20% and 9% respectively. The solid line

refers to ideal conformity of the results. The dotted lines represent a scatter band with a coefficient of two.

Table 2. Experimental fatigue lives for fatigue testing on butt welded joint [33] [35].

Load Set	σ_1 (MPa)	σ_2 (MPa)	n_1 (*1000)	n_2 (*1000)	N_n	N_{n2}
Set 1	104	74	109.9	797.6	549300	1540100
Set 2	89	74	176.1	1029.2	880500	1540100
Set 3	74	89	770.1	545.6	1540100	880500
Set 4	74	104	770.1	418.9	1540100	549300

Table 3. Experimental fatigue lives for fatigue testing on fillet welded joint [33] [35].

Load Set	σ_1 (MPa)	σ_2 (MPa)	n_1 (*1000)	n_2 (*1000)	N_n	N_{n2}
Set 1	93	73	309.9	587.5	619800	1546100
Set 2	83	73	476.1	681.1	952300	1546100
Set 3	73	83	509.2	708.2	1546100	952300
Set 4	73	93	773.0	426.4	1546100	619800

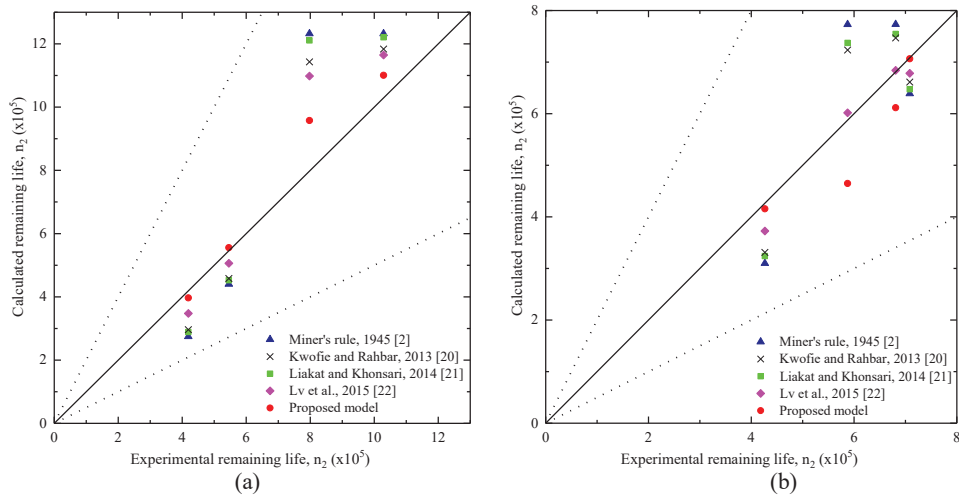


Figure 5. Comparison of calculated fatigue life with experimental life for (a) butt welded joint (b) fillet welded joint

3.3. Application of proposed model under variable amplitude loading (VAL)

The proposed model is also applied to considered welded joints under variable amplitude loading conditions. The fatigue life of both butt and fillet welded joints is predicted using the proposed model. The lives are also predicted using the Miner’s rule recommended by standard codes and standards such as Eurocode. The detail category S-N curves for the joints are taken from the Eurocode [36]. The cycle counting is performed using the rainflow counting method [37]. Finally, the damage accumulation curves are obtained and fatigue lives from proposed model are compared with those obtained using Miner’s rule.

3.3.1. *Considered variable amplitude loading (VAL)*. The variable amplitude loading considered for this study is shown in Figure 6. The stress values are shown for every 0.13 seconds and for a period of one hour. The same stress history is assumed to be repeated until the end of the fatigue life (i.e. the same loading block is assumed to be repeated until the failure point).

3.3.2. *Rainflow counting and mean stress correction*. The cycle counting is performed on the considered VAL using the rainflow counting method [37]. This is followed by the mean stress correction as recommended by Goodman rule [5]. The resulting stress amplitude history is shown in Figure 7.

3.3.3. *Considered detail category S-N curves for welded joints*. The detail category S-N curves of the welded joint details are taken from Eurocode [36]. The parameters of these curves including the fatigue endurance stress limit are shown in Table 4. The stress history after the removal of endurance limit are shown in Figure 8 and Figure 9 for the butt welded and fillet welded joint respectively.

Table 4. S-N curve parameters for considered joints given in Eurocode [36]

Joint	S-N curve parameters				
	$\Delta\sigma_L$	$\Delta\sigma_D$	$\Delta\sigma_C$	m_1	m_2
Butt	20.1	32.3	40	4.3	3.4
Fillet	12.3	21.4	28	6.3	5.4

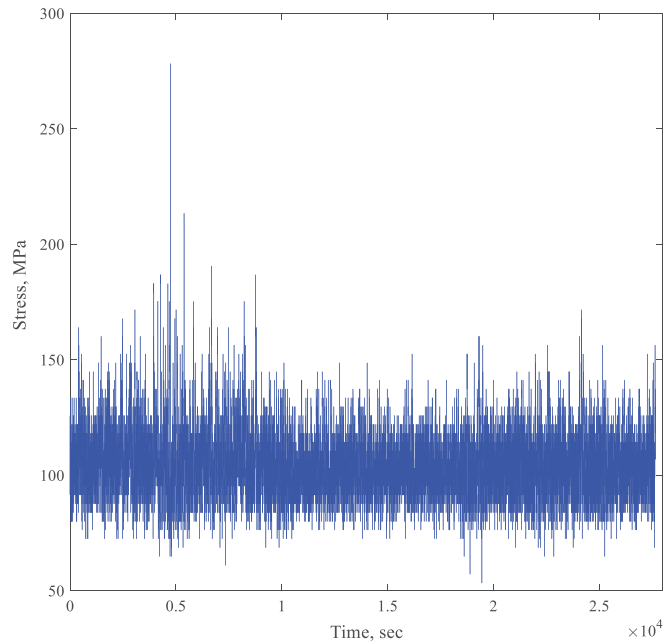


Figure 6. Considered variable amplitude loading for welded joints

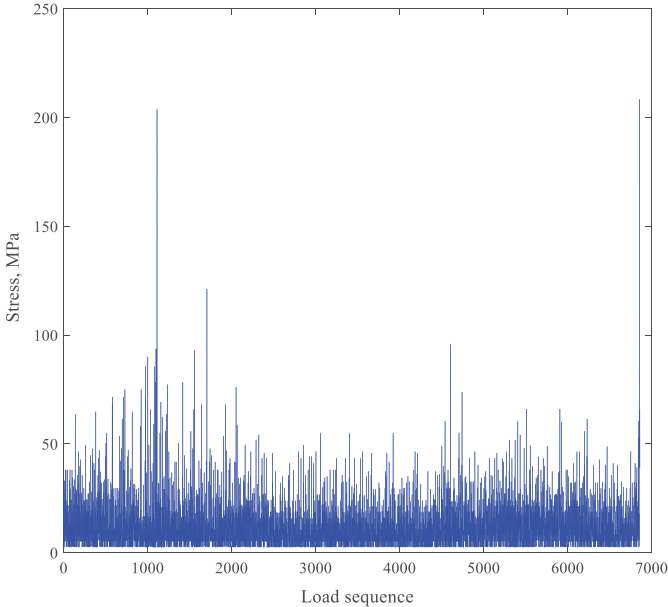


Figure 7. Stress history after mean stress correction

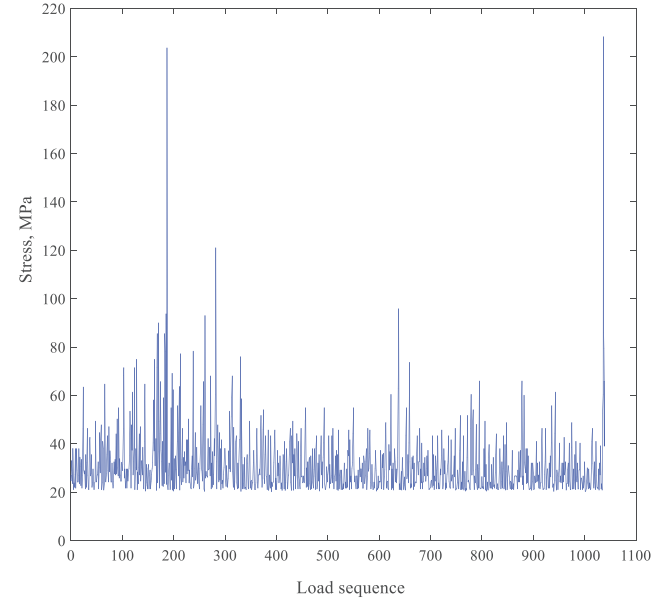


Figure 8. Stress history above endurance for butt welded joint

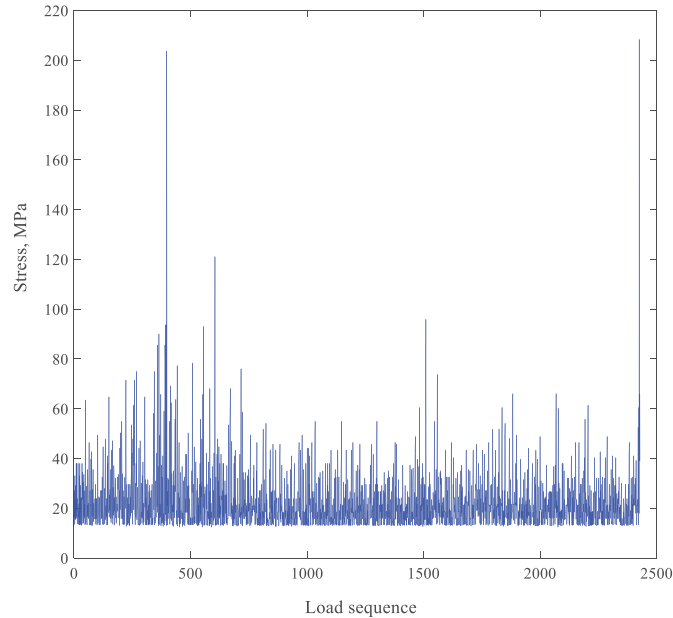


Figure 9. Stress history above endurance for fillet welded joint

3.3.4. Comparison of damage curve and fatigue life. The proposed model is applied to calculate fatigue life of the considered welded joints. The stress amplitude histories shown in Figure 8 and Figure 9 are used for these calculations. The interaction factor in the proposed model is taken as one for this study and the accumulated fatigue damages until failure is shown in Figure 10 and Figure 11 for butt and fillet welds respectively. The damage accumulations using the Eurocode recommended Miner's rule are also shown in Figure 10 and Figure 11.

The fatigue life for the considered joints can be determined from Figure 10 and Figure 11. The fatigue lives are calculated in terms of number of blocks of the VAL considered (i.e. number of repeated blocks) and are shown in Table 5.

Table 5. Fatigue life comparison using proposed model and Eurocode (in blocks)

Joint	Number of blocks of considered VAL		
	Eurocode	Proposed	% difference
Butt	899	829	7.80
Fillet	544	514	5.3

3.4. Discussion and comparison of the results

The proposed model is applied to predict the fatigue lives of welded joints used in several engineering applications. Butt and fillet welded joints were considered in the case study. The application of the fatigue damage model to these joints is shown under both block loadings and variable amplitude loading conditions. The comparisons of the fatigue lives under block loading conditions are shown in Figure 5 (a) and Figure 5 (b) for butt welded and fillet welded joint respectively.

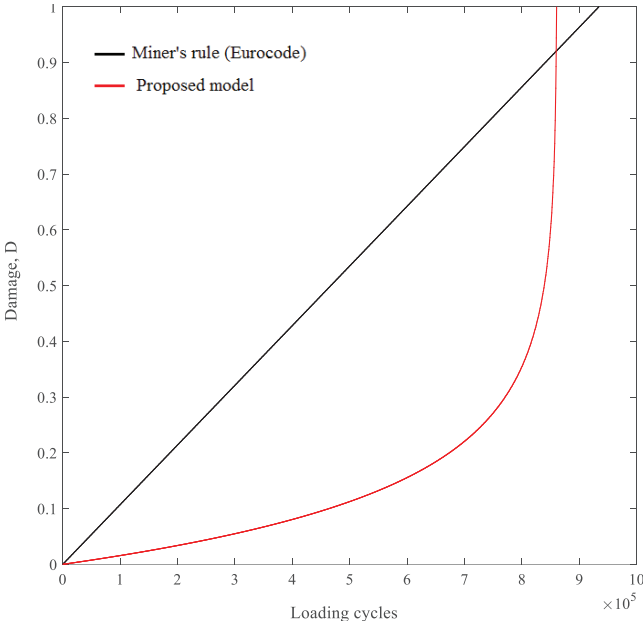


Figure 10. Fatigue damage accumulation using proposed model and Eurocode for butt welded joint

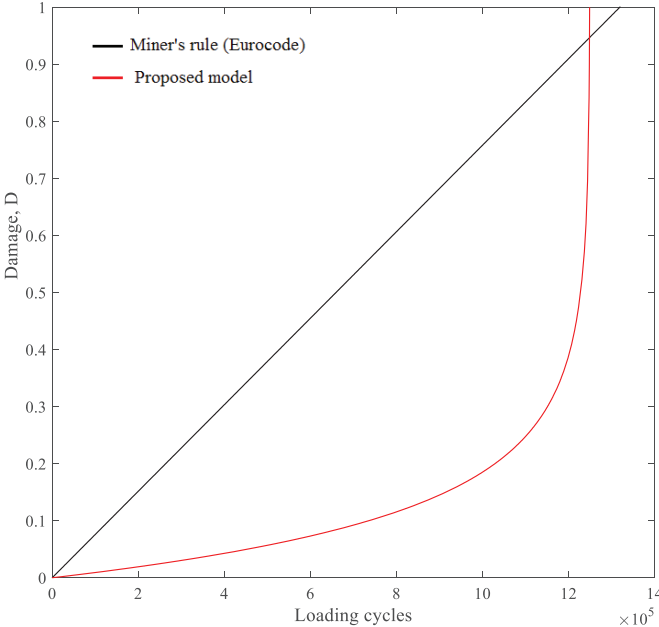


Figure 11. Fatigue damage accumulation using proposed model and Eurocode for fillet welded joint

The predicted lives using the proposed model are in good agreement with the experimental lives compared to Eurocode given Miner's rule. The proposed model predictions are also better compared to earlier models. The sequential law model could not be applied to these joints since full range S-N curve is not available for these detail categories. Using the proposed model, the maximum and average deviations from the experimental results are 20% and 9% respectively for these joints. The scatter bands with a coefficient two is also plotted in all the figures where experimental fatigue life is compared with predicted life. The predicted fatigue lives are all lying within the scatter band.

The application of proposed model is also shown under variable amplitude loading conditions. The variable amplitude loading considered is taken from in-situ measurements for a period of one hour and is assumed to be repeated until the failure. The mean stress zero equivalent stress amplitude history is then derived using the rainflow counting algorithm followed by the mean stress correction. The proposed model requires only the S-N curve parameters of the detailed categories and these were taken as given in the Eurocode. The fatigue damage accumulation curves are shown in Figure 10 and Figure 11 for the butt welded and fillet welded joint respectively. These are compared for both proposed model and the Eurocode (i.e. using the Miner's rule). The predicted fatigue lives are shown in Table 5.

From Figure 10 and Figure 11, it is seen that the damage accumulation curves using the proposed model are nonlinear and are very similar to the damage evolution curves discussed earlier in this paper. This further confirms the real physical damage accumulation behaviour in the material instead of the linear accumulation as assumed by the commonly used Miner's rule given in Eurocode and other design standards. From Table 5, it is seen that the predicted lives using the proposed model are around 8% shorter compared to the Eurocode. This difference may not seem too significant for the design of new structures. However, the proposed model can be used for a more accurate prediction of remaining lives of existing infrastructures such as old bridges, ageing oil/gas platforms and industrial buildings. The remaining life calculations based on Eurocode might result in longer lives than the structures can stand. This shows the importance of applying an accurate fatigue damage model.

4. Conclusions

The paper presents a new fatigue damage model. The proposed model does not require any material parameters, other than the commonly available S-N curve parameters, which are generally used with Miner's rule. The major advantage of proposed model is that it does not require detail material testing or modifications to the S-N curve. Also, unlike earlier models, the proposed model can be applied to design detail categories using the corresponding partially known S-N curve in the design standards. Therefore, the proposed model can be easily implemented by practicing engineers for fatigue analysis of several engineering problems. The model is verified with both the damage evolution curves and fatigue life estimations. It is concluded that the damage curves plotted using the proposed model are in good agreement with the available experimental data for two considered materials. It is also concluded that the fatigue life predictions are more accurate using the proposed model compared to Eurocode given Miner's rule. The application of the proposed model is shown to welded joints used in several engineering applications. The both butt and fillet welded joints are commonly subjected to both block loading and variable amplitude loading conditions. The obtained damage accumulation curves using proposed model confirms the real physical damage accumulation behaviour in the material instead of the linear accumulation as assumed by the commonly used Miner's rule given in Eurocode. It is therefore concluded that the proposed model can be used for better fatigue life predictions and can be easily applied by practicing engineers using only the code-given S-N curves. The applicability, significance and validity of the proposed fatigue damage model should be further verified in the future by applying the model to more case studies.

References

- [1] Naess AA 1985 *Fatigue Handbook* (Trondheim: Tapir)
- [2] Miner MA Cumulative damage in fatigue 1945 *J. Appl. Mech.* **A** pp 159–64
- [3] Eurocode 3 2010 *Design of steel structures – Part 1-9: Fatigue, NS-EN 1993-1-9:2005+NA:2010* (European Standard)
- [4] DNVGL RP C203 2016 *Offshore standard DNVGL-RP-C203: Fatigue Design of Offshore Steel Structures* (Det Norske Veritas and Germanischer Lloyd SE)
- [5] Suresh S 1998 *Fatigue of Materials* (Cambridge: Cambridge University Press)
- [6] Mesmacque G, Garcia S, Amrouche A and Rubio-Gonzalez C 2005 Sequential law in multiaxial fatigue, a new damage indicator *Int. J. Fatigue* **27** pp 461-7
- [7] Leve HL 1969 *Cumulative damage theories. In Metal Fatigue: Theory and Design* (New York: Wiley) p 170
- [8] Marco SM and Starkey WL 1954 A concept of fatigue damage *Trans. of the ASME* **76** 627-32
- [9] Hwang W and Han K S 1986 Cumulative damage models and multi-stress fatigue life prediction *J. Compos. Mater.* **20** pp 125-53
- [10] Manson S, Freche J and Ensign C 1967 Application of a double linear damage rule to cumulative fatigue *Fatigue Crack Propagation, ASTM STP 415* pp 384-412
- [11] Correia O, Jesus A, Blasón S, Calvente M and Fernández-Canteli A. Probabilistic non-linear cumulative fatigue damage of the P355NL1 pressure vessel steel *ASME 2016 pressure vessels and piping conference* **6** pp 17-21
- [12] Manson S and Halford G 1981 Practical implementation of the double linear damage rule and damage curve approach for treating cumulative fatigue damage *Int. J. Fract.* **7** 169-92
- [13] Lemaitre J and Plumtree A 1979 Application of damage concepts to predict creep-fatigue failures *J. Eng. Mater. Technol.* **101** pp 284-92
- [14] Chaboche JL and Lesne PM A non-linear continuous fatigue damage model *Fatig. Fract. Eng. Mater. Struct.* **11** pp 1-7
- [15] Goodin E, Kallmeyer A and Kurath P 2004 Evaluation of nonlinear cumulative damage models for assessing HCF/LCF interactions in multiaxial loadings *Proc. of 9th Nat. Turbine Engine HCF Conf. (North Carolina)*
- [16] Fatemi A and Yang L 1998 Cumulative fatigue damage and life prediction theories: a survey of the state of the art for homogeneous materials *Int. J. Fatigue* **20** pp 9-34
- [17] Shang DG and Yao WX 1999 A nonlinear damage cumulative model for uniaxial fatigue *Int. J. Fatigue* **21** pp 187-94
- [18] Pavlou DG 2002 A phenomenological fatigue damage accumulation rule based on hardness increasing, for the 2024-T42 aluminum *Eng. Struct.* **24** pp 1363-68
- [19] Siriwardane S, Ohga M, Dissanayake R and Taniwaki K 2008 Application of new damage indicator-based sequential law for remaining fatigue life estimation of railway bridges *J. Construct. Steel. Res.* **64** pp 228-37
- [20] Kwofie S and Rahbar N 2013 A fatigue driving stress approach to damage and life prediction under variable amplitude loading *Int. J. Damage Mech.* **22** pp 393-404
- [21] Liakat M and Khonsari MM 2014 An experimental approach to estimate damage and remaining life of metals under uniaxial fatigue loading *Mater. Des.* **57** pp 289-97
- [22] Lv Z, Huang HZ, Zhu SP, Gao H and Zuo F 2015 A modified nonlinear fatigue damage accumulation model *Int. J. Damage Mech.* **24** pp 168-81
- [23] Fernández-Canteli A, Blasón S, Correia JA and De Jesus AM 2014 A probabilistic interpretation of the Miner number for fatigue life prediction *Frattura ed Integrita Strutturale* **30** pp 327-39
- [24] Blasón S, Correia JA, De Jesus AM, Calçada RA and Fernández-Canteli A 2016 A probabilistic analysis of Miner's law for different loading conditions *Struc. Eng. Mech.* **60** pp 71-90
- [25] Correia JA, De Jesus AM, Fernández-Canteli A and Calçada RA 2015 Fatigue damage

- assessment of a riveted connection made of puddle iron from the Fão Bridge using the modified probabilistic interpretation technique *Procedia Eng.* **114** pp 760-7
- [26] Rege K and Pavlou DG 2017 A one-parameter nonlinear fatigue damage accumulation model *Int. J. Fatigue* **98** pp. 234-46
- [27] Huffman PJ and Beckman SP 2013 A non-linear damage accumulation fatigue model for predicting strain life at variable amplitude loadings based on constant amplitude fatigue data *Int. J. Fatigue* **48** pp. 165-169
- [28] Santecchia E, Hamouda AM, Musharavati F, Zalnezhad E, Cabibbo M, El Mehtedi M and Spigarelli S 2016 A review on fatigue life prediction methods for metals *Adv. Mat. Sci. Eng.* **9** pp 1-26
- [29] Silitonga S, Maljaars J, Soetens F and Snijder HH 2013 Survey on damage mechanics models for fatigue life prediction *Heron* **58** pp 25-60
- [30] Aeran A, Siriwardane SC, Mikkelsen O and Langen I 2017 A new nonlinear fatigue damage model based only on SN curve parameters *Int. J. Fatigue* **103** pp 327-341
- [31] Abed FH, Saffarini MH, Abdul-Latif A and Voyiadjis GZ 2017 Flow stress and damage behavior of C45 Steel Over a Range of Temperatures and Loading Rates *J. Eng. Mater. Techno.* **139** pp 1-8
- [32] Fang J, Zhao WZ and Zhang J 2012 Fatigue life prediction of CRH3 carbody based on rigid-flexible coupling model and the master SN curve *Proc. of 1st Int. Work. on High-Speed and Intercity Railways (Berlin)*
- [33] Wang W, Li Q, Liu Z and Wang B 2010 Experimental study on fatigue performance and damage model of aluminum alloy welding joints for high-speed train car body *Proc. of 4th Int. Conf. on Experimental Mechanics (Singapore)*
- [34] Zou H, Li W, Li Q and Wang P 2010 Probabilistic fatigue property of aluminium alloy welded joint for high-speed train *Adv. Mater. Res.* **118** pp 527-31
- [35] Tian J, Liu ZM and He R 2012 Nonlinear fatigue-cumulative damage model for welded aluminum alloy joint of EMU *J. Chin. Railw. Soc.* **34** pp 40-3
- [36] Eurocode 3 2011 *Design of aluminium structures – Part 1-3: Structures susceptible to fatigue, NS-EN 1999-1-3:2007+NAl:2011* (European Standards)
- [37] Downing S and Socie D 1982 Simple rainflow counting algorithms *Int. J. Fatigue* **4** pp 31-40

Paper VI

**A Nonlinear Fatigue Damage Model : Comparison with
Experimental Damage Evolution of S355 (SAE 1020)
Structural Steel and Application to Offshore Jacket
Structures**

Journal Paper

International Journal of Fatigue

May 2019, (under review).

Highlights

Submitted to **International Journal of Fatigue**

May 2019

A nonlinear fatigue damage model: Comparison with experimental damage evolution of S355 (SAE 1020) structural steel and application to offshore jacket structures

Ashish Aeran¹, Ruth Acosta², Sudath C. Siriwardane¹, Peter Starke²,
Ove Mikkelsen¹, Ivar Langen¹, Frank Walther³

¹Department of Mechanical and Structural Engineering and Materials
Science, University of Stavanger,
P.O. Box 8600 Forus, N-4036, Stavanger, Norway

²Department of Materials Science and Materials Testing (WWHK),
University of Applied Sciences Kaiserslautern, D-67659 Kaiserslautern,
Germany

³Department of Materials Test Engineering (WPT), TU Dortmund
University, D-44227 Dortmund, Germany

Corresponding Author: Ashish Aeran ashish.aeran@uis.no

HIGHLIGHTS

(1) A nonlinear fatigue damage model based only on S-N curve parameters is proposed.

(2) Fatigue damage evolution curves are experimentally derived for S355 structural steel based on material physical behavior during cyclic loading.

(3) Material physical behavior is characterized by plastic strain accumulation and changes in electrical resistance and temperature of the microstructure.

(4) Experimentally derived damage evolution curves are compared with theoretically predicted damage using proposed model.

(5) Application of proposed model is shown to an offshore jacket structure and results are compared with conventional approach.

A nonlinear fatigue damage model: Comparison with experimental damage evolution of S355 (SAE 1020) structural steel and application to offshore jacket structures

Ashish Aeran¹, Ruth Acosta², Sudath C. Siriwardane¹, Peter Starke²,
Ove Mikkelsen¹, Ivar Langen¹, Frank Walther³

¹Department of Mechanical and Structural Engineering and Materials Science, University of Stavanger, P.O. Box 8600 Forus, N-4036, Stavanger, Norway

²Department of Materials Science and Materials Testing (WWHK), University of Applied Sciences Kaiserslautern, D-67659 Kaiserslautern, Germany

³Department of Materials Test Engineering (WPT), TU Dortmund University, D-44227 Dortmund, Germany

Corresponding Author: Ashish Aeran ashish.aeran@uis.no

ABSTRACT

Miner's rule is commonly used in fatigue life estimations and is also recommended by design standards. Recently, few models have been proposed to capture loading sequence effects more precisely than the Miner's rule. However, practical applications of these models have not been found due to requirement of additional material parameters. A nonlinear fatigue damage model is recently proposed by the authors

1
2
3
4
5
6
7
8
9
10
11
12
13
14
15
16
17
18
19
20
21
22
23
24
25
26
27
28
29
30
31
32
33
34
35
36
37
38
39
40
41
42
43
44
45
46
47
48
49
50
51
52
53
54
55
56
57
58
59
60
61
62
63
64
65

which does not require any additional material parameters other than the $S-N$ curve. It can be applied by practicing engineers using partially known $S-NS-N$ curves given in design standards including the corresponding detail categories. The model has been verified with several materials for both damage evolution curves and fatigue life estimations. Verification of this model for S355 (SAE 1020) structural steel used in offshore structures is desirable for the industry. Experimental techniques based on characterizing fatigue damage using physical quantities are also recently developed by the authors and are used for this verification. Subsequently, damage evolution curves under load increase tests and constant amplitude tests are developed by observing the changes in plastic strain amplitude, electrical resistance and temperature. The corresponding fatigue strength curve is developed. This curve is used together with proposed damage index for further verification of proposed model for S355 (SAE 1020) structural steel. In the end, application of proposed model is shown to an existing offshore jacket structure and results are compared with conventional approach. Hence, the importance and significance of proposed model is further established.

KEYWORDS: structural steel, fatigue damage model, plastic strain, temperature and resistance measurements, offshore jacket structure.

1
2
3
4
5
6
7
8
9
10
11
12
13
14
15
16
17
18
19
20
21
22
23
24
25
26
27
28
29
30
31
32
33
34
35
36
37
38
39
40
41
42
43
44
45
46
47
48
49
50
51
52
53
54
55
56
57
58
59
60
61
62
63
64
65

1. INTRODUCTION

Cyclic loading on metallic materials causes micro-plastic deformations and, with cyclic softening and/or hardening processes, leads to the formation of characteristic dislocation structures and deformation properties that may be the initial point of fatigue cracks. The fatigue-induced property changes can lead to the formation and propagation of cracks and ultimately to failure. Changes in material's mechanical behavior during cyclic loading are usually characterized by evaluating the accumulated plastic strain amplitude [1,2], which can be expressed as a function of the number of cycles N during loading. Conventional stress-strain hysteresis, change in temperature [3,4] and change in electrical resistance [5,6] were measured with high precision in conducted fatigue experiments. In general, the changes in these physical quantities are directly linked by cross-effects to microstructural changes in the bulk material obtained during quasi-static or fatigue loading.

Developing $S-N$ curve for the design process of structures and components needs to be performed in a quick and cost-effective way. The understanding of fatigue damage evolution is of major importance for the development of fatigue life calculation methods or evaluation models, which are aimed at predicting the lifetime of a specimen, a component or even whole structures during their design life or extended life.

Several approaches like PhyBaL [7], StressLife [8], StrainLife [9] and SteBLife [10] have been developed over the recent 15 years to estimate fatigue strength curves. While the mentioned approaches are

1
2
3
4
5
6
7
8
9
10
11
12
13
14
15
16
17
18
19
20
21
22
23
24
25
26
27
28
29
30
31
32
33
34
35
36
37
38
39
40
41
42
43
44
45
46
47
48
49
50
51
52
53
54
55
56
57
58
59
60
61
62
63
64
65

based on thermometric and electric methods, there are several others based on magnetic, electrochemical and acoustic methods. All these approaches involve extracting material information from few fatigue tests only and thereby reducing both experimental and financial efforts. As a result, these approaches offer the possibility to investigate even more fatigue relevant parameters like mean stresses, residual stresses, material conditions, elevated temperatures etc. with a fewer number of specimens, than the conventional way to generate a simple $S-N$ curve.

Cumulative fatigue damage due to variable amplitude or random loading is generally determined using Miner's rule [11]. Miner's rule does not consider loading sequence effects and can lead to unreliable life predictions [12,13]. A number of fatigue damage theories have been proposed in the past to overcome these shortcomings [14-17]. However, application of these model requires either determination of additional material parameters or modifications to the $S-N$ curve of detail categories. Moreover, such additional material parameters are not readily available in design standards and codes. As a result, practicing engineers find it difficult to apply these models to structural engineering problems.

A new nonlinear fatigue damage model was recently proposed by the authors [18]. This model does not require determination of any additional material parameters other than the fatigue strength curve ($S-N$ curve) given in the design standards. As a result, the model can also be applied to structural details for a better fatigue life estimation. The model has been verified with experimental test results

1
2
3
4
5
6
7
8
9
10
11
12
13
14
15
16
17
18
19
20
21
22
23
24
25
26
27
28
29
30
31
32
33
34
35
36
37
38
39
40
41
42
43
44
45
46
47
48
49
50
51
52
53
54
55
56
57
58
59
60
61
62
63
64
65

for several materials. Verification has been shown for both fatigue damage evolution and fatigue lives [18]. The aim of this paper is to show further verification of this model based on experimentally observed damage evolution characterized through physical quantities during the cyclic loading. This verification is shown for S355 (SAE 1020) structural steel used extensively in both onshore and offshore structures. In addition, application of this model is also shown to an existing offshore jacket structure for better life estimation compared to conventional approach.

Initially, the paper presents the recently proposed nonlinear fatigue damage model. Experimental measurements of fatigue damage of S355(SAE 1020) structural steel specimens are presented thereafter. The fatigue damage is experimentally measured for both constant amplitude tests (CAT) as well as for load increase tests (LIT) where the stress amplitude was increased in steps. Relevant *S-N* curves are obtained using the StressLife method. These experimental results are then compared with theoretically predicted damage using proposed nonlinear model in order to verify the model further for S355 (SAE 1020) structural steel. In the end, application of proposed model is shown to an existing offshore jacket structure and fatigue damage are compared with conventional approach.

2. PROPOSED NONLINEAR FATIGUE DAMAGE MODEL

A nonlinear fatigue damage model has been proposed recently by the authors and the damage index is given in Equation (1) [18]. The damage for a given stress level is determined using the damage evolution

1 curve of the considered material. This damage is then transferred to
 2
 3
 4 the next load level by determining the effective number of cycles
 5
 6
 7 using the proposed load interaction factor. The physical meaning of
 8
 9 the concept is to assume the same damage state of the material, while
 10
 11 transferring the loading state from one stress level to the next and
 12
 13 determining the effective number of cycles required to cause this
 14
 15 damage.
 16
 17
 18
 19
 20

$$21 \quad D_i = 1 - \left[1 - \frac{n_i}{N_i}\right]^{\delta_i} = 1 - \left[1 - \frac{n_{(i+1),eff}}{N_{i+1}}\right]^{\frac{\delta_{i+1}}{\mathbb{Q}_{i+1}}} \quad (1)$$

22 where D_i is the damage at load level i when member is subjected to a
 23
 24 certain stress amplitude (or range) σ_i for n_i number of cycles and
 25
 26
 27
 28
 29
 30
 31
 32
 33
 34
 35
 36
 37
 38
 39
 40
 41
 42
 43
 44
 45
 46
 47
 48
 49
 50
 51
 52
 53
 54
 55
 56
 57
 58
 59
 60
 61
 62
 63
 64
 65

$$59 \quad \delta_i = \frac{-1.25}{\ln N_i} \quad (2)$$

$$60 \quad \mathbb{Q}_i = \left(\frac{\sigma_{i-1}}{\sigma_i}\right)^2 \quad (3)$$

1
2
3
4
5
6
7
8
9
10
11
12
13
14
15
16
17
18
19
20
21
22
23
24
25
26
27
28
29
30
31
32
33
34
35
36
37
38
39
40
41
42
43
44
45
46
47
48
49
50
51
52
53
54
55
56
57
58
59
60
61
62
63
64
65

The damage at load level $i+1$ can be determined using Equation (4) and Equation (5).

$$D_{i+1} = 1 - \left[1 - \frac{n_{(i+1),total}}{N_{i+1}} \right]^{\delta_{i+1}} \quad (4)$$

where

$$n_{(i+1),total} = n_{(i+1),eff} + n_{(i+1)} \quad (5)$$

where n_{i+1} is the number of cycles for stress state σ_{i+1} . Also, $n_{(i+1),total}$ is the total number of cycles for stress state σ_{i+1} obtained using the proposed concept. More details of the proposed model and associated parameters can be found in a authors' recent publication [18].

3. EXPERIMENTAL MEASUREMENT OF FATIGUE DAMAGE

3.1 Material and specimen geometry

The S355 (SAE 1020) steel has its chemical composition as well as the mechanical properties in accordance to standard DIN EN 10025-2. The chemical composition and the mechanical properties are given in **Table 1** and **Table 2**, respectively.

Table 1.

Table 2.

The geometry of the fatigue specimen (**Figure 1a**) is characterized through a transition from the cylindrical shaft with a diameter of 12 mm by a radius of 11.5 mm to the cylindrical gauge length with a diameter of 5.8 mm. Due to a smooth tangential shaft-gauge length-

1 transition, the stress concentration factor K_t is below 1.003 and can
2
3
4 be therefore neglected. The surface was polished to a roughness of R_z
5
6
7 = 6 μm , which is the 10-point roughness value. The surface topography
8
9 evaluated through a confocal microscope can be seen in **Figure 1b**.

10
11
12
13
14 **Figure 1a.**

15
16 **Figure 1b.**

17 18 19 20 21 **3.2 Experimental Setup**

22 Stress-controlled load increase tests (LIT) and constant amplitude
23
24 tests (CAT) were carried out at ambient temperature with a frequency
25
26 of 5 Hz on a servohydraulic testing system type EHF-L 25 kN by
27
28 Shimadzu using a sinusoidal load-time function at a load ratio of $R =$
29
30
31
32
33
34
35
36
37
38
39
40
41
42
43
44
45
46
47
48
49
50
51
52
53
54
55
56
57
58
59
60
61
62
63
64
65
-1. The experimental setup is given as a schematically drawing and a
photograph in **Figure 2**.

A LIT and two CATs were performed until specimen failure. In order
to characterize the microstructure-based fatigue behavior in detail,
besides the conventional mechanical stress-strain hysteresis
measurement by means of the plastic strain amplitude $\varepsilon_{a,p}$, also the
change in temperature ΔT and the change in electrical resistance ΔR
was measured. During the fatigue tests, ΔT was calculated from the
temperature on the surface of the specimen, continuously measuring
along the gauge length by an infrared camera.

This quantitative change is directly related to deformation-induced
changes of the microstructure in the bulk material and is considered
to represent the current fatigue state. Since metallic materials are

1
2 very good heat conductors, the microstructure related dissipated
3
4 energy is superimposed by heat transfer processes, which requires a
5
6 temperature stabilized grip system for the servohydraulic testing
7
8 system.
9

10
11
12
13 **Figure 2.**
14
15
16

17
18 For temperature measurements, three fields (5 × 5 pixels) were defined
19
20 along the specimen, one in the middle of the gauge length (T_1) and two
21
22 at each shaft (T_2 , T_3). The change in temperature was calculated in
23
24 accordance with Equation (6) below:
25
26

$$\Delta T = T_1 - 0.5 \times (T_2 + T_3) \quad (6)$$

27
28
29
30
31
32
33

34
35 The diameter of the shafts is much bigger than the diameter of the
36
37 gauge length and due to this the elastic portion of the change in
38
39 temperature, as well as ambient influences, are reduced from T_1
40
41 leading to ΔT , which is proportional to the plastic strain amplitude
42
43 $\varepsilon_{a,p}$ and is dedicated to the plastic deformation progress in the gauge
44
45 length of the specimen.
46
47

48
49 The theoretical background can be deduced from the consideration of
50
51 the stress-strain hysteresis loop. The area of the hysteresis loop
52
53 describes the energy that must be applied to plastically deform the
54
55 specimen during fatigue loading. Since energy cannot simply be
56
57 extinguished, it is transformed into the internal energy U and the
58
59 heat energy Q [4]. The term U enables microstructural changes such as
60
61
62
63

1
2
3
4
5
6
7
8
9
10
11
12
13
14
15
16
17
18
19
20
21
22
23
24
25
26
27
28
29
30
31
32
33
34
35
36
37
38
39
40
41
42
43
44
45
46
47
48
49
50
51
52
53
54
55
56
57
58
59
60
61
62
63
64
65

dislocation reactions, micro- and macro-cracking as well as their propagation processes. The predominant proportion of about 90 % of the deformation energy dissipates as heat, that is why the temperature change can be correlated directly with the plastic deformation or the cumulative damage. In the case of metallic materials, the change in temperature due to the dissipated heat energy can be easily measured on the specimens' surface due to the very good heat conduction.

For temperature measurements, the surface of the specimen was painted with high emissivity black paint, obtaining an emission factor of 0.97 and the change in the emissivity was neglected even if the effective temperature changes are relatively small (< 10K).

For the sake of thermal stability as well as the accuracy during long test intervals, the infrared camera has been modified by an active cooling system (**Figure 2**).

To get the thermal stability of the specimen grips, a cooling system based on Peltier-elements with water coolant was developed, which is a basic requirement in order to use temperature-sensitive measurement techniques.

For highly sensitive resistometric measurements, the specimen was subjected to a direct current of $I = 5 \text{ A}$ and the change in electrical resistance ΔR was accurately measured using two wires at the transition areas between the specimens' gauge length and clamping shafts. For the connection to the data acquisition device, copper cables with a cross-section of 0.22 mm^2 and a length of 1.50 mm were used, and the welding process was performed without additives in order to increase the reproducibility of electrical resistance measurements.

1
2 Even for mean stress-free loading, the electrical resistance R and its
3
4 change depends up to the initiation of macrocracks exclusively on the
5
6 specific electrical resistance ρ^* , which is a function of deformation-
7
8 induced microstructural changes.
9

10 11 **3.3 Load increase and constant amplitude tests**

12
13 Load increase tests (LIT) allow estimating the fatigue limit of
14
15 materials with one specimen only. In Figure 3, the stress amplitude
16
17 σ_a , starting at $\sigma_{a,start} = 100$ MPa with a stepwise increase of $\Delta\sigma_a = 20$
18
19 MPa each $\Delta N = 9 \times 10^3$ cycles, the plastic strain amplitude $\varepsilon_{a,p}$, the
20
21 change in temperature ΔT as well as the change in electrical
22
23 resistance ΔR are plotted versus the number of cycles for a S355 (SAE
24
25 1020) steel specimen. The change in temperature calculated in
26
27 accordance to Equation (6) as well as the other measurands are shown
28
29 in **Figure 3** together with the stress amplitude σ_a from $N = 54 \times 10^3$
30
31 cycles up to specimen failure at a number of cycles to failure of $N_f =$
32
33 117,201 and a load level of $\sigma_a = 360$ MPa.
34
35
36
37
38
39
40
41
42

43 **Figure 3.**

44
45
46
47 From $N = 63 \times 10^3$ and $\sigma_a = 240$ MPa for ΔR and $N = 72 \times 10^3$ and $\sigma_a = 260$
48
49 MPa for ΔT , respectively, slight changes in the slopes can be observed
50
51 indicating the first micro-plastic deformations. In the case of the
52
53 plastic strain amplitude first changes occur for $\sigma_a = 280$ MPa, which
54
55 underlines that ΔT and ΔR are much more sensitive to the first
56
57 microstructural changes than the conventional strain measurement.
58
59
60
61
62
63
64
65

1
2 Based on this result, the fatigue limit (point of transition) can be
3
4 estimated with a value of $\sigma_a = 240/260$ MPa.
5

6
7 In addition to the LIT, two CATS were performed. The stress
8
9 amplitudes for both CATs are chosen above the point of transition. The
10
11 frequency was kept constant for all fatigue tests, which possibly
12
13 leads to an influence of the mechanical stress rate, which was not
14
15 considered separately.
16
17

18
19 In the following cyclic deformation curves for stress amplitudes of
20
21 $\sigma_a = 280$ MPa and 320 MPa (**Figure 4**) based on the plastic strain
22
23 amplitude, the change in temperature and the change in electrical
24
25 resistance vs. the number of cycles are plotted.
26
27
28
29
30

31 **Figure 4.**
32
33
34

35
36 The cyclic deformation behavior is characterized by varying incubation
37
38 intervals indicated by constant values of $\varepsilon_{a,p}$, ΔT and ΔR parallel to
39
40 the X-axis until a first increase is detected which is related to
41
42 cyclic softening processes of the S355 (SAE 1020) steel. After passing
43
44 10% N_f , the slope becomes smaller and stays constant until 75 % N_f is
45
46 reached. The final increase is caused by the propagation of
47
48 macrocracks leading to a fictitious secondary cyclic softening
49
50 dominated by the reduction in the effective cross-section within the
51
52 plastically deformed specimen's gauge lengths.
53
54
55

56 **3.4 S-N curve estimation using StressLife approach**

57
58 The StressLife_{tc} (tc: trend curve) approach gives comprehensive
59
60 information regarding the load-function related deformation behavior
61
62
63
64
65

1
2 and thus the load-lifetime relation by means of an $S-N$ curve of a
3
4 material by using only one load increase test (LIT) and two constant
5
6 amplitude tests (CAT). The procedure is described in detail in [8].
7
8 The material's response can be characterized through different
9
10 measurands, among others the total strain amplitude, change in
11
12 temperature and the change in electrical resistance. The calculation
13
14 shown in **Figures 5** and **Figure 6** was performed on the basis of
15
16 temperature data and is compared with StressLife calculations for also
17
18 the total strain amplitude as well as the change in electrical
19
20 resistance (**Figure 6b**).

21
22 In the following, Morrow [19], Manson-Coffin [20] and Basquin [21]
23
24 laws are combined into one single equation in order to calculate the
25
26 $S-N$ data for the S355 (SAE 1020) steel.

27
28 The first step in the StressLife_{tc} procedure is the LIT which was
29
30 already shown in **Figure 3**. From the traditional point of view, the
31
32 material response for stress-controlled tests is the total and plastic
33
34 strain amplitude, but this can also be transferred to other measuring
35
36 methods based on temperature or any changes of magnetic or electric
37
38 parameters and due to this it can be written in a generalized manner.
39
40 The feasibility of this practice has been verified in numerous
41
42 completed investigations [7].

43
44 For the further calculation, the stress amplitude is plotted vs. the
45
46 material response in terms of a generalized Morrow plot [8] shown in
47
48 **Figure 5a** for the change in temperature.

1
2
3
4
5
6
7
8
9
10
11
12
13
14
15
16
17
18
19
20
21
22
23
24
25
26
27
28
29
30
31
32
33
34
35
36
37
38
39
40
41
42
43
44
45
46
47
48
49
50
51
52
53
54
55
56
57
58
59
60
61
62
63
64
65

From this diagram a mostly elastic and a mostly plastic range can be identified and described independently of each other mathematically according to Morrow expressed through Equation (7).

$$\sigma_a = K_{e/p/CAT'} \times (M)^{n_{e/p/CAT'}} \tag{7}$$

From Equation (7) and the differentiation into a mostly elastic and mostly plastic response (**Figure 5a**), the fatigue strength exponent *b* (mostly elastic) as well as the fatigue ductility exponent *c* (mostly plastic) can be calculated by using Equations (8) and (9).

$$b = \frac{-n_e'}{5n_e' + 1} \tag{8}$$

$$c = \frac{-1}{5n_p' + 1} \tag{9}$$

As previously explained for the term "material response", the measured value *M* is the change in temperature and can be specified into an elastic (*M_e*) and a plastic (*M_p*) portion in Equation (10).

$$M_t = M_e + M_p \tag{10}$$

M_e can be represented by a generalized Basquin equation (Equation (11)), where in the case of strain measurements *B* is expressed through $\sigma_f' \times E^{-1}$ (σ_f' = fatigue strength coefficient, *E* = Young's modulus).

$$M_e = B \times (2N_f)^b \tag{11}$$

1
2 M_p can be described by Manson-Coffin (Equation (12)), where C
3
4 corresponds to the fatigue ductility coefficient σ_f' , if strain is the
5
6 measured value.
7
8
9

$$10 \quad M_p = C \times (2N_f)^c \quad (12)$$

11
12
13
14
15
16 If Equation (12) and (11) are used in Equation (10), then Equation
17
18 (13) is obtained:
19

$$20 \quad M_{1/2} = B \times (2N_{f,1/2})^b + C \times (2N_{f,1/2})^c \quad (13)$$

21
22
23
24
25
26
27
28 As it is already shown in **Figure 4**, two CATs ($\sigma_{a,2} < \sigma_{a,1}$) are
29
30 performed leading to different number of cycles to failure ($N_{f,2} > N_{f,1}$)
31
32 as well as different values of the material response ($M_2 < M_1$) at a
33
34 defined fatigue stage, e.g. $0.5 \times N_f$.
35
36
37
38
39

$$40 \quad C = \frac{(2N_{f,1})^b \times M_2 - (2N_{f,2})^b \times M_1}{(2N_{f,2})^c \times (2N_{f,1})^b - (2N_{f,1})^c \times (2N_{f,2})^b} \quad (14)$$

41
42
43
44
45
46 Since there are each two values for N_f and M , C (Equation (14)) and
47
48 B (Equation (15)) can be evaluated through this.
49
50
51
52
53

$$54 \quad B = \frac{M_1 - C \times (2N_{f,1})^c}{(2N_{f,1})^b} \quad (15)$$

1
2 In consequence of Equations (11) and (12), the elastic as well as
3
4 plastic portion of the material response can be plotted vs. the number
5
6 of cycles to failure, which is shown in **Figure 5b** as slopes indicated
7
8
9 with *b* and *c*.
10

11
12
13
14 **Figure 5a.**

15
16
17 **Figure 5b.**

18
19
20
21 The summation of both curves leads to a change in temperature-number
22
23 of cycles to failure ($\Delta T-N_f$) curve. According to the simplification of
24
25 Ramberg-Osgood [22], the elastic behavior can be assumed to be linear.
26
27 By extrapolation of the elastic portions of $\Delta T_{320 \text{ MPa}}$ ($CAT_{320 \text{ MPa}}$) and
28
29 $\Delta T_{280 \text{ MPa}}$ ($CAT_{280 \text{ MPa}}$) to a σ_a -value ($CAT_{260 \text{ MPa calc.}}$) slightly above the
30
31 transition point from a mostly elastic to mixed elastic-plastic
32
33 behavior, ΔT_e for σ_a of $CAT_{260 \text{ MPa calc.}}$ can be calculated. By using the
34
35 relationship between ΔT_e and the $\Delta T-N_f$ curve, ΔT can be determined for
36
37
38
39
40 $CAT_{260 \text{ MPa calc.}}$ (**Figure 6a**).
41

42
43 With this third calculated point, K_{CAT}' and n_{CAT}' can now be evaluated
44
45 according to Equation (7).
46

47
48 If Equation (13) is used in Equation (7), then Equation (16)
49
50 follows, the parameters *C*, *B*, K_{CAT}' and n_{CAT}' being determined in the
51
52 preceding steps. Based on Equation (16), the *S-N* curve can be
53
54
55 calculated.
56

$$\sigma_a = K_{CAT}' \times (B \times (2N_f)^b + C \times (2N_f)^c)^{n_{CAT}'} \quad (16)$$

1
2 **Figure 6b** gives an impression regarding the capability of the
3
4 StressLife_{tc} approach, which enables the calculation of the materials'
5
6 fatigue life based on one LIT and two CATs and is in very good
7
8 accordance compared to the conventional determined lifetimes from
9
10 constant amplitude tests. The diagram shows StressLife calculations
11
12 based on the total strain amplitude, the change in temperature and the
13
14 change in electrical resistance in comparison with the two CATs from
15
16 the StressLife calculation at stress amplitudes of 280 and 320 MPa as
17
18 well as two additional CATs at 300 and 340 MPa. All conventional
19
20 determined *S-N* data show a very good accordance to the calculated
21
22 ones, which underlines the high capability of the StressLife approach.
23
24
25
26
27
28
29
30

31 **Figure 6a.**

32 **Figure 6b.**

33
34
35
36
37
38 This procedure was already shown for normalized SAE 1040 steel in
39
40 [8]. The results of this work as well as [8] underline that the
41
42 StressLife_{tc} approach could lead to an enormous reduction in time and
43
44 costs, while the experimental efforts will be also reduced, whereas
45
46 significant financial as well as scientific advantages can be reached.
47
48 However, it must be noted that the material behavior can sometimes
49
50 scatter strongly. In many cases this depends on the material itself
51
52 but may also be due to the material or surface condition. For this
53
54 reason, the results calculated according to StressLife_{tc} must always be
55
56 considered critically. Besides that, this method gives a wealth of
57
58 information regarding the cyclic deformation behavior, which makes it
59
60
61
62
63
64
65

1
2 a valuable tool for material characterization under cyclic loading.
3
4 For example, it might be possible to compare results of stress- and
5
6 strain-controlled fatigue tests with one another and even to convert
7
8 them for a first estimation. Therefore, the separation of a total
9
10 deformation into elastic and plastic portions as it is known from *S-N*
11
12 curves evaluated under total strain control is a basic requirement.
13
14

15
16 It was not in the scope of this paper to provide a statistic
17
18 validation of the calculated $StressLife_{tc}$ curves through conventional
19
20 determined *S-N* datasets, rather, it should be shown that short-term
21
22 methods as *StressLife* can generate datasets for simulation or
23
24 modelling activities.
25
26
27
28
29
30

31 **4. COMPARISON OF PROPOSED MODEL WITH EXPERIMENTAL FATIGUE DAMAGE OF** 32 33 **S355 (SAE 1020) STRUCTURAL STEEL** 34 35

36 The theoretically predicted damage (D_{model}) using proposed model are
37
38 compared with above determined damage evolution characterized through
39
40 physical quantities (plastic strain amplitude, change in temperature
41
42 and change in electrical resistance). For this comparison, the
43
44 cumulated signals are first calculated from the experimentally
45
46 measured continuous material response based on change in above
47
48 physical quantities. The comparison for the case of a load increase
49
50 test (LIT) is shown in **Figure 7**. Comparison for the two constant
51
52 amplitude tests (CAT) performed at stress amplitudes 280 MPa and 320
53
54 MPa is shown in **Figure 8** and **Figure 9** respectively. The experimental
55
56 results for above LIT and CAT are presented earlier in Section 3.3.
57
58
59
60
61
62
63
64
65

1
2
3
4
5
6
7
8
9
10
11
12
13
14
15
16
17
18
19
20
21
22
23
24
25
26
27
28
29
30
31
32
33
34
35
36
37
38
39
40
41
42
43
44
45
46
47
48
49
50
51
52
53
54
55
56
57
58
59
60
61
62
63
64
65

Figure 7.

Figure 8.

Figure 9.

From above figures, it can be seen that there is a good agreement between the proposed damage curve using the proposed model and the measured physical parameters representing the fatigue behavior of the material. There are still some deviations from the experimental damage evolution especially in the case of CAT at 320 MPa. However, the predicted final fatigue life in all considered cases is found in good agreement with experimental life as shown in **Figure 10.**

Figure 10.

5. APPLICATION OF PROPOSED MODEL TO ESTIMATE FATIGUE DAMAGE OF a JACKET STRUCTURE

The proposed model is applied to a bottom fixed offshore jacket structure and fatigue damage at one of the joints is estimated. The damage is also computed using the conventional approach. Fatigue assessment is performed using the hot spot stress-based approach. Initially, the details of considered jacket structure is provided. The hydrodynamic parameters are thereafter discussed followed by time domain fatigue analysis using Wajac software [23]. The considered waves for fatigue analysis are mentioned and fatigue damage at one of the joints is calculated in the end using the proposed model and conventional approach.

5.1 Considered offshore jacket structure

1
2
3
4
5
6
7
8
9
10
11
12
13
14
15
16
17
18
19
20
21
22
23
24
25
26
27
28
29
30
31
32
33
34
35
36
37
38
39
40
41
42
43
44
45
46
47
48
49
50
51
52
53
54
55
56
57
58
59
60
61
62
63
64
65

The considered platform is referred to as Platform A in this study and is one of the heaviest platforms in the North Sea. The platform is supported on an 8-legged jacket structure installed in a water depth of 123 meters. The legs are arranged in a 2 x 4 rectangular grid and battered to a slope of approximately 1:8. The topsides and jacket weights are 23,600 tonnes and 17,400 tonnes respectively. The structure is modelled in Sesam GeniE software [24] and the model along with its dimensions is shown in **Figure 11**. The members are modelled as beam elements and supports are modelled as spring elements whose stiffness are defined as per the seabed properties from the geotechnical reports provided by the client.

Figure 11.

5.2. Considered hydrodynamic parameters

The hydrodynamic parameters for jacket members are considered as per the design basis of the structure and the Norsok standard [25]. The values of drag and inertia coefficients for both smooth and rough members(along with anodes) are given in **Table 3**. The drag coefficient of rough members is increased by 10% due to the anodes. Marine growth and flooding are also considered as per the design basis. Also, a kinematic factor of 0.95 is considered to account for wave spreading as per the Norsok standard [25].

Table 3.

1
2
3
4
5
6
7
8
9
10
11
12
13
14
15
16
17
18
19
20
21
22
23
24
25
26
27
28
29
30
31
32
33
34
35
36
37
38
39
40
41
42
43
44
45
46
47
48
49
50
51
52
53
54
55
56
57
58
59
60
61
62
63
64
65

5.3. Time domain fatigue analysis of considered joint

A time domain fatigue analysis is performed for one of the joints of the jacket structure. The waves selected for this analysis are taken from the design brief provided by the Client and are given in **Table 4**. For each seastate, a random irregular sea is generated based on a wave spectrum. The wave spectrum used in this study is JONSWAP wave spectrum for the generation of irregular sea [26].

Table 4.

Eight random irregular seastates are generated for various significant wave heights each representing a 3-hour seastate. The eight seastates are ordered randomly in a sequence and the sequence in this combined 24-hour irregular seastate is shown in **Table 5**.

Table 5.

Multi-step static time-domain analysis is performed separately for each 3-hour seastate. The combined 24-hour irregular seastate is repeated to determine structural fatigue damage after 25 and 40 years.

5.4. Considered joint and determination of hotspot stresses

The considered joint for fatigue damage evaluation is shown in **Figure 12a**. The joint has three braces connected to the main leg in the splash zone as shown in **Figure 12b**. Brace Bm1425 is found to be the

1
2
3
4
5
6
7
8
9
10
11
12
13
14
15
16
17
18
19
20
21
22
23
24
25
26
27
28
29
30
31
32
33
34
35
36
37
38
39
40
41
42
43
44
45
46
47
48
49
50
51
52
53
54
55
56
57
58
59
60
61
62
63
64
65

most critical brace at this joint and results are presented for this brace.

Figure 12a.

Figure 12b.

The fatigue damage is evaluated for the brace member Bm1425 of considered joint. Forces and moments in the brace member were extracted from the global finite element analysis at the end of each time step of 1 second in 24-hour simulation. The time histories of axial force, in-plane and out-of-plane moment in the member are shown in **Figure 13**. The nominal axial and bending stress ranges were subsequently determined. The hot spot stress concentration factors for considered joint members were also calculated using the DNV guidelines [27]. The nominal stress ranges were combined using the method of superposition wherein hot spot stresses were evaluated at eight locations around the circumference of the intersection for each of the load combinations using formulae given in the guidelines. The hot spot stresses were determined for considered brace member and are shown in **Figure 14**.

Figure 14.

5.5. Determination of fatigue damage for considered joint

The cycle counting is performed using the rainflow method followed by the determination of fatigue damage using the Miner's rule and

1
2
3
4
5
6
7
8
9
10
11
12
13
14
15
16
17
18
19
20
21
22
23
24
25
26
27
28
29
30
31
32
33
34
35
36
37
38
39
40
41
42
43
44
45
46
47
48
49
50
51
52
53
54
55
56
57
58
59
60
61
62
63
64
65

proposed non-linear model. The interaction factor is taken as one for this study. The damages are calculated for brace member in the considered joint and the results are given in **Table 6**.

Table 6.

There are significant deviations between the fatigue damage predicted using proposed model and using conventional approach. The predicted damage is almost seven times lesser than that predicted using Miner's rule after 25 years lifetime. However, the damage using proposed model is more than 3 times lesser than using Miner's rule at the end of 40 years. These observations in the damage deviations confirm the nonlinear behavior of fatigue damage evolution in the material and structure. It is to be noted that the considered joint might not be the most critical joint of the structure for fatigue damage. Therefore, fatigue life of the structure cannot be decided based on Table 6. However, the aim of this study is to compare the fatigue damage using proposed model with the use of conventional approach and this has been shown for one of the typical joints. It is recommended that such a comparison should be done for all the joints or fatigue critical joints for estimation of fatigue life of the whole structure. This has also been identified as the scope of further works.

6. CONCLUSIONS

Following conclusions are made based on this study:

1
2
3
4
5
6
7
8
9
10
11
12
13
14
15
16
17
18
19
20
21
22
23
24
25
26
27
28
29
30
31
32
33
34
35
36
37
38
39
40
41
42
43
44
45
46
47
48
49
50
51
52
53
54
55
56
57
58
59
60
61
62
63
64
65

1. Changes in physical quantities (plastic strain, temperature and resistance) during cyclic loading can reasonably characterize the fatigue behaviour of the material and fatigue damage can be evaluated based on cyclic deformation, temperature and electrical resistance curves.
2. Detailed material information can be extracted from a small number of fatigue tests using the StressLife approach as compared to conventional methods. As a result, use of such method could lead to an enormous reduction in time and costs involved in numerous experiments.
3. Proposed nonlinear fatigue damage model overcomes the shortcomings of commonly used Miner's rule and gives better fatigue damage predictions for variable/random loading states. The model doesn't require any additional material parameters, other than the commonly available *S-N* curve. It can be applied to design detail categories (structural details) using the corresponding partially known *S-N* curve in the design standards.
4. Proposed model can be applied to engineering structures for a better estimation of fatigue assessment. It can be easily used by practicing engineers based only on the code-given *S-N* curves. Application of proposed model to an offshore jacket structure shows the importance of precise fatigue model in real life.

ACKNOWLEDGMENT

The authors from the research group in Norway gratefully acknowledge the financial support provided by the Norwegian Ministry of Education during this project. The authors from the research groups in Germany

1
2 would like to thank their funding foundations, e.g. German Research
3
4 Foundation (Deutsche Forschungsgemeinschaft, DFG) and Federal Ministry
5
6 of Economics and Technology (Bundesministerium für Wirtschaft und
7
8 Technologie, BMWi), for the financial support of related research
9
10 work.
11
12

13
14 The authors would also thank Shimadzu Europe/Germany and Micro-Epsilon
15
16 for their support in technical equipment provision.
17
18
19
20

21 REFERENCES

22
23 [1] P. Lukáš, M. Klesnil. Cyclic stress-strain response and fatigue
24 life of metals in low amplitude region. *Materials Science and*
25 *Engineering* 1973;11:345-56.
26
27

28 [2] A. Brazenas, D. Vaiciulis. Determination of fatigue curve
29 parameters at cyclic strain limited loading according to the
30 mechanical characteristics of power energy structural materials.
31 *Nuclear Engineering and Design* 2011; 241:3596-04.
32
33

34 [3] F. Curà, A. E. Gallinatti, R. Sesana. Dissipative aspects in
35 thermographic methods. *Fatigue & Fracture of engineering materials &*
36 *structures* 2012;35:1133-47.
37
38

39 [4] G. Meneghetti, R. B. Atzori. A two-parameter, heat energy-based
40 approach to analyze the mean stress influence on axial fatigue
41 behavior of plain steel specimens. *Int J Fatigue* 2016;82:60-70.
42
43

44 [5] M. A. Omari, I. Sevostianov. Estimation of changes in the
45 mechanical properties of stainless steel subjected to fatigue loading
46 via electrical resistance monitoring. *Int J Engineering Science*
47 *2013;65:40-8.*
48
49

50 [6] P. Starke, F. Walther, D. Eifler. Model-based correlation between
51 electrical resistance and the dislocation structure of fatigued ICE R7
52 wheel steel. *MP Materials Testing* 2018;60:669-76.
53
54

55 [7] P. Starke, F. Walther, D. Eifler. "PHYBAL" a short-time procedure
56 for a reliable fatigue life calculation. *Advanced Engineering*
57 *Materials* 2010;12:276-82.
58
59

60 [8] P. Starke. StressLife_{tc} - NDT-related assessment of the fatigue
61 life of metallic materials. *MP Materials Testing* 2019;91(4):297-03.
62
63

1
2
3
4
5
6
7
8
9
10
11
12
13
14
15
16
17
18
19
20
21
22
23
24
25
26
27
28
29
30
31
32
33
34
35
36
37
38
39
40
41
42
43
44
45
46
47
48
49
50
51
52
53
54
55
56
57
58
59
60
61
62
63
64
65

[9] R. Acosta, P. Starke, C. Boller, M. Jamrozy, M. Klein, M. Knyazeva, F. Walther, K. Heckmann, J. Sievers, T. Schopf, X. Schuler. StrainLife: Efficient fatigue life data generation for an enhanced ageing assessment of metallic components. Proceedings of the ASME 2018 Pressure Vessels and Piping Conference 2018;1-8.

[10] P. Starke, H. Wu. Use of non-destructive testing methods in a new one-specimen test strategy for estimating fatigue data. Int J Fatigue 2018;111:177-85.

[11] A. Almar-Naess. Fatigue handbook. Tapir Publishers, Trondheim, Norway; 1985.

[12] S. Suresh. Fatigue of materials. Cambridge UK: Cambridge University Press; 1998.

[13] G. Mesmacque, S. Garcia, A. Amrouche, C. Rubio-Gonzalez. Sequential law in multiaxial fatigue, a new damage indicator. Int J Fatigue 2005;27(4):461-7.

[14] J. L. Chaboche, P. M. Lesne. A non-linear continuous fatigue damage model. Fatig Fract Eng Mater Struct 1988;11(1):1-17.

[15] D. G. Shang, W. X. Yao. A nonlinear damage cumulative model for uniaxial fatigue. Int J Fatigue 1999;21(2):187-94.

[16] P. J. Huffman, S. P. Beckman. A non-linear damage accumulation fatigue model for predicting strain life at variable amplitude loadings based on constant amplitude fatigue data. Int J Fatigue 2013;48:165-9.

[17] E. Santecchia, A. M. S. Hamouda, F. Musharavati, E. Zalnezhad, M Cabibbo, M. El Mehtedi, S. Spigarelli. A review on fatigue life prediction methods for metals. Adv Mater Sci Eng 2016; 9573524:1-26.

[18] A. Aeran, S. C. Siriwardane, O. Mikkelsen, I. Langen. A new nonlinear fatigue damage model based only on SN curve parameters. Int J Fatigue 2017;103:327-41.

[19] J. D. Morrow. Cyclic plastic strain energy and fatigue of metals. Internal friction, damping and cyclic plasticity. American Society for Testing and Materials 1964;45-87.

[20] M. Ricotta. Simple expressions to estimate the Manson-Coffin curves of ductile cast irons. Int J Fatigue 2015;78:38-45.

[21] H. Basquin. The exponential law on endurance tests. American Society for Testing and Materials 1910;10:625-630.

1
2
3
4
5
6
7
8
9
10
11
12
13
14
15
16
17
18
19
20
21
22
23
24
25
26
27
28
29
30
31
32
33
34
35
36
37
38
39
40
41
42
43
44
45
46
47
48
49
50
51
52
53
54
55
56
57
58
59
60
61
62
63
64
65

[22] J. Li, Z. Zhang, C. Li. An improved method for estimation of Ramberg-Osgood curves of steels from monotonic tensile properties. *Fatigue & Fracture of engineering materials & structures* 2016;39:412-426

[23] Det Norske Veritas. Wave and Current Loads on Fixed Rigid Frame Structures. Wajac user manual. July 2018.

[24] Det Norske Veritas. Concept design and analysis of offshore structures. Sesam user manual Genie Vol. 1. March 2014.

[25] Standard NORSOK. Actions and action effects. 2017. N-003. January 2017.

[26] Chakrabarti SK. Hydrodynamics of offshore structures. Boston: Computational Mechanics Publications. 1987.

[27] Det Norske Veritas. Fatigue design of offshore steel structures. 2016. DNVGL-RP-C-203. April 2016.

Submitted to **International Journal of Fatigue**

May 2019

A nonlinear fatigue damage model: Comparison with experimental damage evolution of S355 (SAE 1020) structural steel and application to offshore jacket structures

Ashish Aeran¹, Ruth Acosta², Sudath C. Siriwardane¹, Peter Starke²,
Ove Mikkelsen¹, Ivar Langen¹, Frank Walther³

¹Department of Mechanical and Structural Engineering and Materials Science, University of Stavanger,
P.O. Box 8600 Forus, N-4036, Stavanger, Norway

²Department of Materials Science and Materials Testing (WWHK), University of Applied Sciences Kaiserslautern, D-67659 Kaiserslautern, Germany

³Department of Materials Test Engineering (WPT), TU Dortmund University, D-44227 Dortmund, Germany

Corresponding Author: Ashish Aeran ashish.aeran@uis.no

FIGURES AND TABLES

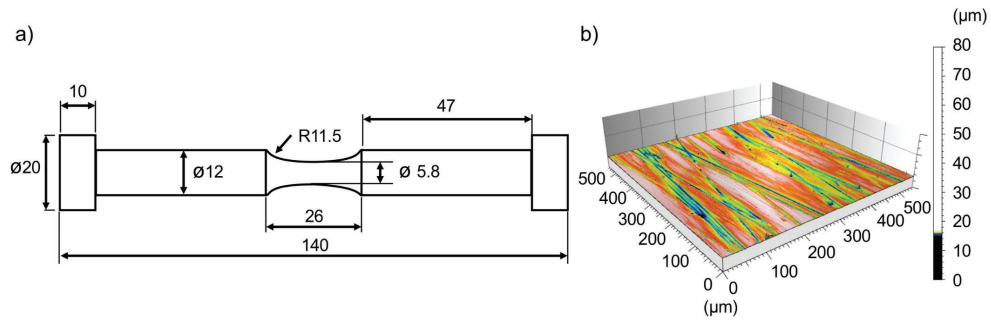


Figure 1(a) Specimen geometry for fatigue tests and **(b)** topography of polished specimen surface.

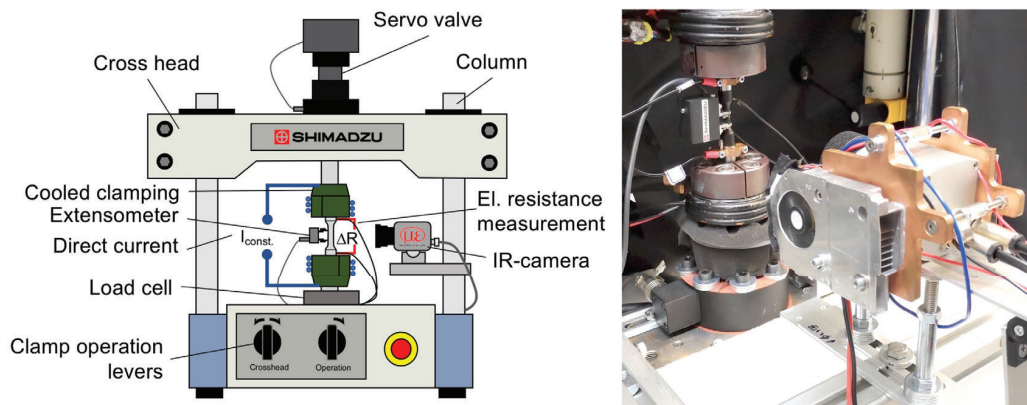


Figure 2. Experimental setup.

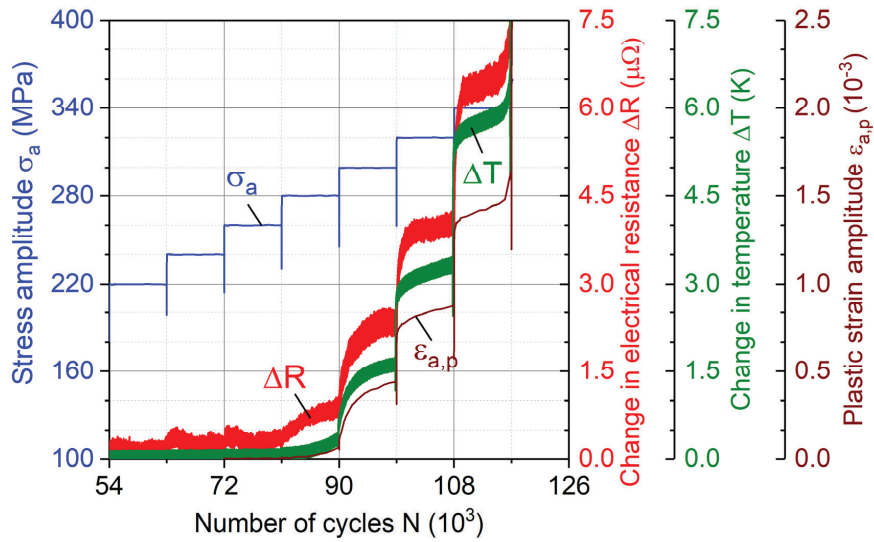


Figure 3. Load increase test results for S355 (SAE 1020) structural steel.

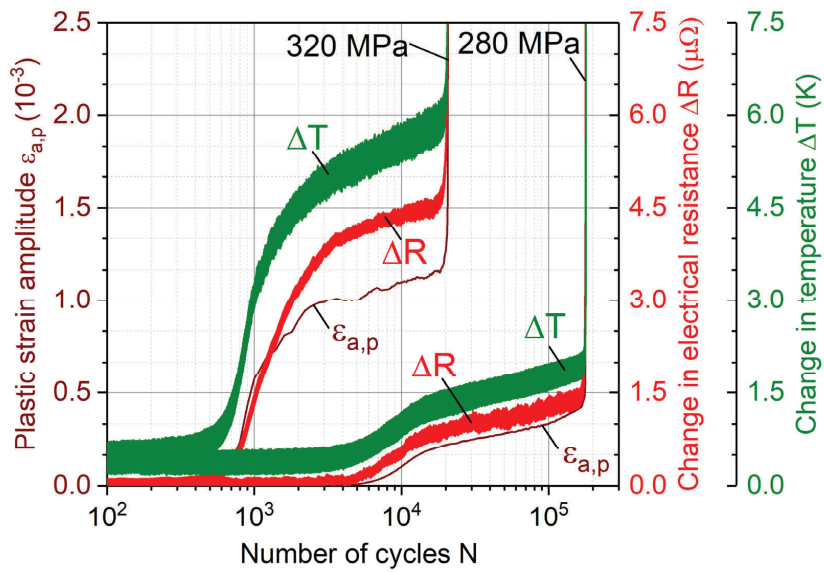
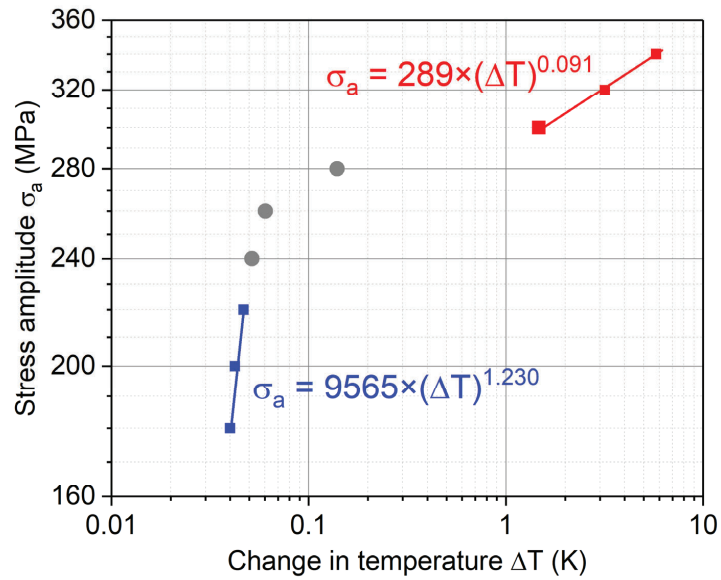
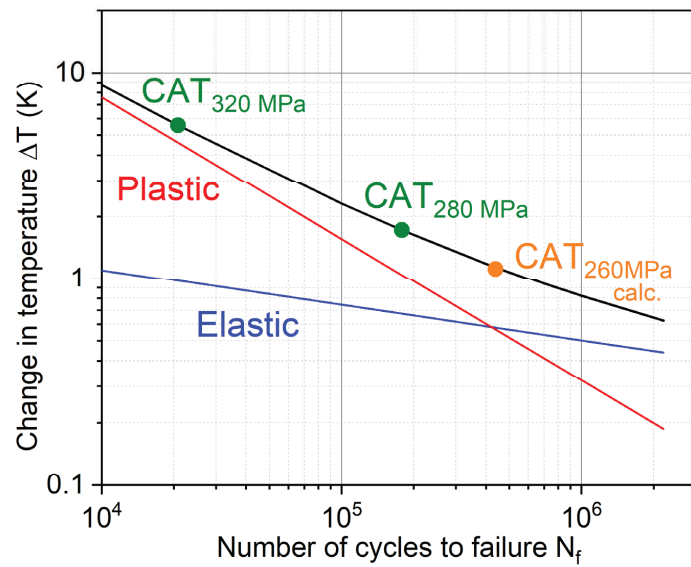


Figure 4. Constant amplitude test results for S355 (SAE 1020) structural steel.

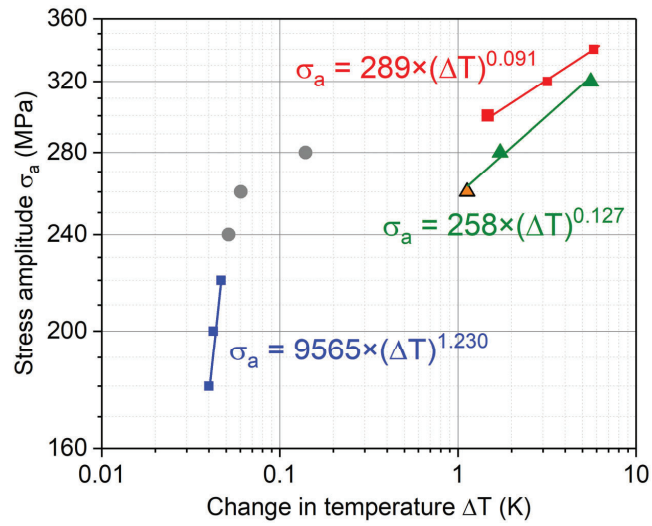


(a)

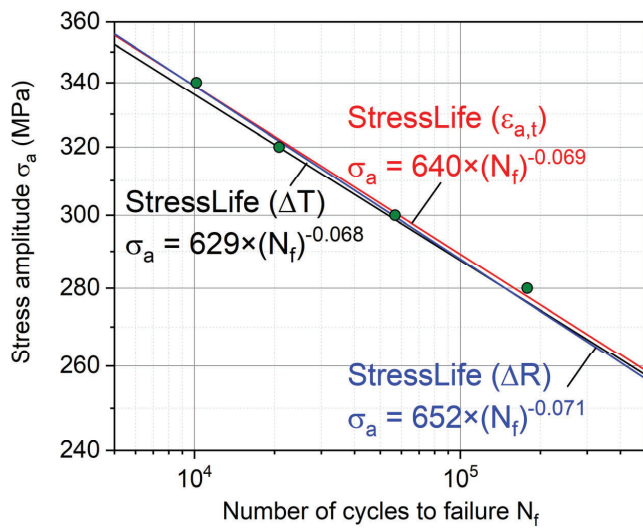


(b)

Figure 5. (a) Change in temperature with stress amplitude during LIT
 (b) ΔT - N_f curve during CATs for S355 (SAE 1020) structural steel.



(a)



(b)

Figure 6. (a) Change in temperature with stress amplitude during LIT and CATs (b) comparison of the calculated StressLife_{t_c}-curves with conventionally determined S-N data of S355 (SAE 1020) structural steel.

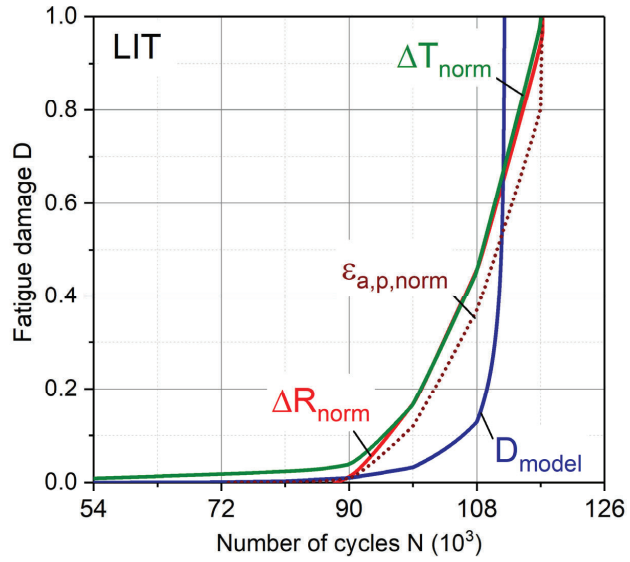


Figure 7. Comparison of experimental and calculated fatigue damage for LIT.

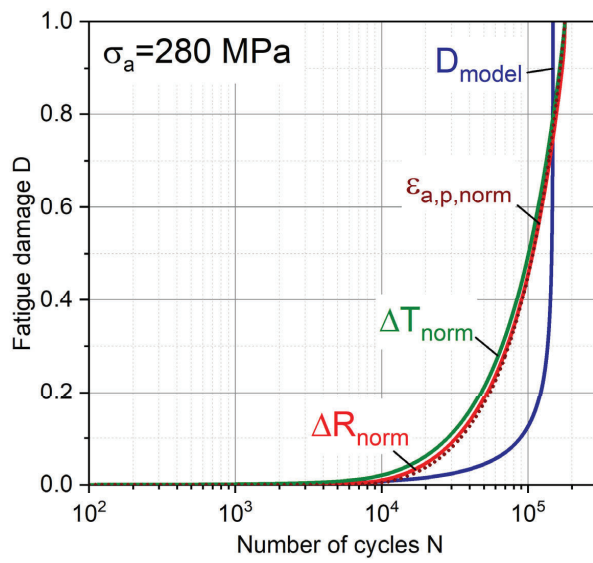


Figure 8. Comparison of experimental and calculated fatigue damage for CAT under $\sigma_a = 280$ MPa.

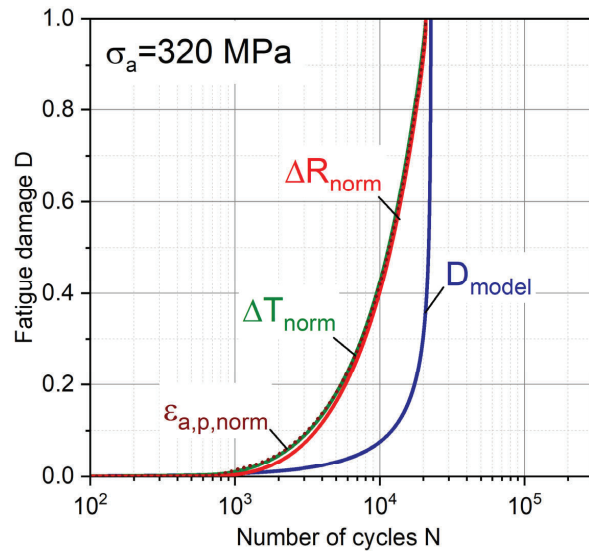


Figure 9. Comparison of experimental and calculated fatigue damage for CAT under $\sigma_a = 320$ MPa.

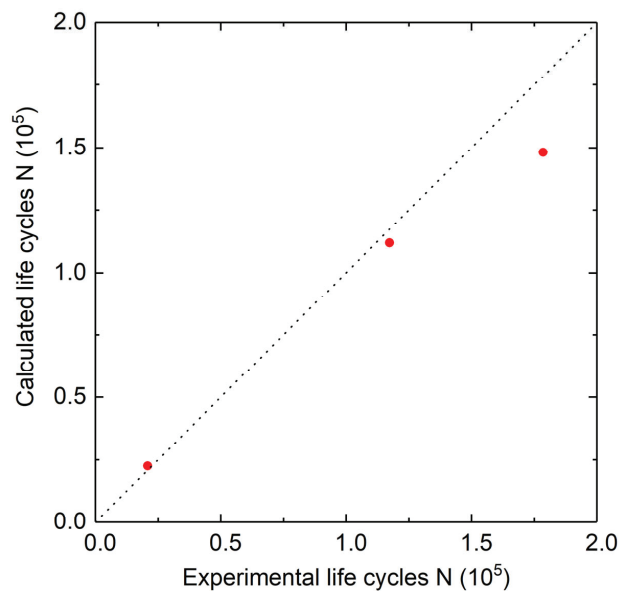


Figure 10. Experimental versus calculated life for fatigue life estimations under LIT and CATs.

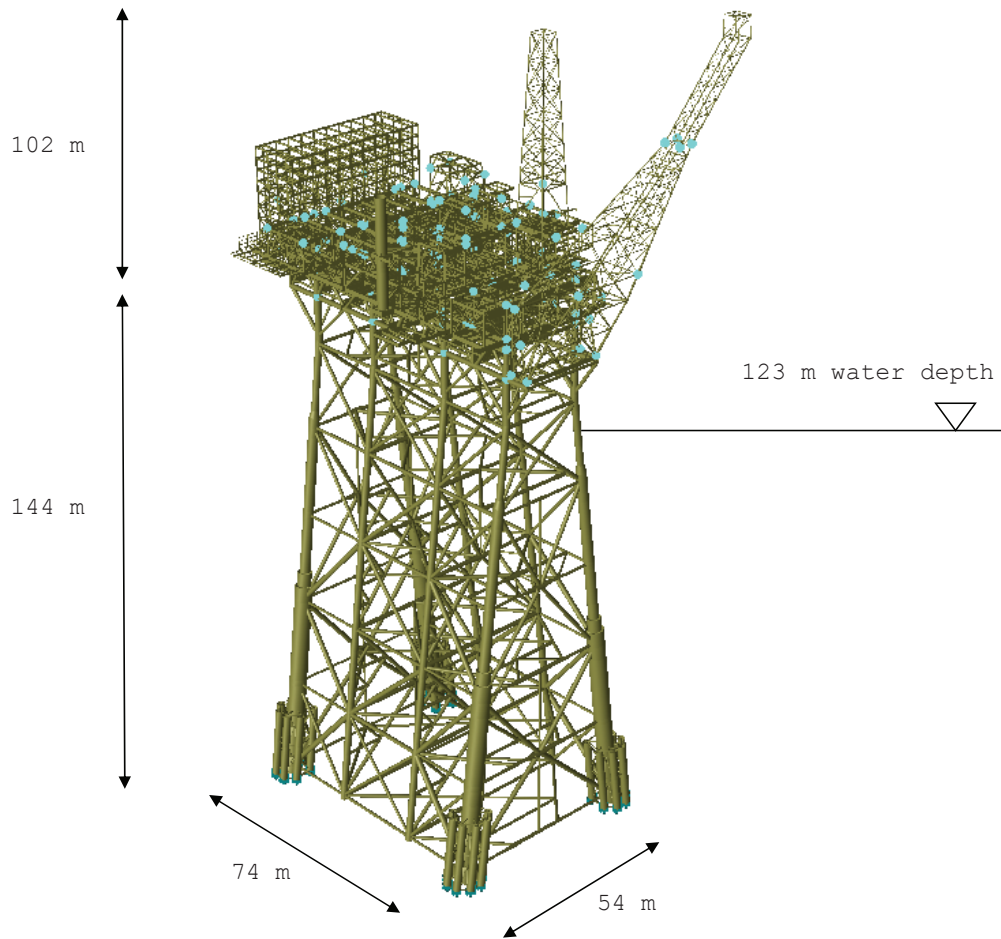


Figure 11. Finite element model of considered jacket type offshore structure and its dimensions.

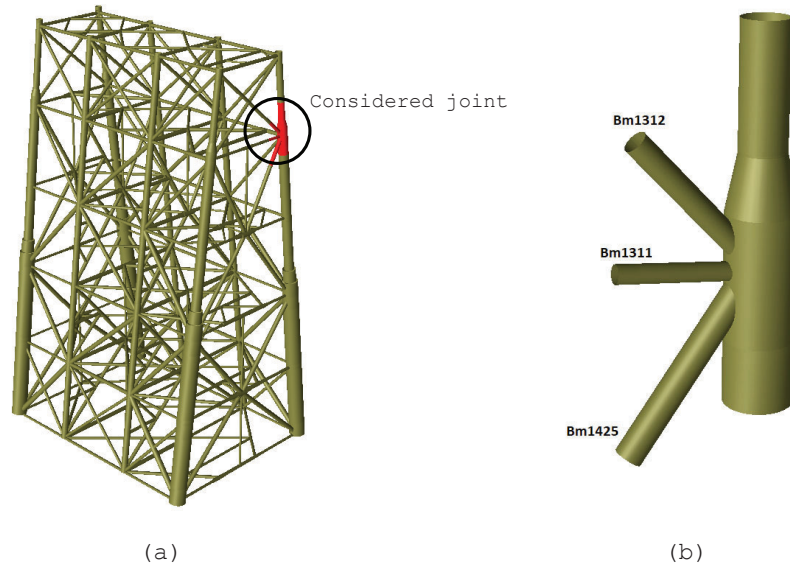
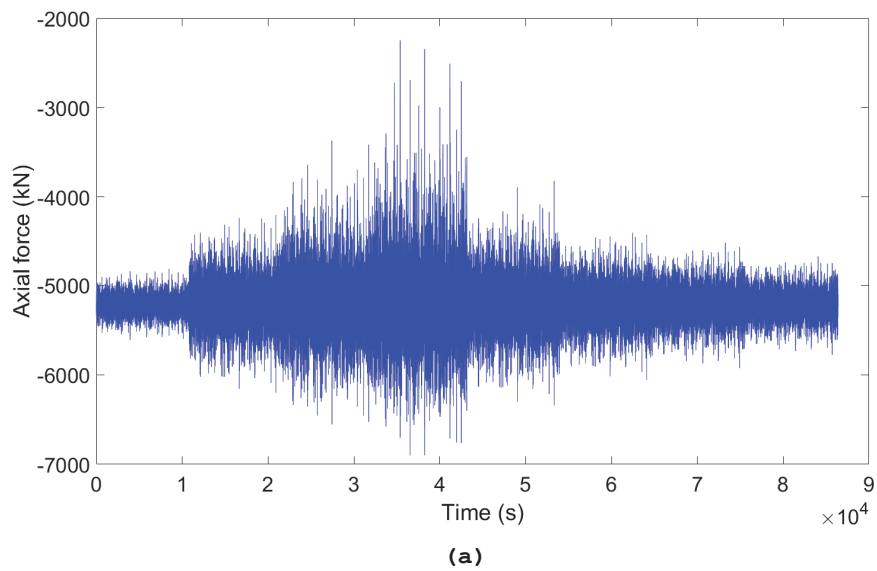
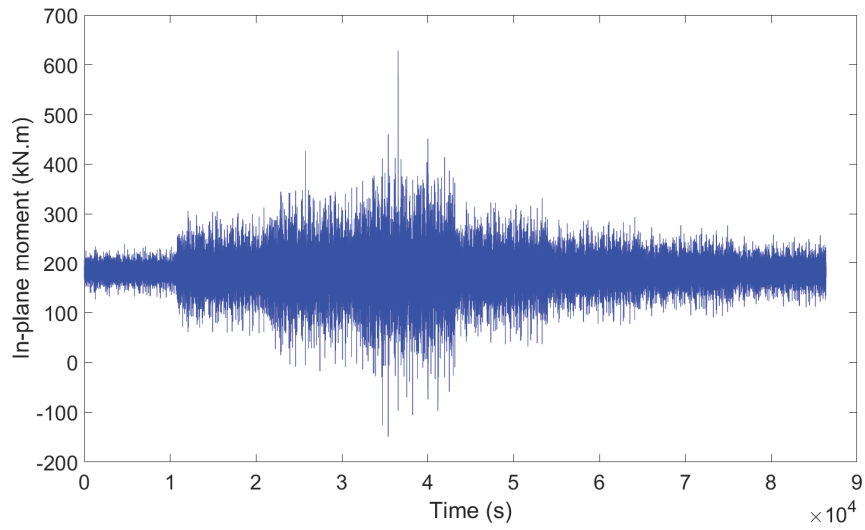
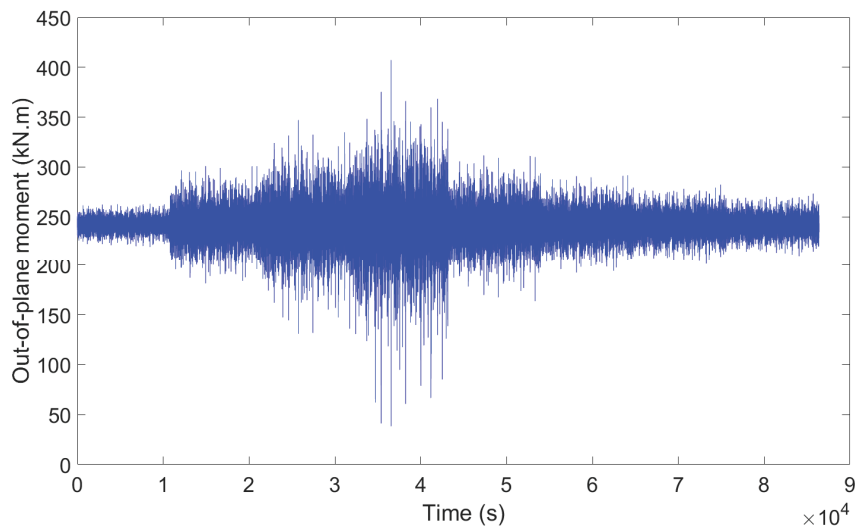


Figure 12. (a) Finite element model of jacket structure and considered joint (b) Considered joint and its members.





(b)



(c)

Figure 13. 24-hour time series for in considered brace member for **(a)** axial force **(b)** in-plane moment **(c)** out-of-plane moment.

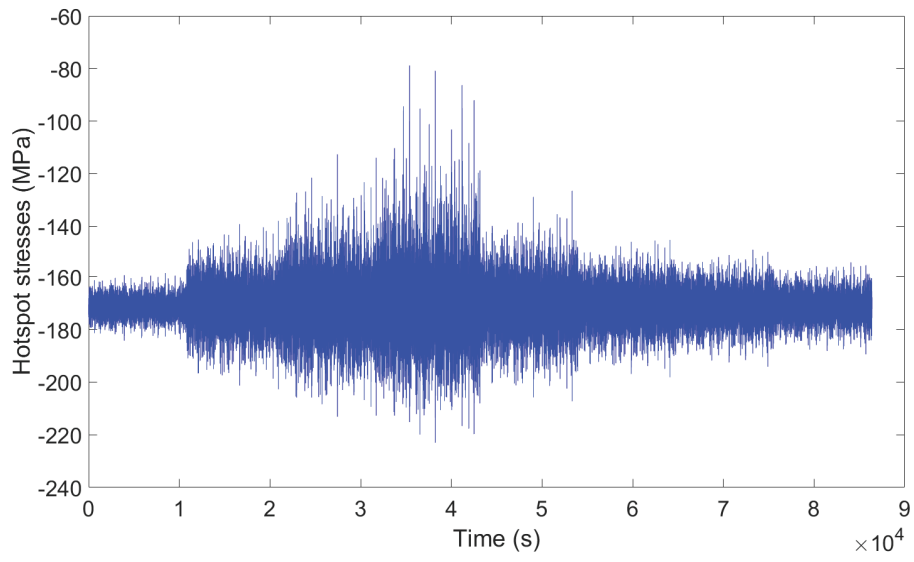


Figure 14. 24-hour time series for hot spot stresses in considered brace member.

Table 1. Chemical composition of SAE 1020 (German designation S355 J2+AR), manufacturer's information.

(wt.-%)	C	Si	Mn	P	S	Cr	Mo	Ni
	0.12	0.24	1.08	0.019	0.023	0.13	0.03	0.14

Table 2. Mechanical properties of SAE 1020 (German designation S355), manufacturer's information.

Parameters	Value
Yield strength R_e (MPa)	455
Tensile strength R_m (MPa)	600
Ultimate strain A (%)	22
Notch impact strength KCV ($J \cdot cm^{-2}$)	144

Table 3. Considered hydrodynamic coefficients for jacket members.

Members	Hydrodynamic coefficients	
	C_d	C_m
Smooth members (116.4m and above)	0.65	1.6
Rough members and anodes (seabed to 116.4m)	1.05*1.1	1.2

Table 4. Considered fatigue waves for time domain fatigue analysis.

Sea state	1	2	3	4	5	6	7	8
H_s (m)	3	4	5	6	7	8	10	13
T_p (sec)	7.5	8.5	8.5	9.5	9.5	9.5	10.5	11.5

Table 5. Considered sequence of waves for time domain fatigue analysis

Sequence	Arrangement of seastates in the sequence							
Order	1	5	7	8	6	4	3	2

Table 6 Fatigue damage in critical brace Bm1425 of considered joint

Damage calculation	Miner's rule	Proposed model
After 25 years	0.57	0.08
After 40 years	0.91	0.24

Paper VII

**Novel Non-linear Relationship to Evaluate the Critical
Plane Orientation**

Journal Paper

International Journal of Fatigue

July 2019, Volume 124, Pages 537-543.



Contents lists available at ScienceDirect

International Journal of Fatigue

journal homepage: www.elsevier.com/locate/ijfatigue

Novel non-linear relationship to evaluate the critical plane orientation

Ashish Aeran^a, Sabrina Vantadori^{b,*}, Andrea Carpinteri^b, Sudath C. Siriwardane^a, Daniela Scorza^b^a Department of Mechanical and Structural Engineering and Materials Science, University of Stavanger, P.O. Box 8600 Forus, N-4036 Stavanger, Norway^b Department of Engineering & Architecture, University of Parma, Parco Area delle Scienze 181/A, 43124 Parma, Italy

ARTICLE INFO

Keywords:

Critical plane
Fatigue life
Fatigue strength ratio
Multiaxial loading

ABSTRACT

Damage in offshore structures is mainly due to fatigue multiaxial stress state at structural joints, and fatigue strength assessment of such joints through the critical-plane criterion is well-accepted by the scientific community. A novel relationship to estimate the critical plane orientation is proposed in the present paper. Such a relationship is implemented in the stress-based critical-plane criterion by Carpinteri et al., which is applicable to any metallic material under multiaxial constant amplitude fatigue loading. Fatigue life of specimens made of different metallic materials is herein evaluated by using such a criterion. The experimental fatigue life of each specimen examined is compared with the analytical one. The relationship above seems to be a useful tool for estimations of fatigue life under multiaxial loading.

1. Introduction

Fatigue is a major cause of failure in offshore structures: almost 25% of all structural damages requiring repair is classified as fatigue damage [1–3]. Under service loading conditions, the joints of such structures are subjected to multiaxial stress state. The joint safety can be assessed through criteria based on nominal stresses, hot-spot stresses, and notch stresses [2]. Then, the detail category-based S-N curves in design standards are used for fatigue life estimation of such structural details, as in the case of tubular joints. These criteria are also based on the stress concentration factors (SCFs).

However, the fatigue damage due to multiaxial stress state is not exactly the same as that evaluated by employing an equivalent uniaxial stress together with SCFs. Moreover, the above criteria cannot be used for multiplanar complex joints or stiffened joints [4].

Therefore, more accurate and easier criteria to design the above structures are needed, by representing the actual stress state more precisely. Several criteria proposed over the past decades to capture the multiaxial stress state can be broadly classified into four categories: (a) stress-based criteria, (b) strain-based criteria, (c) energy-based criteria, and (d) fracture mechanics-based criteria [5]. Note that, while the stress-based criteria are suitable for high-cycle fatigue regime (where the major part of the lifetime is spent during the crack initiation stage) and strain-based criteria for low-cycle fatigue regime (where crack propagation takes a much larger amount of the overall fatigue lifetime), the energy-based criteria can be adopted for both these regimes [6–9]. Even though the strain energy is a scalar quantity, such a damage

parameter can be used to evaluate the orientation of crack initiation and propagation, as is proved in Ref. [9]. However, energy criteria based on SWT (Smith-Watson-Topper) parameter can lead to some uncertainty since the cycles are extracted from the shear direction. This might result in scattering of results as is reported in Ref. [9].

In the context of the above criteria, the critical plane-based approach is often recommended, providing high accuracy in the fatigue assessment of engineering components [10]. Strain energy-based criteria employing the critical plane concept have recently been proposed by some researchers [11,12]. Towards the end of the 20th century, mesoscopic scale (grain scale) fatigue damage theories were developed, wherein some grains undergo local plasticity while the rest of the matrix behaves elastically [13–15]. Mesoscopic scale criteria were used in conjunction with the critical plane-based approach and energy criteria as well [16,17]. Though these criteria yield good results, their application by the designer community is still a challenge, since determination of the model parameters depends on complex processes of error optimization.

The stress-based criteria can be further categorised based on the type of stress: empirical equivalent stress, stress invariants, average stress, and critical plane stress [18]. The earliest works included classical yield theories of Lamé and Tresca as well as the von Mises criterion, based on equivalent stress formulations [19]. Thereafter, several other formulations of equivalent stress were proposed, followed by criteria based on stress-invariants and averaged stress [20–24]. Though these approaches give us unsatisfactory results especially under non-proportional loading, the von Mises criterion is still widely used due to

* Corresponding author.

E-mail address: sabrina.vantadori@unipr.it (S. Vantadori).<https://doi.org/10.1016/j.ijfatigue.2019.02.012>

Received 3 January 2019; Received in revised form 3 February 2019; Accepted 9 February 2019

Available online 11 February 2019

0142-1123/© 2019 Elsevier Ltd. All rights reserved.

Nomenclature	
a, b, c	parameters of the relationship proposed in Eq. (7) [–]
C_a, C_m	amplitude and mean of the shear component of stress vector [MPa]
E_{RMS}	root mean square logarithmic error [–]
k	inverse slope of S-N curve under fully reversed normal stress [cycle/MPa]
k^*	inverse slope of S-N curve under fully reversed shear stress [cycle/MPa]
N_a, N_m	amplitude and mean of the normal component of stress vector [MPa]
N_{cal}	calculated number of loading cycles to failure [cycles]
N_{exp}	experimental number of loading cycles to failure [cycles]
$N_{eq,a}$	equivalent normal stress amplitude [MPa]
N_0	number of loading cycles corresponding to $\sigma_{af,-1}$ stress level [cycles]
N_0^*	number of loading cycles corresponding to $\tau_{af,-1}$ stress level [cycles]
$W(t)$	weight function [–]
t	time instant [s]
T	period of the cyclic loading [s]
T_{RMS}	mean square error [–]
β	angle between $\hat{1}$ -direction and normal to the critical plane as per Eq. (7) [°]
δ	original formulation of angle between $\hat{1}$ -direction and normal to the critical plane as per Eq. (3) [°]
ϕ, θ, ψ	principal Euler angles [°]
$\hat{\phi}, \hat{\theta}, \hat{\psi}$	averaged values of principal Euler angles [°]
σ_u	ultimate tensile strength [MPa]
$\sigma_{af,-1}$	fully-reversed normal stress fatigue strength [MPa]
$\sigma_1, \sigma_2, \sigma_3$	instantaneous principal stresses [MPa]
$\tau_{af,-1}$	fully-reversed shear stress fatigue strength [MPa]

its simplicity of application.

Towards the beginning of 21st Century, Carpinteri and co-workers proposed a multiaxial fatigue criterion based on the critical plane approach, for assessment of metallic structural components under multiaxial constant amplitude cyclic loadings [25–28]. This criterion requires the determination of a critical plane orientation, followed by an equivalent stress evaluation performed on such a plane. Note that the critical plane may or may not be coincident with the fatigue fracture plane.

In more detail, the evaluation of the critical plane orientation according to the Carpinteri et al. criterion is performed in two stages: first, averaged principle stress directions at the material verification point are computed; then, the normal to the critical plane, defined by means of an off-angle is estimated. Such an off-angle is a material characteristic depending only on the fatigue strength ratio $\sigma_{af,-1}/\tau_{af,-1}$ of the material, being $\sigma_{af,-1}$ and $\tau_{af,-1}$ the fatigue strengths under fully-reversed normal stress and shear stress, respectively.

Several off-angle expressions have been proposed in the literature, the original one being a non-linear expression by Carpinteri et al. [25]. This expression can only be employed for materials with a fatigue strength ratio in the range from $1/\sqrt{3}$ to 1. Subsequently, some relationships have been presented by Walat et al. in 2014 [29]. Recently, Carpinteri et al. in 2017 have proposed another off-angle expression [30]. Although such an expression provides more accurate fatigue lifetime results than those determined by using the original one, there are still slight deviations from the experimental results. Moreover, the expression does not exactly meet the boundary conditions for both elastic-brittle and elastic-plastic materials.

In the present paper, a novel relationship to compute the off-angle is proposed in order to improve fatigue life estimation deduced through the Carpinteri et al. criterion. Several metallic material tests under biaxial loading are analysed, and some conclusions are drawn. The results in terms of fatigue lifetime are compared with those derived by employing the original expression of the off-angle.

2. The Carpinteri et al. criterion

The flowchart of the Carpinteri et al. criterion [25–28] is shown in Fig. 1. Let us consider a body subjected to constant amplitude multiaxial cyclic loading. The material is characterised by the tensile ultimate strength σ_u and the following fatigue properties: fatigue strength under fully reversed normal stress $\sigma_{af,-1}$ evaluated at N_0 loading cycles, inverse slope of the S-N curve under fully reversed normal stress, k ($\sigma^k N = C_\sigma$), fatigue strength under fully reversed shear stress $\tau_{af,-1}$ evaluated at N_0^* loading cycles, and inverse slope of the S-N curve under fully reversed shear stress, k^* ($\tau^{k^*} N = C_\tau$).

The time-varying stress state at the verification material point P (that is, the point where fatigue assessment is performed), expressed with respect to the fixed frame XYZ , can be described by means of the stress tensor σ . The instantaneous principal stress directions 1, 2 and 3 (being $\sigma_1 \geq \sigma_2 \geq \sigma_3$) at point P can be worked out from σ . The instantaneous reference frame $P123$ can be defined through the principal Euler angles ϕ, θ and ψ . Being such angles time-varying, the averaged values $\hat{\phi}, \hat{\theta}$ and $\hat{\psi}$ and consequently the averaged reference frame $P\hat{1}\hat{2}\hat{3}$ can be determined as follows (Fig. 2):

$$\hat{\phi} = \int_0^T \phi(t) W(t) dt, \quad \hat{\theta} = \int_0^T \theta(t) W(t) dt \quad \text{and} \quad \hat{\psi} = \int_0^T \psi(t) W(t) dt \quad (1)$$

being $W(t)$ a weight function given by

$$W(t) = \begin{cases} 0, & \sigma_1(t) < \sigma_{1,max} \\ 1, & \sigma_1(t) = \sigma_{1,max} \end{cases} \quad (2)$$

where t is the time, T is the period of the cyclic loading, and $\sigma_{1,max}$ is the maximum value of σ_1 during T .

The normal w to the critical plane is assumed to be correlated to the above $\hat{1}$ -direction through the original expression of the off-angle δ (rotation to be performed in the $\hat{1}\hat{3}$ plane, Fig. 2):

$$\delta = \frac{3}{2} \left[1 - \left(\frac{\tau_{af,-1}}{\sigma_{af,-1}} \right)^2 \right] 45^\circ \quad (3)$$

Let us consider the stress vector related to the above verification point P on the critical plane. The time-history of the normal component of the stress vector can be defined by means of a scalar period function, characterised by the mean value N_m and the amplitude N_a , the normal component direction being fixed with respect to time. As far as the shear component of the stress vector is concerned, the vector field has to be defined, the shear component direction being time-varying. More precisely, such a field may be described by a vector, representing the mean value C_m , and a scalar quantity, representing the amplitude C_a . The procedure proposed by Araujo et al. [31] is here implemented to compute C_m and C_a .

Finally, according to the Carpinteri criterion, the number of loading cycles to failure, N_{cal} , can be obtained from the solution of the following expression:

$$\sqrt{N_{eq,a}^2 + (\sigma_{af,-1}/\tau_{af,-1})^2 (N_{cal}/N_0)^{-2/k} (N_0^*/N_{cal})^{-2/k^*} C_a^2} = \sigma_{af,-1} (N_{cal}/N_0)^{-1/k} \quad (4)$$

where $N_{eq,a}$ (representing the amplitude of an equivalent normal stress) is given by

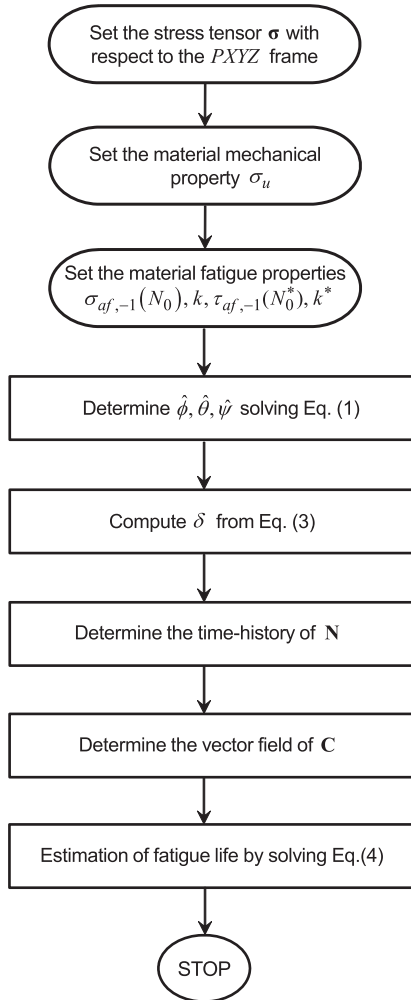


Fig. 1. Flowchart of the Carpinteri et al. criterion.

$$N_{a,eq} = N_u + \sigma_{af,-1} \left(\frac{N_m}{\sigma_u} \right) \quad (5)$$

taking into account the diagram of Goodman.

3. A novel relationship to evaluate the off-angle

3.1. Formulation of the logistic curve (S-curve)

Now a novel expression is proposed to compute the above off-angle, named β in the following in order to distinguish it from the original expression (δ in Eq. (3)).

The novel relationship is based on a logistic curve, also named S-curve, whose general expression is given by [32]:

$$f(x) = \frac{1}{1 + e^{-\alpha(x-x_0)}} \quad (6)$$

where x is the variable, and α and x_0 are the slope and inflection point

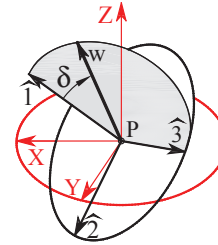


Fig. 2. Frame $\hat{P}\hat{1}\hat{1}\hat{2}\hat{3}$ of the averaged principal stresses, off-angle in the $\hat{1}\hat{1}$ plane, and normal w to the critical plane.

of the curve, respectively. According to Eq. (6), the following relationship is proposed:

$$\beta \left(\frac{\sigma_{af,-1}}{\tau_{af,-1}} \right) = \frac{a}{1 + e^{-b[(\sigma_{af,-1}/\tau_{af,-1}) - c]}} \quad (7)$$

which represents an advancement of Eq. (6), due to an additional parameter a instead of 1 at the numerator of Eq. (6). Such an optimization allows to govern the peak value of the curve. The unit of β is degree, and the variable is the fatigue strength ratio $\sigma_{af,-1}/\tau_{af,-1}$. The dimensionless parameters a , b , c define peak value, slope and inflection point of the curve, respectively.

3.2. Parametric study of the proposed logistic curve (S-curve)

A parametric study is here performed to analyse the influence of the parameters a , b , c on the shape of the proposed logistic curve (Eq. (7)).

Parameter a determines the peak value of the curve, as is shown in Fig. 3, where different curves are plotted by varying a from 30 to 50 and taking b and c as constants.

The slope of the curve is governed by parameter b , as is shown in Fig. 4, where different curves are plotted by varying b from 15 to 35 and taking a and c as constants.

Parameter c determines the inflection point of the curve, as is shown in Fig. 5, where different curves are plotted by varying c from 1.0 to 2.0 and taking b and c as constants. It can also be said that this parameter governs the shifting of the curve along the abscissa axis.

3.3. S-curve calibration

In order to calibrate the S-curve described by Eq. (7), some fatigue test data available in the literature are examined. They are related to the following metallic materials: five steels (mild steel D30 and hard steel 982FA [33], SM45C [34], SUS304 [35], 10HNAP [36]), two cast irons (GGG40 and GTS45 [36]), and CuZn40Pb2 brass [37]. The specimens are smooth and subjected to combined in-phase normal loading (tension or bending) and torsion loading, with loading ratio equal to

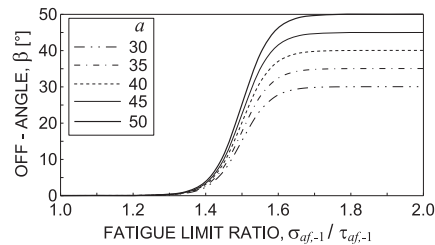


Fig. 3. S-curve shape, by varying the value of the parameter a ($b = 25$ and $c = 1.5$).

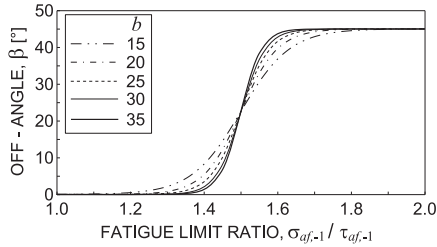


Fig. 4. S-curve shape by varying the value of the parameter b ($a = 45$ and $c = 1.5$).

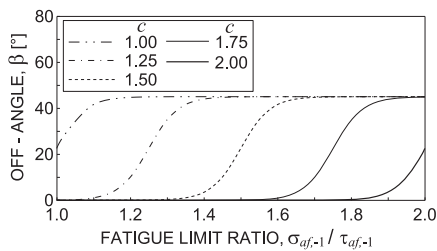


Fig. 5. S-curve shape by varying the value of the parameter c ($a = 45$ and $b = 25$).

– 1.0. The fatigue strength under normal loading and that under torsion loading are listed in Table 1, together with the corresponding loading cycle numbers N_0 and N_0^* , respectively.

First of all, for each experimental data related to the above metallic materials, the estimated fatigue life N_{cal} is computed from Eq. (4) by varying β from 0° to 45° with a step equal to 1° . Note that the angle β varies in such a range, being equal to 0° for very hard metals ($\sigma_{af,-1}/\tau_{af,-1} = 1$) and equal to 45° for mild/hard metals ($\sigma_{af,-1}/\tau_{af,-1} = \sqrt{3}$). The series of planes considered by varying β from 0° to 45° are candidate planes where to perform the fatigue assessment, that is to say, one of them is adopted as the critical plane. The critical plane is the verification plane not experimentally measurable; it is herein assumed to be different from the experimentally measurable fatigue fracture plane.

Then, for each of the above materials, the value of the root mean square logarithmic error is computed for 45 times, corresponding each one to a different value of β ranging from 0° to 45° :

$$E_{RMS} = \sqrt{\frac{\sum_{i=1}^n \log^2 \frac{N_{exp}}{N_{cal}}}{n}} \quad (8)$$

where n is the total number of the experimental data for a given

Table 1
Fatigue properties of the examined metallic materials.

Material	Ref.	$\sigma_{af,-1}$ [MPa]	N_0 [cycles]	k	$\tau_{af,-1}$ [MPa]	N_0^* [cycles]	k^*
GGG40	[36]	257.067	10^6	10.95	237.413	10^6	12.41
CuZn40Pb2	[37]	243.990	10^6	5.86	194.480	10^6	17.17
GTS45	[36]	284.259	$2.5(10)^5$	19.40	224.762	$2.5(10)^5$	12.80
SUS304	[35]	213.717	$2.5(10)^3$	7.04	156.906	$2.5(10)^3$	8.70
SM45C	[34]	341.964	10^5	10.30	243.835	10^5	18.60
D30	[33]	178.265	$2(10)^6$	10.75	119.117	$2(10)^6$	9.20
982FA	[33]	338.007	10^6	12.10	218.127	10^6	18.60
10HNAP	[36]	386.598	$2(10)^6$	9.50	206.304	$2(10)^6$	8.20
IC2	[33]	102.651	10^6	8.80	88.862	10^6	19.50
30CrNiMo8	[38]	630.957	10^5	8.05	419.043	10^5	24.62
PA4 (6082-T6)	[39]	153.947	$2(10)^6$	8.00	91.391	$2(10)^6$	7.70

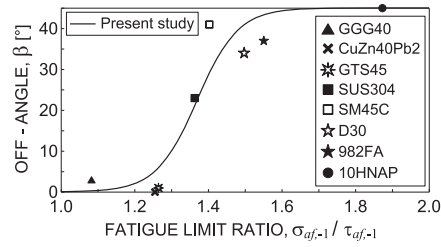


Fig. 6. Proposed S-curve: data employed to perform the regression analysis, and plot of the curve characterised by $a = 45$, $b = 18$, and $c = 1.37$.

metallic material, N_{exp} is the experimental multiaxial fatigue life, and N_{cal} is the estimated life. The corresponding mean square error T_{RMS} is computed as follows:

$$T_{RMS} = 10^{E_{RMS}} \quad (9)$$

Finally, for each metallic material examined, the off-angle $\beta_{T_{RMS,min}}$ corresponding to the minimum value $T_{RMS,min}$ of the mean square error is registered. The experimental values of $\beta_{T_{RMS,min}}$ against $\sigma_{af,-1}/\tau_{af,-1}$ are represented in Fig. 6 by using symbols, whereas the curve plotted is determined as is described below.

The experimental data shown in Fig. 6 are the starting point of the procedure of the S-curve calibration. As a matter of fact, a regression analysis is performed on such data, where the parameters a , b , c are made to vary in order to minimise the regression coefficient. The results obtained are $a = 45$, $b = 18$, and $c = 1.37$, with a regression coefficient equal to 0.97, and the proposed S-curve (Eq. (7)) is plotted with a continuous line. Note that such a curve satisfies with a good accuracy the aforementioned experimental observations, that is to say: $\beta = 0.056^\circ$ when $\sigma_{af,-1}/\tau_{af,-1} = 1$, whereas $\beta = 44.934^\circ$ when $\sigma_{af,-1}/\tau_{af,-1} = \sqrt{3}$.

3.4. Comparison between the novel curve and other literature relationships

By comparing the proposed curve (Eq. (7) with $a = 45$, $b = 18$, and $c = 1.37$) with the original one (Eq. (3)), it can be observed that there is significant deviation between such two curves (see Fig. 7).

In the same Figure, a slight deviation can be observed between the herein proposed relationship and that presented in Ref. [30], especially for very hard metals ($\sigma_{af,-1}/\tau_{af,-1} \rightarrow 1$) because the expression in Ref. [30] does not exact fulfil the zero boundary condition when $\sigma_{af,-1}/\tau_{af,-1} = 1$. For hard and mild/hard metallic materials, instead, such two curves show a good agreement with an average deviation of about 1%. Note that the curve presented in Ref. [30] can be considered as a particular case of that described by Eq. (7) taking the S-curve parameters equal to $a = 43.5$, $b = 20$, and $c = 1.36$.

The orientation of the fracture plane is connected to the averaged principal stress directions, and does not depend on the β angle.

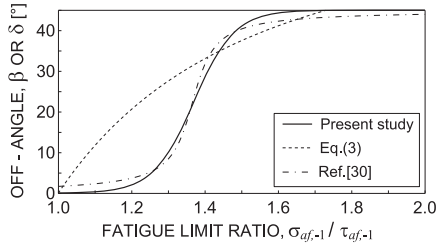


Fig. 7. Comparison between off-angle relationships: present study (Eq. (7) with $a = 45$, $b = 18$, and $c = 1.37$), original curve (Eq. (3)), and expression in Ref. [30].

Therefore, to verify the accuracy of the proposed expression for β angle, comparing the estimated fatigue life with the experimental fatigue life seems to be more appropriate than comparing the estimated fracture plane with the experimental one. The comparison related to the fracture plane could be meaningful for materials characterised by small values of β angle, because the fracture plane in such cases tends to coincide with the critical plane (verification plane). However, to the best knowledge of the authors, no data related to the fracture plane orientation are available in the literature for GGG40, CuZn40Pb2 and GTS45.

4. Verification of the novel relationship

Let us consider the fatigue test data used for S-curve calibration [33–37] and other experimental data available in the literature, related to the following metallic materials: steel (30CrNiMo8 [38]), cast iron (IC2 [33]), and aluminium alloy (PA4 or 6082-T6 [39]). The specimens are smooth and subjected to the same type of loading as that used for tests in Refs. [33–37]. The fatigue strengths under both normal and torsion loading are listed in Table 1, together with the corresponding loading cycle numbers N_0 and N_0^* , respectively.

Now, by employing Eq. (7) with $a = 45$, $b = 18$, $c = 1.37$ instead of Eq. (3), the Carpinteri et al. criterion is applied to such experimental data [33–39] in order to compute the number of loading cycles to failure, N_{cal} . The values of the mean square error T_{RMS} are plotted in Fig. 8. A quite good accuracy is deduced in terms of fatigue life estimation since T_{RMS} is lower than 3.5 for all examined materials.

Note that the curve in Fig. 6 is calibrated by taking into account eight (8) materials, but it is used to determine the critical plane orientation for eleven (11) materials, that is, the effect of the proposed curve on fatigue life is assessed by examining three (3) further materials (IC2, 982FA and 10HNAP) which are not considered for the curve calibration.

Then, the Carpinteri et al. criterion is applied according to its original formulation (Eq. (3)). The computed values of the mean square error are shown in Fig. 9. Such results are worse than the previous ones (in Fig. 8), being T_{RMS} much greater than 3.0 for many materials.

In Fig. 10, experimental data are compared with theoretical evaluations. The solid line indicates $N_{cal} = N_{exp}$ (all results above such a line are conservative), the dashed lines correspond to N_{cal}/N_{exp} equal to 0.5 and 2, respectively, and the dash-dot lines correspond to N_{cal}/N_{exp} equal to 1/3 and 3, respectively. In more detail, the fatigue life estimations in Fig. 10(a) are determined through the novel relationship (Eq. (7) with $a = 45$, $b = 18$, $c = 1.37$), whereas those in Fig. 10(b) are deduced through the original formulation (Eq. (3)). It can be observed that, for the materials being examined, there is significant difference between the two expressions in medium-cycle fatigue regime ($10^4 \leq N_{exp} \leq 10^6$) compared to the high-cycle fatigue regime. In the case of high-cycle fatigue regime, the values are different but not very scattered.

For the materials and fatigue loadings being examined, it can be

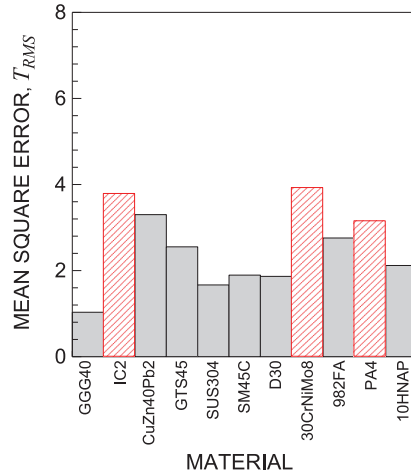


Fig. 8. Mean square error T_{RMS} by employing the novel off-angle relationship (Eq. (7) with $a = 45$, $b = 18$, $c = 1.37$). Results obtained from experimental data not used in the regression analysis are shown with diagonal hatching.

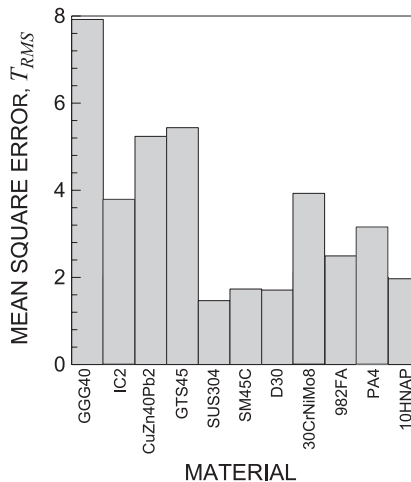


Fig. 9. Mean square error, T_{RMS} , by employing the original off-angle relationship (Eq. (3)).

observed that 83% of the results fall within the 3x band and 67% within the 2x band by employing the novel relationship, whereas 84% of the results fall within the 3x band and 65% within the 2x band by employing the original formulation. According to such percentages, the two relationships above seem to produce results with a very similar accuracy.

To better estimate the reliability of such two relationships, the mean square error (T_{RMS}) values have to be examined because they take into account how far the results are from the solid line $N_{cal} = N_{exp}$. Since the average of T_{RMS} is equal to 2.18 by using the novel relationship (average computed on the 11 T_{RMS} values in Fig. 8) against 3.10 by using the original expression (average computed on the 11 T_{RMS} values in Fig. 9), the accuracy of the novel relationship results is greater than that of the original expression ones.

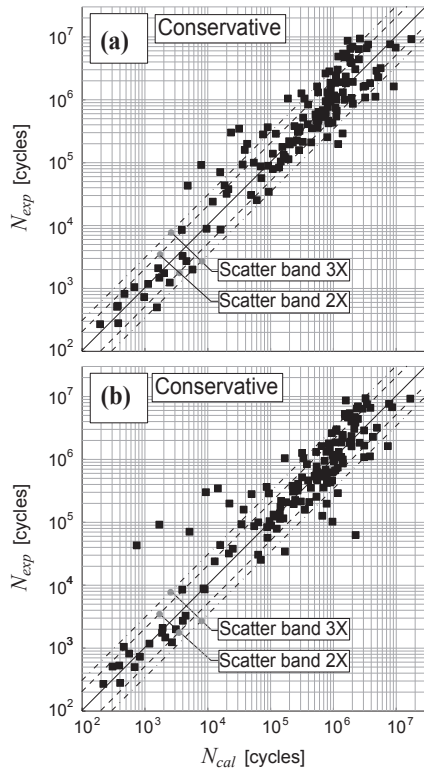


Fig. 10. Experimental fatigue life vs predicted fatigue life for each experimental data set analysed, by applying: (a) the novel relationship, (b) the original relationship. All results above the solid line $N_{cal} = N_{exp}$ are conservative.

Note that the fatigue life N_{cal} is computed in Ref. [30] by applying a criterion different from that here employed as far as both equivalent stress amplitude evaluation and fatigue life computation are concerned. As a matter of fact, the criterion used in Ref. [30] consists in determining the amplitude of an equivalent stress (acting on the critical plane) evaluated by linearly combining the amplitude of the normal stress vector component with the amplitude of the shear stress vector component (both related to the critical plane), the latter being calculated as is reported in Ref. [39]. The fatigue life is then estimated by using the S-N curve.

Instead, the criterion here employed (Refs. [25–28]) consists in determining the amplitude of an equivalent stress (acting on the critical plane) evaluated by a non-linear combination (Eq. (4)) of the amplitude of an equivalent normal stress vector component (normal to the critical plane, Eq. (5)) with the amplitude of the shear stress vector component acting on the same plane, the latter being computed as is reported in Ref. [31]. The fatigue life is then estimated by exploiting the Basquin expression and obtaining Eq. (4).

5. Conclusions

A novel off-angle relationship to evaluate the critical plane orientation is proposed in the present paper. Such a relationship is used in conjunction with Carpinteri et al. criterion in order to improve the accuracy in fatigue life estimation of any metallic material under multiaxial constant amplitude fatigue loading.

Several tests on metallic materials under biaxial loading are available in the literature. The fatigue life for each test examined has been computed by employing both the novel relationship and the original off-angle expression, and then such results have been compared with the experimental fatigue life.

A good agreement has been observed between experimental data and theoretical life estimations when the novel relationship is used since the mean square error is equal to about 2, while such an error is equal to about 3 when the original expression is adopted.

The novel relationship used together with the Carpinteri et al. criterion seems to be a useful tool to obtain life estimations for any metallic material under multiaxial loading. Such a relationship should be further assessed in the case of both different materials and different loadings. As a matter of fact, it can be employed to estimate the critical plane orientation even in the case of metallic specimens under variable amplitude loading. However, for such a type of loading, the present criterion cannot be used to evaluate the fatigue life, but other criteria formulated in time- or in frequency-domain have to be used, as is detailed in Ref. [28].

Acknowledgements

The authors gratefully acknowledge the financial support provided by the Norwegian Ministry of Education and Research and the Italian Ministry for University and Technological and Scientific Research (MIUR), Research Grant PRIN 2015 No. 2015JW9NJT on “Advanced mechanical modeling of new materials and structures for the solution of 2020 Horizon challenges”.

References

- [1] Almar-Naess A. Fatigue handbook. Trondheim, Norway: Tapir Publishers; 1985.
- [2] Haagenen PJ. Fatigue of tubular joints and fatigue improvement methods. *Prog Struct Mat Eng* 1997;1:96–106.
- [3] Lotsberg I. Fatigue design of marine structures. Cambridge: Cambridge University Press; 2016.
- [4] Saini DS, Karmakar D, Ray-Chaudhuri S. A review of stress concentration factors in tubular and non-tubular joints for design of offshore installations. *J Ocean Eng Sci* 2016;1:186–202.
- [5] Wei H, Liu Y. A critical plane-energy model for multiaxial fatigue life prediction. *Fatigue Fract Eng Mater Struct* 2017;40:1973–83.
- [6] Zhu SP, Liu Y, Liu Q, Yu ZY. Strain energy gradient-based LCF life prediction of turbine discs using critical distance concept. *Int J Fatigue* 2018;113:33–42.
- [7] Zhu SP, Yu ZY, Liu Q, Ince A. Strain energy-based multiaxial fatigue life prediction under normal/shear stress interaction. *Int J Damage Mech* 2018. <https://doi.org/10.1177/1056789518786031>. [in press].
- [8] Feng ES, Wang XG, Jiang C. A new multiaxial fatigue model for life prediction based on energy dissipation evaluation. *Int J Fatigue* 2019;122:1–8.
- [9] Portugal I, Olave M, Urresti I, Zurutuza A, López A, Muñiz-Calvente M, et al. A comparative analysis of multiaxial fatigue models under random loading. *Eng Struct* 2019;182:112–22.
- [10] Zhu SP, Yu ZY, Correia J, De Jesus A, Berto F. Evaluation and comparison of critical plane criteria for multiaxial fatigue analysis of ductile and brittle materials. *Int J Fatigue* 2018;112:279–88.
- [11] Carpinteri A, Berto F, Campagnolo A, Fortese G, Ronchei C, Scorza D, et al. Fatigue assessment of notched specimens by means of a critical plane-based criterion and energy concepts. *Theor Appl Fract Mech* 2016;84:57–63.
- [12] Lu C, Melendez J, Martínez-Esnaola JM. Modelling multiaxial fatigue with a new combination of critical plane definition and energy-based criterion. *Int J Fatigue* 2018;108:109–15.
- [13] Papadopoulos IV, Davoli P, Gorla C, Filippini M, Bernasconi A. A comparative study of multiaxial high-cycle fatigue criteria for metals. *Int J Fatigue* 1997;19:219–35.
- [14] Morel F. A fatigue life prediction method based on a mesoscopic approach in constant amplitude multiaxial loading. *Fatigue Fract Eng Mater Struct* 1998;21:241–56.
- [15] Dang Van K, Bignonnet A, Fayard JL, Janosch JJ. Assessment of welded structures by a local multiaxial fatigue approach. *Fatigue Fract Eng Mater Struct* 2001;24:369–76.
- [16] Morel F, Palin-Luc T, Froustey C. Comparative study and link between mesoscopic and energetic approaches in high cycle multiaxial fatigue. *Int J Fatigue* 2001;23:317–27.
- [17] Huyen N, Flaceliere L, Morel F. A critical plane fatigue model with coupled mesoplasticity and damage. *Fatigue Fract Eng Mater Struct* 2008;31:12–28.
- [18] Liu Y, Mahadevan S. Multiaxial high-cycle fatigue criterion and life prediction for metals. *Int J Fatigue* 2005;27:790–800.
- [19] von Mises R. *Mechanik der festen Körper im plastisch-deformablen Zustand*.

- Nachrichten von der Gesellschaft der Wissenschaften zu Göttingen, Mathematisch-Physikalische Klasse 1913:582–92.
- [20] Gough HJ, Pollard HV. The strength of metals under combined alternating stresses. *Proc Inst Mech Eng* 1935;131:3–18.
- [21] Crossland B. Effect of large hydrostatic pressures on the torsional fatigue strength of an alloy steel. *Proceedings of the international conference on fatigue of metals*. London: Institution of Mechanical Engineers; 1956. p. 184–94.
- [22] Papadopoulos IV. Long life fatigue under multiaxial loading. *Int J Fatigue* 2001;23:839–49.
- [23] Li B, De Freitas M. A procedure for fast evaluation of high-cycle fatigue under multiaxial random loading. *J Mech Des* 2002;124:558–63.
- [24] You BR, Lee SB. A critical review on multiaxial fatigue assessments of metals. *Int J Fatigue* 1996;18:235–44.
- [25] Carpinteri A, Spagnoli A. Multiaxial high-cycle fatigue criterion for hard metals. *Int J Fatigue* 2001;23:135–45.
- [26] Carpinteri A, Spagnoli A, Vantadori S. Multiaxial fatigue life estimation in welded joints using the critical plane approach. *Int J Fatigue* 2009;31:188–96.
- [27] Carpinteri A, Spagnoli A, Vantadori S. Multiaxial fatigue assessment using a simplified critical plane-based criterion. *Int J Fatigue* 2011;33:969–76.
- [28] Carpinteri A, Spagnoli A, Vantadori S, Bagni C. Structural integrity assessment of metallic components under multiaxial fatigue: the C-S criterion and its evolution. *Fatigue Fract Eng Mater Struct* 2013;36:870–83.
- [29] Walat K, Lagoda T. Lifetime of semi-ductile materials through the critical plane approach. *Int J Fatigue* 2014;67:73–7.
- [30] Carpinteri A, Kurek M, Lagoda T, Vantadori S. Estimation of fatigue life under multiaxial loading by varying the critical plane orientation. *Int J Fatigue* 2017;100:512–20.
- [31] Araújo J, Carpinteri A, Ronchei C, Spagnoli A, Vantadori S. An alternative definition of the shear stress amplitude based on the maximum rectangular hull method and application to the C-S (Carpinteri-Spagnoli) criterion. *Fatigue Fract Eng Mater Struct* 2014;37:764–71.
- [32] Cristóbal JR. The S-curve envelope as a tool for monitoring and control of projects. *Procedia Comput Sci* 2017;121:756–61.
- [33] Nishihara T, Kawamoto M. The strength of metals under combined alternating bending and twisting. *Japan: Memoirs of the College of Engineering, Kyoto Imperial University*; 1941.
- [34] Lee SB, Miller KJ, Brown MW. A criterion for fully reversed out of phase torsion and bending. *Multiaxial fatigue*. Philadelphia, USA: ASTM STP 853; 1985. p. 553–68.
- [35] Sakane M, Ohnami M, Sawada M. Fracture modes and low cycle biaxial fatigue life at elevated temperature. *J Eng Technol* 1987;109:236–43.
- [36] Pawliczek R. Badanie wpływu parametrów obciążenia i geometrii karbu na trwałość przy zmiennym zginaniu i skręcaniu. *Opole: Rozprawa doktorska Politechnika Opolska*; 2001. [in Polish].
- [37] Müller A. Zum Festigkeitsverhalten von mehrachsiger stochastisch beanspruchten Gußeisen mit Kugelgraphit und Tempergu. *Darmstadt: Fraunhofer – Institut für Betriebsfestigkeit*; 1994.
- [38] Sanetra C. Untersuchungen zum Festigkeitsverhalten bei mehrachsiger Randombeanspruchung unter Biegung und Torsion *Dissertation Technische Universität Clausthal*; 1991.
- [39] Niesłony A, Lagoda T, Walat K, Kurek M. Multiaxial fatigue behaviour of AA6068 and AA2017A aluminium alloys under in-phase bending with torsion loading condition. *Mat-wiss U Werkstofftech* 2014;45:947–52.

